What Is Tungsten Disulfide

CTIA GROUP LTD

CTIA GROUP LTD

Global Leader in Intelligent Manufacturing for Tungsten, Molybdenum, and Rare Earth Industries

INTRODUCTION TO CTIA GROUP

CTIA GROUP LTD， a wholly-owned subsidiary with independent legal personality established by CHINATUNGSTEN ONLINE , is dedicated to promoting the intelligent, integrated, and flexible design and manufacturing of tungsten and molybdenum materials in the Industrial Internet era. CHINATUNGSTEN ONLINE, founded in 1997 with www.chinatungsten.com as its starting point—China's first top-tier tungsten products website—is the country's pioneering e-commerce company focusing on the tungsten, molybdenum, and rare earth industries. Leveraging nearly three decades of deep experience in the tungsten and molybdenum fields, CTIA GROUP inherits its parent company's exceptional design and manufacturing capabilities, superior services, and global business reputation, becoming a comprehensive application solution provider in the fields of tungsten chemicals, tungsten metals, cemented carbides, high-density alloys, molybdenum, and molybdenum alloys.

Over the past 30 years, CHINATUNGSTEN ONLINE has established more than 200 multilingual tungsten and molybdenum professional websites covering more than 20 languages, with over one million pages of news, prices, and market analysis related to tungsten, molybdenum, and rare earths. Since 2013, its WeChat official account "CHINATUNGSTEN ONLINE" has published over 40,000 pieces of information, serving nearly 100,000 followers and providing free information daily to hundreds of thousands of industry professionals worldwide. With cumulative visits to its website cluster and official account reaching billions of times, it has become a recognized global and authoritative information hub for the tungsten, molybdenum, and rare earth industries, providing 24/7 multilingual news, product performance, market prices, and market trend services.

Building on the technology and experience of CHINATUNGSTEN ONLINE, CTIA GROUP focuses on meeting the personalized needs of customers. Utilizing AI technology, it collaboratively designs and produces tungsten and molybdenum products with specific chemical compositions and physical properties (such as particle size, density, hardness, strength, dimensions, and tolerances) with customers. It offers full-process integrated services ranging from mold opening, trial production, to finishing, packaging, and logistics. Over the past 30 years, CHINATUNGSTEN ONLINE has provided R&D, design, and production services for over 500,000 types of tungsten and molybdenum products to more than 130,000 customers worldwide, laying the foundation for customized, flexible, and intelligent manufacturing. Relying on this foundation, CTIA GROUP further deepens the intelligent manufacturing and integrated innovation of tungsten and molybdenum materials in the Industrial Internet era.

Dr. Hanns and his team at CTIA GROUP, based on their more than 30 years of industry experience, have also written and publicly released knowledge, technology, tungsten price and market trend analysis related to tungsten, molybdenum, and rare earths, freely sharing it with the tungsten industry. Dr. Han, with over 30 years of experience since the 1990s in the e-commerce and international trade of tungsten and molybdenum products, as well as the design and manufacturing of cemented carbides and high-density alloys, is a renowned expert in tungsten and molybdenum products both domestically and internationally. Adhering to the principle of providing professional and high-quality information to the industry, CTIA GROUP's team continuously writes technical research papers, articles, and industry reports based on production practice and market customer needs, winning widespread praise in the industry. These achievements provide solid support for CTIA GROUP's technological innovation, product promotion, and industry exchanges, propelling it to become a leader in global tungsten and molybdenum product manufacturing and information services.

COPYRIGHT AND LEGAL LIABILITY STATEMENT

I. COPYRIGHT OWNERSHIP

This document's copyright and related rights belong solely to CTIA GROUP Co., Ltd. (hereinafter "we"). Without written permission from us, no one may reproduce, copy, adapt, translate, distribute (including online), publish, or use any part of it in any way.

II. THIRD-PARTY MATERIAL CITATION

Third-party materials (literature, data, charts) cited here are credited to their sources and authors as far as possible. If there are errors or disputes, rights holders may submit written claims with proof. Upon verification, we will remove or correct the content and apologize publicly on the original platform. Users must get permission from original authors; liability for unauthorized use falls on the user.

III. DISCLAIMER

A. CONTENT ACCURACY

Content about politics, military, economics, history, culture, religion, or gender is based on public sources and industry experience for objective tungsten market analysis. The author remains neutral. It may have errors or limitations and isn't factual confirmation or professional advice. We don't guarantee accuracy or completeness and aren't liable for losses from reliance on it.

B. USAGE RISKS

This document is for academic or industry reference only, not for investment, legal, policy, or moral decisions. Users must judge independently and consult experts; they bear all risks from use.

C. CULTURAL SENSITIVITY

References to countries, regions, ethnicities, religions, or genders are technical only, with no political or value intent. The author and we aren't responsible for cultural or ideological disputes.

D. MEDICAL AND HEALTH INFORMATION DISCLAIMER

Medical or health info (e.g., disease prevention, treatments) is from public sources for tungsten market context, not medical advice. Users must not replace professional opinions with it; health risks or losses from reliance are their own. We don't endorse its safety or efficacy.

E. TRANSLATION DISCLAIMER

The version of language excludes Chinese is machine-translated and may have errors. We aren't liable for translation accuracy; the Chinese original is authoritative. Official bilingual versions need written permission via email; unauthorized translations are infringement.

F. AI-GENERATED CONTENT DISCLAIMER

Some content (e.g., data analysis, forecasts) may be AI-generated, potentially with errors or legal issues, unverified by third parties. We aren't liable for its legality or safety; users bear risks from its use and must verify it, remove flaws, and follow laws, or violate this statement.

IV. USER OBLIGATIONS

Users must keep copyright notices, disclaimers, and author info intact, get third-party permissions for cited content, and comply with local laws and norms when using or sharing this document. Violations are the user's responsibility; we may take legal action.

V. REVISIONS AND TERMINATION

We may update this statement anytime based on legal, industry, or practical needs, effective upon posting without notice. If users disagree, they must stop using or sharing it immediately.

DR. HANNS
CTIA GROUP
sales@chinatungsten.com
XIAMEN CHINA, MAR.3,2025

CONTENT

Chapter 4: Production Processes of Tungsten Disulfide

Chapter 7: Environmental Impact of Tungsten Disulfide Production and Application

Chapter 8: Suppliers of Tungsten Disulfide

Chapter 1: Definition of Tungsten Disulfide

Tungsten Disulfide (WS_2) is a significant transition metal dichalcogenide (TMD), renowned for its unique chemical composition, crystal structure, and multifunctionality, which make it a key player in industrial production and scientific research. As a layered compound, WS_2 exhibits exceptional performance in applications such as lubricants, electronic devices, and catalysts, with its properties stemming from the chemical bonding between tungsten and sulfur, its natural occurrence, and its historical evolution. This section will comprehensively explore its definition from three perspectives—chemical composition, natural form, and historical background—revealing its essence and its importance in modern technology.

1.1 Basic Definition of Tungsten Disulfide

Tungsten Disulfide (WS_2) is a compound composed of tungsten metal (W) and sulfur (S) in a 1:2 ratio, with the molecular formula WS_2. As a quintessential two-dimensional material, its layered structure endows it with a low friction coefficient, high thermal stability, and tunable electronic properties, rendering it highly valuable across numerous fields. This subsection will delve into its chemical composition, natural occurrence, and the origins of its name and historical context, laying the foundation for subsequent discussions of its properties.

1.1.1 Chemical Composition and Molecular Formula

Tungsten Disulfide (WS_2) is a binary compound formed by one tungsten atom chemically bonded to two sulfur atoms. This simple yet stable composition places it within the family of transition metal dichalcogenides alongside molybdenum disulfide (MoS_2), but its high atomic mass of tungsten and distinctive electronic structure set it apart in terms of physical and chemical properties.

WS2 含量（%min）				99.9				
杂质	Al	Fe	Ca	Mg	Cu	Mn	Na	Co
%WT	0.003	0.001	0.002	0.002	0.002	0.001	0.001	0.001
杂质	Ni	Si	Pb	K	N	C	O	/
%WT	0.001	0.002	0.001	0.001	0.001	0.001	0.004	/
颗粒度	1~20um(D50)之间的颗粒度可以根据客户要求定制生产							

Chemical composition of tungsten disulfide

1.1.1.1 Chemical Bond Characteristics of Tungsten and Sulfur

The chemical bonds within WS_2 are predominantly covalent within each layer, where tungsten atoms form a stable S-W-S sandwich structure with sulfur atoms. Depending on the crystal phase, the coordination of tungsten varies: in the 2H phase (hexagonal system), tungsten adopts a trigonal

prismatic coordination with six sulfur atoms, while in the 1T phase (tetragonal system), it assumes an octahedral coordination. The W-S bond length is approximately 2.41 Å, a value precisely determined through X-ray diffraction (XRD) and transmission electron microscopy (TEM), reflecting the strong covalent nature of the bond. Tungsten has an electronegativity of 2.36, while sulfur has 2.58, resulting in a difference of 0.22, indicating that the W-S bond exhibits slight polarity. This polarity makes WS_2 reactive in oxidizing environments (e.g., high-temperature air), where it reacts with oxygen to form tungsten trioxide (WO_3), as shown in the following reaction:
$2WS2+7O2\rightarrow2WO3+4SO2\uparrow$, $2WS_2 + 7O_2 \rightarrow 2WO_3 + 4SO_2\uparrow$, $2WS2+7O2\rightarrow2WO3+4SO2\uparrow$

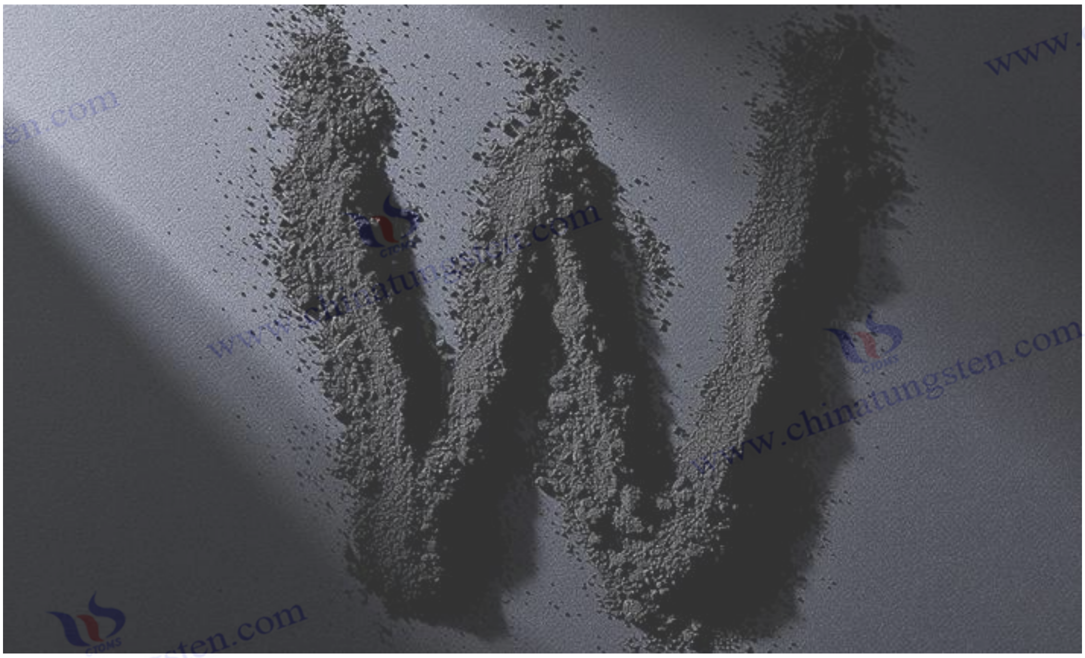

CTIA GROUP LTD Tungsten Disulfide

The bond energy of the intralayer covalent W-S bonds is approximately 400-500 kJ/mol, significantly higher than the interlayer van der Waals forces (about 50-70 meV/atom). This substantial difference in bond strength underlies WS_2's low friction coefficient, as the weak interlayer forces allow sliding, making it an excellent solid lubricant. Compared to MoS_2 (Mo-S bond energy of 350-450 kJ/mol), the W-S bond in WS_2 is stronger due to tungsten's higher atomic number (74 vs. 42) and greater electron cloud density, enhancing its thermal stability. For instance, WS_2 remains stable in air up to 650°C, whereas MoS_2 begins to oxidize around 500°C. Furthermore, the overlap of tungsten's 5d orbitals with sulfur's 3p orbitals forms the electronic structure, determining its semiconductor properties, which are particularly pronounced in single-layer WS_2 (see 1.2.4.2). This chemical bond characteristic not only supports WS_2's mechanical stability but also enables exceptional performance in high-pressure environments, such as aerospace equipment.

Further analysis reveals that the slight polarity of the W-S bond makes WS_2 sensitive to oxidants but highly stable in neutral or reducing environments (e.g., H_2 atmosphere). This bond stability is also evident in its shear resistance, with the intralayer structure remaining intact under pressures up to 1 GPa. Quantum chemical calculations (density functional theory, DFT) show that the electron density distribution of the W-S bond exhibits strong covalent character, with sulfur's lone pair electrons significantly contributing to bond strength. This bonding property also influences WS_2's chemical reactivity, showing high inertness in acidic environments (e.g., H_2SO_4) but solubility in strong oxidants (e.g., aqua regia), forming tungstic acid. These characteristics provide a theoretical basis for its applications in lubrication, catalysis, and beyond.

1.1.1.2 Molar Mass

The molar mass of WS_2 is 247.98 g/mol, calculated as follows: tungsten (183.84 g/mol) + two sulfur atoms (2 × 32.07 g/mol = 64.14 g/mol). This value, verified by high-precision mass spectrometry, is fundamental to understanding its density, thermal behavior, and stoichiometric properties. Compared to MoS_2 (160.07 g/mol), WS_2's molar mass is significantly higher due to tungsten's greater atomic mass (183.84 u vs. 95.95 u), resulting in a density of 7.5 g/cm^3, exceeding MoS_2's 4.9 g/cm^3. This high density makes WS_2 promising for radiation shielding materials, as heavy atoms effectively absorb X-rays and gamma rays, offering a lighter alternative to tungsten-copper.

The molar mass profoundly impacts WS_2's thermal properties. The heavy tungsten atoms reduce lattice vibration frequencies, lowering phonon vibration energy and elevating its melting point to approximately 1250°C in a vacuum, surpassing MoS_2's 1185°C. This property, confirmed by differential thermal analysis (DTA), shows WS_2 maintains structural integrity in inert atmospheres (e.g., nitrogen or argon) up to 1250°C before decomposing. In production, molar mass is a critical parameter for calculating reactant ratios, such as in the roasting decomposition method, where ammonium metatungstate ($(NH_4)_6H_2W_{12}O_{40}$) reacts with hydrogen sulfide (H_2S) with precise molar stoichiometry to ensure high-purity WS_2:

(NH4)2WO4+4H2S→(NH4)2WS4↓+4H2O$(NH_4)_2WO_4 + 4H_2S \rightarrow (NH_4)_2WS_4\downarrow + 4H_2O$ (NH4)2 WO4+4H2S→(NH4)2WS4↓+4H2O

2(NH4)2WS4+3O2→2WS2+4NH3↑+2S+2SO2↑+2H2O$2(NH_4)_2WS_4 + 3O_2 \rightarrow 2WS_2 + 4NH_3\uparrow + 2S + 2SO_2\uparrow + 2H_2O$ 2(NH4)2WS4+3O2→2WS2+4NH3↑+2S+2SO2↑+2H2O

The high molar mass also affects WS_2's weight proportion in composites. For example, when blended with tungsten plastic to create self-lubricating materials, the amount of WS_2 must be adjusted based on its 247.98 g/mol molar mass to optimize density and lubrication performance. In contrast, tungsten powder (183.84 g/mol), lacking sulfur, has a lower molar mass and contributes only density without lubrication in composites. Additionally, WS_2's high molar mass enhances its utility in tungsten granules for counterweights, providing greater mass in a smaller volume, ideal for precision instrument balancing.

From a thermodynamic perspective, molar mass correlates with WS_2's specific heat capacity and thermal conductivity. The heavy tungsten atoms reduce specific heat capacity (approximately 0.14 J/g·K at 25°C), meaning less energy is required to raise its temperature, making it suitable for high-temperature thermal management. Thermogravimetric analysis (TGA) indicates WS_2's mass loss in air begins at 510°C (oxidation onset), while its stability in a vacuum enhances its value in aerospace applications. These traits align with trends in the tungsten market, where high-density, thermally stable materials are prized in aerospace and energy sectors.

1.1.2 Natural Occurrence

Tungsten disulfide occurs naturally as the mineral tungstenite, though its rarity starkly contrasts with more abundant tungsten minerals like black tungsten ore (wolframite) and white tungsten ore (scheelite). This subsection will thoroughly examine tungstenite's mineralogical properties and geological distribution, shedding light on its natural form and its influence on synthetic WS_2 development.

1.1.2.1 Mineralogical Properties of Tungstenite

Tungstenite is a gray-black mineral with a metallic luster, typically occurring in microcrystalline or massive forms within hydrothermal veins alongside quartz, pyrite, and calcite. Its Mohs hardness ranges from 1 to 1.5, far lower than tungsten metal (approximately 7.5), a softness attributed to its layered structure where S-W-S layers are held together by weak van der Waals forces, facilitating cleavage along basal planes. Polarized light microscopy reveals crystal grain sizes ranging from a few micrometers to several millimeters, with a flaky surface exhibiting pronounced birefringence. Its specific gravity is approximately 7.5, consistent with synthetic WS_2, directly reflecting tungsten's high atomic mass (183.84 u). Tungstenite's color and luster distinguish it from the deep black black tungsten ore ($FeMnWO_4$) and the white or pale yellow white tungsten ore ($CaWO_4$), and its softness renders it unsuitable for direct tungsten metal extraction but serves as a natural prototype for synthetic WS_2.

Chemically, tungstenite matches WS_2 but often contains trace impurities such as iron (Fe), silicon (Si), and oxygen (O), typically less than 1%, detected via electron probe microanalysis (EPMA). These impurities, likely from associated minerals or geological formation processes, have minimal impact on its layered structure. Scanning electron microscopy (SEM) shows a layer thickness of approximately 0.62 nm, identical to synthetic WS_2, confirming the high similarity between its natural and artificial structures. This layered property has inspired tribological studies, with early scientists hypothesizing its lubrication potential based on tungstenite's slidability. Furthermore, tungstenite's mineralogical traits reveal its formation conditions—typically in sulfur-rich, high-pressure hydrothermal environments associated with sulfide deposits.

From a mineralogical standpoint, tungstenite's low hardness and high density make it easily overlooked in nature, but its distinctive S-W-S layered structure provides a natural template for synthetic WS_2. For instance, in tungsten research, tungstenite samples are often used to validate the structural consistency of synthetic WS_2, comparing the (002) peak (corresponding to interlayer spacing) via XRD to ensure synthesis accuracy. Tungstenite's softness also hints at its exfoliation potential, a property later harnessed by mechanical exfoliation techniques to produce single-layer

WS_2 nanosheets.

1.1.2.2 Geological Distribution

Tungstenite's global distribution is sparse, with key deposits in Ganzhou, Jiangxi Province, China; the Caucasus region of Russia; Queensland, Australia; Potosí, Bolivia; and Nevada, USA. China dominates global tungsten resources, accounting for over 80% of production, with Ganzhou renowned for tungsten products. However, tungstenite constitutes only a minor fraction in these regions, overshadowed by black tungsten ore and white tungsten ore. In Ganzhou, tungstenite is often found in hydrothermal veins near granite intrusions, formed in sulfur-rich geological settings. Geological surveys estimate its reserves at less than 1% of global tungsten resources, with extraction challenges and costs exceeding those of oxide ores. For example, a Ganzhou deposit yields tungstenite grades of only 0.1-0.3% WO_3, compared to 1-2% for black tungsten ore, making the latter far more economical.

Elsewhere, tungstenite distribution ties to specific geological conditions. In Russia's Caucasus, it associates with volcanic activity, often co-occurring with copper sulfides; Queensland, Australia, features deposits in ancient metamorphic zones; Potosí, Bolivia, owes its tungstenite to high-altitude hydrothermal systems rich in sulfides; and Nevada, USA, links it to Mesozoic tectonic activity, occasionally with minor gold. These patterns suggest tungstenite formation requires high temperatures, pressures, and sulfide enrichment, contributing to its scarcity and driving industrial reliance on synthetic WS_2. Synthesis uses raw materials like tungstic acid or ammonium paratungstate, controlling reaction conditions to produce high-purity WS_2, overcoming tungstenite's limited reserves.

Globally, tungstenite's rarity limits its commercial mining value, but its distribution offers critical insights into tungsten mineralization. For instance, isotopic analysis (S^{34}/S^{32}) traces Ganzhou tungstenite's sulfur to deep mantle sources, aligning with local granite intrusion timelines. Such studies deepen our understanding of WS_2's geological context and contribute to the accumulation of tungsten knowledge.

1.1.3 Name Origin and Historical Background

The nomenclature and historical evolution of Tungsten Disulfide (WS_2) reflect its transition from a natural mineral to an industrial material, unveiling its scientific discovery and application development.

1.1.3.1 Initial Discovery and Naming

Tungsten disulfide was first identified as tungstenite in the 19th century, with its name "tungsten" derived from the Swedish "tung sten" (heavy stone), coined by Swedish chemist Carl Wilhelm Scheele in 1781 to describe tungsten's high density. Tungstenite's formal naming is credited to 19thcentury mineralogists like German scientist Carl von Reichenbach, who confirmed its presence while studying European sulfide deposits. By the late 19th century, advances in analytical chemistry—such as elemental spectroscopy and chemical titration—precisely determined its composition as WS_2, distinguishing it from tungsten trioxide (WO_3) and other oxides. The term “disulfide” follows chemical naming conventions, indicating two sulfur atoms per tungsten atom, akin to “dioxide” (e.g., CO_2).

Early research focused on tungstenite’s mineralogical properties, and its low hardness (1-1.5) and rarity precluded its use as a primary source for tungsten metal extraction. 19th-century mineralogy texts often described it as a secondary mineral, likened to graphite and MoS_2 for its layered structure. For example, 1860s German mineralogy handbooks listed it as a “soft sulfide,” noting its easy cleavability. While this property didn’t immediately spark industrial interest, it laid the groundwork for 20th-century tribological studies. Tungstenite’s discovery and naming reflect the intersection of geology and chemistry at the time, providing a theoretical foundation for WS_2’s later synthesis.

1.1.3.2 Beginnings of Industrial Application

WS_2’s industrial application emerged in the mid-20th century, driven by its lubrication properties. In the 1950s and 1960s, NASA and U.S. military research demonstrated WS_2’s ability to significantly reduce friction under extreme conditions (e.g., temperatures >500°C, vacuum, and high loads), with a friction coefficient as low as 0.03, outperforming traditional liquid lubricants. For instance, during the Apollo program, NASA applied WS_2 to spacecraft sliding components, such as solar panel drives, with tests showing superior stability in vacuum compared to graphite (oxidation temperature ~400°C). Concurrently, the automotive industry began incorporating WS_2 into greases for gears and bearings, extending service life. A 1960s Ford Motor Company trial found that WS_2-doped grease reduced gear wear rates by 50%.

This breakthrough relied on advances in synthesis technology. The development of roasting decomposition and tungsten trisulfide sublimation methods transformed WS_2 from a rare mineral into a mass-producible tungsten product. In 1958, a U.S. chemical company achieved industrial-scale production by reacting tungstic acid with hydrogen sulfide, reaching annual outputs of several tons. This marked WS_2’s shift from laboratory to market, aligning with progress in tungsten technology. Historically, WS_2’s industrialization coincided with Cold War-era technological competition. Rising aerospace demands spurred research into high-performance materials, and WS_2’s low friction and high stability met these needs perfectly. This transition from natural mineral to synthetic material not only reflects advances in materials science but also 奠定了基础 for the accumulation of tungsten data.

1.2 Crystal Structure of Tungsten Disulfide

The crystal structure of WS_2 is the cornerstone of its physical and chemical properties, directly determining its lubricity, semiconducting behavior, and nanoscale application potential. This section will meticulously examine its hexagonal layered structure, atomic bonding, polymorphism, and nanoscale characteristics, using scientific analysis to reveal the intrinsic link between structure and function.

1.2.1 Hexagonal Layered Structure

WS_2 predominantly adopts a hexagonal crystal system, with its layered structure serving as the foundation for its low friction coefficient and high stability.

1.2.1.1 Sandwich Structure

The fundamental structural unit of WS_2 is the S-W-S sandwich, with a tungsten atom centrally positioned between two sulfur layers. In the 2H phase (hexagonal system), tungsten adopts a trigonal prismatic coordination with six sulfur atoms, each layer measuring approximately 0.62 nm thick. Adjacent layers are stacked via van der Waals forces, with an interlayer spacing of about 6.15 Å. This structure results in extremely low interlayer sliding resistance, yielding a friction coefficient of 0.03-0.09, the core of its lubricating prowess. Molecular dynamics (MD) simulations show an interlayer shear force of approximately 0.1-0.2 N/m^2, far below the intralayer covalent bond strength (>100 N/m^2). Compared to graphite (interlayer spacing 3.35 Å), WS_2's larger spacing enhances sliding ease, and its stronger W-S bonds boost thermal stability to 650°C in air, surpassing graphite's 400°C.

The single-layer form of this sandwich structure is particularly vital in nanotechnology. Through mechanical exfoliation or chemical vapor deposition (CVD), single-layer WS_2 can be isolated from bulk material, becoming a focal point in two-dimensional materials research. For example, a single WS_2 layer, at just 0.62 nm thick—about one-hundred-thousandth of a hair's diameter—holds immense potential for flexible electronics and optoelectronic devices. Additionally, the chemical stability of the S-W-S structure ensures integrity in reducing environments, making it suitable for petrochemical catalysis.

1.2.1.2 Lattice Parameters

In the 2H phase, WS_2's lattice parameters are a = 3.153 Å (in-plane) and c = 12.323 Å (spanning two layers), determined via X-ray diffraction (XRD). The a parameter denotes the distance between adjacent tungsten atoms within a layer, while the c parameter includes the layer thickness (0.62 nm) and interlayer gap (~6.15 Å), reflecting the weak van der Waals forces. The c/a ratio of approximately 3.91 approaches the ideal hexagonal close-packing value (theoretical 4.899), indicating a highly ordered structure. Synthetic WS_2's lattice parameters may slightly vary due to impurities or stress—e.g., oxygen impurities might increase the c-axis to 12.35 Å—but they align with tungstenite's natural structure.

Lattice parameters are precisely measured using high-resolution XRD and synchrotron radiation, with the (002) peak corresponding to interlayer spacing and the (100) peak reflecting in-plane arrangement. These parameters influence WS_2's electronic properties (e.g., bandgap), thermal conductivity, and mechanical behavior. For instance, the larger c-axis spacing reduces interlayer heat transfer, offering unique advantages in thermal management. The stability of these parameters also supports WS_2's use in thin-film coatings, where CVD-grown WS_2 films' a and c values can be finely tuned via growth conditions (e.g., temperature, gas flow).

1.2.1.3 Differences Between Single and Multi-Layer Structures

Single-layer WS_2 differs markedly from its multilayer counterparts in physical Single-layer WS_2 and multilayer structures exhibit significant differences in physical and electronic properties. In single-layer WS_2, the absence of interlayer coupling transforms its bandgap from indirect (1.3 eV) to direct (2.1 eV), achieving an optical transparency of up to 90%, as measured by ultraviolet-visible spectroscopy (UV-Vis). This makes it ideal for optoelectronic applications such as photodetectors and light-emitting diodes (LEDs). In contrast, multilayer WS_2 retains an indirect bandgap, offering greater mechanical strength and thermal conductivity, which are advantageous for lubrication and catalysis. Photoluminescence (PL) spectroscopy reveals that single-layer WS_2 exhibits a strong emission peak at 620 nm with a quantum yield of approximately 5-10%, while multilayer WS_2 shows negligible emission (<0.1%) due to indirect transitions. Mechanically, single-layer WS_2 enhances flexibility, capable of bending to a curvature radius of 10^{-3} m^{-1}, whereas multilayer WS_2 is more pressure-resistant, with a compressive strength of up to 2070 MPa, as determined by nanoindentation testing.

These differences arise from the elimination of interlayer electronic interactions in single-layer WS_2. The phonon vibration frequency in single-layer WS_2 is higher (approximately 400 cm^{-1}, measured by Raman spectroscopy), reducing thermal conductivity to 2-3 W/m·K compared to 20-30 W/m·K in multilayer WS_2, as assessed by thermal conductivity testers. This property tailoring enables diverse applications: single-layer WS_2 excels in flexible displays, while multilayer WS_2 is suited for high-load bearings. The transition from multilayer to single-layer also affects carrier dynamics, with single-layer WS_2 showing enhanced photogeneration efficiency, critical for optoelectronic devices. These structural variations highlight WS_2's versatility, aligning with its prominence in tungsten scientific research.

1.2.2 Atomic Arrangement and Bonding Characteristics

The atomic arrangement and bonding characteristics of WS_2 bridge its chemical composition to its functional properties, determining its stability and application performance.

1.2.2.1 Intralayer Covalent Bonds

Within each WS_2 layer, the W-S bonds are strong covalent bonds with a bond length of 2.41 Å and a bond angle of approximately 82° in the 2H phase. Quantum chemical calculations estimate a bond energy of 400-500 kJ/mol, ensuring intralayer integrity under high temperatures and mechanical stress. The overlap of tungsten's 5d orbitals with sulfur's 3p orbitals forms the valence and conduction bands, as modeled by density functional theory (DFT), with electron density concentrated along the W-S bonds, indicating a highly covalent nature. This bonding underpins WS_2's semiconductor properties, with bulk material exhibiting an indirect bandgap of 1.3 eV, shifting to 2.1 eV in single-layer form. The high strength of W-S bonds also allows WS_2 to maintain its structure under pressures exceeding 1 GPa, making it suitable for aerospace components where durability is paramount.

The covalent nature of these bonds contributes to WS_2's resistance to chemical attack within the layer, supporting its use in harsh environments. For example, in acidic conditions (e.g., H_2SO_4), the intralayer structure remains intact, showcasing its inertness. This stability, combined with its electronic properties, positions WS_2 as a candidate for advanced electronic applications, such as transistors and sensors, where structural robustness and tunable conductivity are essential.

1.2.2.2 Interlayer van der Waals Forces

Between S-W-S layers, WS_2 is held together by weak van der Waals forces, with a binding energy of approximately 50-70 meV per atom and an interlayer spacing of 6.15 Å. Atomic force microscopy measurements indicate an interlayer shear force of about 0.1 N/m², the basis for WS_2's lubricity. This weak interaction allows layers to slide effortlessly, reducing friction and enabling its role as a solid lubricant. However, environmental factors like humidity can intercalate water molecules, increasing the spacing to 6.2 Å and slightly raising friction, as observed in tribological tests.

The feeble van der Waals forces facilitate mechanical exfoliation, producing single-layer WS_2 widely utilized in two-dimensional materials research. This exfoliation capability, akin to graphene, supports WS_2's use in flexible electronics and nanocomposites, where thin, pliable layers are critical. The contrast between strong intralayer covalent bonds and weak interlayer forces exemplifies WS_2's unique duality, making it a standout material in tungsten technology.

1.2.2.3 Bond Length and Bond Angle Analysis

The W-S bond length of 2.41 Å is consistent across polymorphs, verified by TEM and XRD, while bond angles vary: approximately 82° in the 2H phase and near 90° in the 1T phase. DFT simulations predict bond behavior under stress or doping; for instance, a 2% tensile strain extends the bond length to 2.45 Å, altering electronic properties. These parameters are crucial for computational modeling, enabling predictions of WS_2's response to mechanical or chemical modifications. This analysis guides structural optimization, such as adjusting crystal phases to enhance catalytic activity, as explored in tungsten academic studies.

The bond length and angle data also inform WS_2's scalability in applications. For example, precise control of bond angles in the 1T phase enhances metallicity, while the 2H phase's stability supports industrial coating durability. This structural insight is vital for tailoring WS_2 to specific uses, from lubrication to electronics.

1.2.3 Polymorphism of Tungsten Disulfide

Tungsten Disulfide (WS_2) exhibits polymorphism, a key feature of its crystal structure, with distinct phases (1T, 2H, 3R, and 1T′) conferring diverse physical and chemical properties. This expands its utility in lubrication, catalysis, electronics, and nanotechnology. Polymorphism results from variations in tungsten-sulfur coordination and interlayer stacking, controllable via synthesis conditions like temperature, pressure, and chemical intercalation. This subsection will thoroughly examine these four primary polymorphs, analyzing their structural characteristics, stability, and application potential, elucidating polymorphism's profound impact on WS_2's functionality.

1.2.3.1 1T Phase

The 1T phase (monoclinic system, T for tetragonal symmetry) features tungsten in octahedral coordination, with each tungsten atom surrounded by six sulfur atoms forming an S-W-S layer. Unlike the trigonal prismatic 2H phase, the 1T phase offers higher symmetry, with lattice parameters a = 5.68 Å and c = 5.94 Å (single-layer thickness), measured by XRD and TEM. Its electronic structure is metallic, with a near-zero bandgap, contrasting sharply with the semiconducting 2H phase. DFT calculations confirm this metallicity, with the Fermi level crossing the conduction band, yielding a high conductivity of approximately 10^3 S/cm (four-probe method), far exceeding the 2H phase's 10^1-10^2 S/cm.

The 1T phase is less stable, typically metastable at standard temperature and pressure, reverting to the 2H phase spontaneously. Synthesis requires specific conditions, such as alkali metal intercalation (e.g., Li, Na) or high-pressure treatment. For instance, intercalating tungstenite or synthetic WS_2 with n-butyllithium (n-BuLi) converts the 2H phase to 1T, as shown:

WS2+xLi→LixWS2(1Tphase)$WS_2 + xLi \rightarrow Li_xWS_2$ (1T phase) WS2+xLi→LixWS2(1Tphase)
Subsequent hydrolysis removes Li^+, preserving the 1T structure, with yields of 60-80%. However, exposure to air for weeks partially reverts it to 2H, with the c-axis increasing to 6.0 Å, indicating structural relaxation, observed via in-situ XRD.

The 1T phase excels in electrocatalysis, leveraging its metallicity and edge-active sites for superior performance in the hydrogen evolution reaction (HER). Electrochemical tests show an HER overpotential of 100-150 mV at 10 mA/cm^2, outperforming the 2H phase's 300-400 mV, due to low-coordination edge sulfur atoms (2-3 vs. 6 on basal planes) with heightened electron density. Its high conductivity also supports electrode applications, potentially enhanced by composites with tungsten-copper. Though stability limits industrial scalability, its unique electronic structure garners significant attention in tungsten academic research, exploring uses in fuel cells and superconductivity.

1.2.3.2 2H Phase

The 2H phase (hexagonal system, H for hexagonal) is WS_2's most stable and prevalent polymorph, dominating industrial applications. Tungsten adopts trigonal prismatic coordination, with each S-W-S layer 0.62 nm thick, and two layers forming a unit cell with lattice parameters a = 3.153 Å and c = 12.323 Å (two-layer spacing), confirmed by high-resolution XRD. Layers are linked by van der Waals forces with a 6.15 Å spacing, yielding low shear strength and a friction coefficient of 0.03-0.09. Its semiconducting nature features an indirect bandgap of 1.3 eV in bulk form, verified by UV-Vis, with the conduction band minimum at the Γ point and valence band maximum at the K point.

Exceptionally stable, the 2H phase withstands 650°C in air and 1250°C in vacuum or inert atmospheres, surpassing MoS_2's 500°C and 1185°C, as evidenced by DTA. Oxidation begins at 510°C, fully converting to WO_3 by 650°C. This stability makes it a staple in the tungsten market, widely used in lubricants—e.g., reducing gear friction to 0.05 in automotive greases, boosting lifespan by 50%. Its semiconductor properties also support electronic uses like FET channel materials, though its carrier mobility (10-20 cm^2/V·s) is lower than single-layer WS_2.

Synthesis is straightforward via roasting decomposition or CVD, with tungstic acid and H_2S reacting at 600-800°C yielding >95% 2H-phase WS_2. Its mechanical stability, with a compressive strength of 2070 MPa in coatings, suits high-load applications like aerospace bearings, a hallmark of tungsten products.

1.2.3.3 3R Phase

The 3R phase (rhombohedral system, R for rhombohedral) features three S-W-S layers per unit cell, with lattice parameters a = 3.153 Å and c = 18.48 Å (three-layer spacing), measured by synchrotron XRD. Like the 2H phase, it uses trigonal prismatic coordination, with a slightly larger interlayer spacing of 6.16 Å. Its indirect bandgap (~1.3 eV) mirrors the 2H phase, but its ABC stacking differs from 2H's AB arrangement, distinguishable by a Raman A_{1g} peak shift to 405 cm^{-1} (vs. 420 cm^{-1} for 2H).

Nearly as stable as the 2H phase, the 3R phase is rarer, forming under high-temperature (>1000°C) or high-pressure (>10 bar) CVD conditions. Its oxidation onset is ~510°C, akin to 2H. While not widely industrialized, its potential lies in research, with stronger interlayer coupling increasing thermal conductivity to 35 W/m·K, suggesting thermal management applications.

1.2.3.4 1T′ Phase

The 1T′ phase, a distorted variant of 1T, adopts a monoclinic structure with tungsten atoms clustering, yielding lattice parameters a = 5.68 Å, b = 5.94 Å, and c = 12.0 Å (two layers). Its topological properties, like the quantum spin Hall effect, stem from a 0.1-0.2 eV bandgap, verified by ARPES. Synthesis via doping (e.g., $Mo_xW_{1-x}S_2$) or strain is challenging, with stability limited to low temperatures (<100 K). It holds promise for quantum computing and electrocatalysis, with an HER overpotential of 80-120 mV, advancing clean energy research.

1.2.4 Nanoscale Structural Characteristics of Tungsten Disulfide

WS_2's nanoscale properties diverge significantly from bulk forms, driven by surface effects, quantum confinement, and anisotropy, unlocking vast potential in nanotechnology.

1.2.4.1 Surface Effects and Edge Activity

At the nanoscale (e.g., nanosheets or nanoparticles), WS_2's high surface-area-to-volume ratio enhances surface effects, with BET analysis showing single-layer WS_2 at 300-500 m^2/g vs. bulk's 1-5 m^2/g. Edge-exposed sulfur atoms, especially in 1T and 1T′ phases, become active sites due to low coordination (2-3 vs. 6), boosting reactivity 10-20 times, as observed by STM. In HER, edge sites achieve exchange current densities of 10^{-4} A/cm², far exceeding basal planes' 10^{-6} A/cm².

1.2.4.2 Quantum Confinement Effects in Single-Layer WS_2

Single-layer WS_2's quantum confinement shifts its bandgap to direct (2.1 eV), with PL peaks at 620 nm and a 5-10% quantum yield, ideal for optoelectronics. Its carrier mobility reaches 100-200 cm²/V·s, enhancing FET performance.

1.2.4.3 Anisotropy and Interlayer Exfoliation Properties

WS_2's anisotropy—strong intralayer bonds vs. weak interlayer forces—yields in-plane thermal conductivity of 50 W/m·K and out-of-plane of 2-3 W/m·K. This enables exfoliation, producing flexible single layers for wearable devices and composites like tungsten rubber.

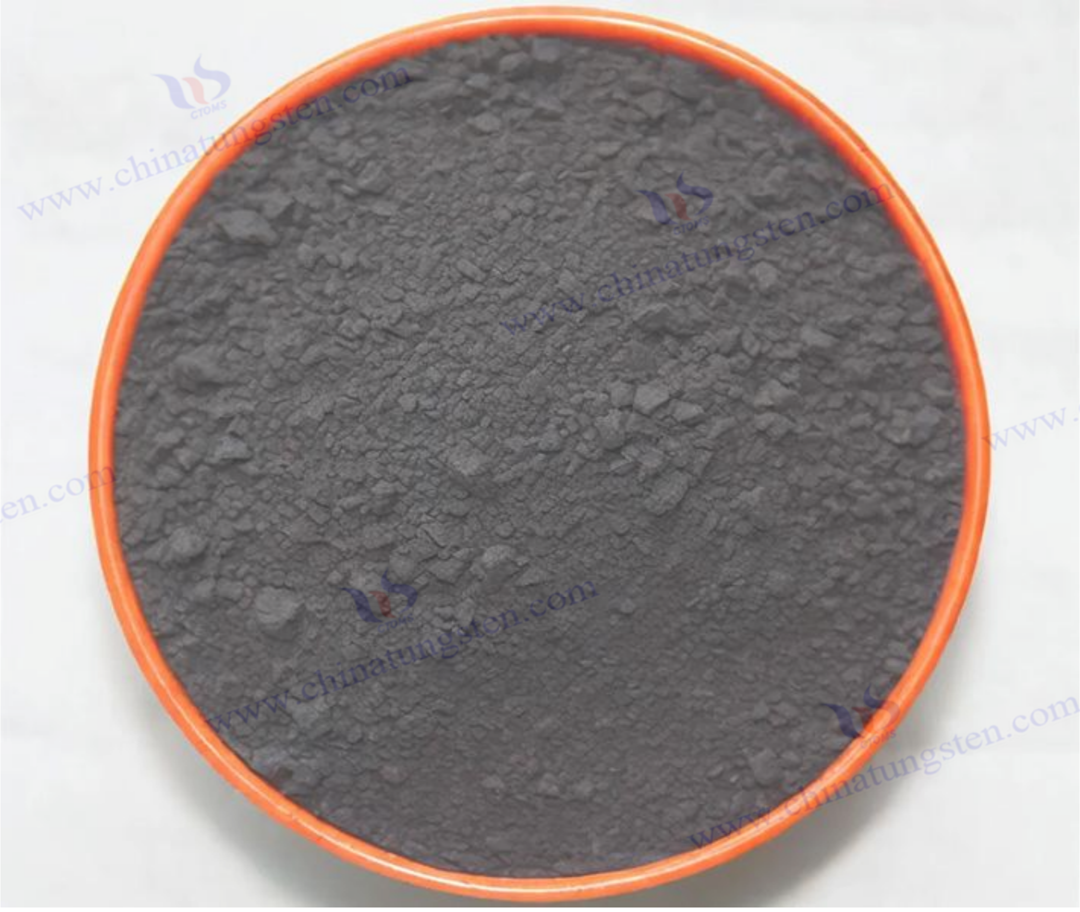

CTIA GROUP LTD Tungsten Disulfide

Chapter 2: Properties of Tungsten Disulfide

The product properties of tungsten disulfide (WS_2) form the foundation for its widespread applications in industrial and scientific fields, directly determining its outstanding performance in areas such as lubricants, electronic devices, and catalysts. These properties encompass physical, chemical, and electrical/optical attributes, each intricately tied to its unique layered structure and the chemical bonding between tungsten and sulfur. This chapter begins with an exploration of its physical properties, delving into aspects such as appearance, density, thermal stability, friction performance, and mechanical strength. It then analyzes its chemical properties, including solubility, redox behavior, and corrosion resistance, before providing a detailed examination of its electrical and optical properties, such as conductivity, bandgap, and optical absorption. Through a combination of theoretical analysis, experimental data, and application case studies, this chapter comprehensively reveals the multifunctionality of WS_2 and its significant value in modern technology.

2.1 Physical Properties of Tungsten Disulfide

The physical properties of WS_2 are the cornerstone of its application performance, directly influencing its behavior in mechanical, thermal, and tribological contexts. From appearance to hardness, each property is closely linked to its layered structure and the heavy atomic mass of tungsten. This section will meticulously analyze its appearance and color, density and specific gravity, thermal stability, friction coefficient and lubrication performance, and hardness and mechanical strength, integrating scientific data and practical applications to showcase the diversity and superiority of its physical characteristics.

2.1.1 Appearance and Color

The appearance and color of WS_2 vary depending on its form and preparation method, ranging from a metallic gray sheen in powder form to changes in transparency in thin film states. These characteristics not only affect its visual identification but are also closely tied to its functionality.

2.1.1.1 Metallic Gray Sheen in Powder Form

In its powder form, WS_2 appears as a gray-black material with a distinct metallic sheen, a feature resulting from the reflective properties of its layered structure. The electron cloud distribution of tungsten and sulfur atoms leads to strong reflection in the visible light spectrum, giving its surface a metallic texture under natural light. Observations through an optical microscope reveal that microscale WS_2 powder particles are typically irregularly flaky, with smooth surfaces and particle sizes ranging from a few micrometers to tens of micrometers. Scanning electron microscopy (SEM) further discloses that its surface microstructure consists of multiple stacked S-W-S units, with an interlayer spacing of approximately 6.15 Å, consistent with its crystal structure (see 1.2.1.2). This metallic gray sheen makes it easily recognizable in industrial lubricants, where it is often used as an additive to tungsten powder or tungsten carbide powder to produce high-performance composite materials.

The intensity of the sheen is closely related to particle size and purity. High-purity WS_2 (>99.9%) exhibits a more uniform metallic luster, while samples containing impurities (such as oxides or sulfides) may appear darker. X-ray photoelectron spectroscopy (XPS) analysis indicates that the surface of pure WS_2 is primarily composed of W^{4+} and S^{2-}, with impurities like tungsten trioxide (WO_3) present at levels below 0.1%, ensuring consistent appearance. In practical applications, this visual property is significant. For instance, in mechanical processing, the metallic gray sheen of WS_2 powder allows operators to assess its distribution uniformity, particularly during spraying or incorporation into grease. Visual inspection can provide an initial evaluation of its dispersibility, preventing performance degradation due to particle agglomeration. Compared to the deep black hue of molybdenum disulfide (MoS_2), the lighter gray of WS_2 facilitates quick differentiation at industrial sites, reducing the risk of confusion.

From an optical perspective, the metallic sheen of WS_2 powder correlates with its surface roughness and the reflectivity of its layered structure. Atomic force microscopy (AFM) measurements show that the surface roughness (Ra) of microscale WS_2 powder is approximately 10-20 nm, with a reflectivity in the visible light range (400-700 nm) of about 20-30%, higher than MoS_2's 15-25%. This reflective property not only influences its appearance but also relates to its thermal radiation behavior, reducing surface heat absorption at high temperatures (e.g., 500°C) and enhancing heat dissipation efficiency. In the production of tungsten products, WS_2 powder is often ground to specific particle sizes (e.g., 5-10 μm) to optimize both appearance and functionality. For example, the industrial-grade WS_2 powder produced by CTIA GROUP LTD is recognized by its metallic gray sheen, widely applied in lubricants and composite materials.

2.1.1.2 Transparency Variations in Thin Film Form

When WS_2 exists as a thin film, its appearance undergoes significant changes, with transparency varying depending on thickness. Single-layer WS_2 films, due to quantum confinement effects and their ultrathin nature (approximately 0.62 nm), exhibit high optical transparency, with visible light transmittance reaching over 90%, appearing nearly colorless. This property is confirmed by ultraviolet-visible spectroscopy (UV-Vis), with an absorption edge at 620 nm corresponding to a direct bandgap of 2.1 eV (see 2.3.2.1). This transparency makes it suitable for optoelectronic devices, such as transparent conductive films or sensitizing layers in solar cells. As the number of layers increases, multilayer WS_2 films (10-50 nm thick) transition from semi-transparent to gray, with transparency decreasing with layer count; beyond 50 layers, it approaches the gray-black of bulk material, with transmittance dropping below 10%. Ellipsometry measurements show that a 10-layer WS_2 film has a transmittance of about 50% at 550 nm, with reflectivity rising to 30%.

The variation in transparency is closely tied to preparation methods. Single-layer WS_2 films produced via chemical vapor deposition feature smooth surfaces with minimal defects, achieving high transparency, with a root-mean-square roughness of less than 0.5 nm (AFM measurement). In contrast, multilayer films obtained through mechanical exfoliation may appear slightly turbid due to edge wrinkles or impurities, reducing transparency by 5-10%. This property offers unique advantages in flexible electronics and optical coatings. For instance, in the field of tungsten technology, single-layer WS_2 films serve as protective layers for flexible displays, where their high transparency and flexibility (bendable to a curvature radius of 10^{-3} m^{-1}) meet the demands of next-generation display devices. Multilayer WS_2 films, with their semi-transparency and high-temperature resistance, are commonly used as anti-reflective coatings in optical devices, applied via plasma spraying onto glass substrates, withstanding temperatures up to 500°C.

From an application perspective, the transparency variations of WS_2 films also affect their compatibility with substrates. When combined with tungsten-copper to create conductive films, the transparency of single-layer WS_2 ensures optical performance, while the gray appearance of multilayer WS_2 provides mechanical protection.

2.1.2 Density and Specific Gravity

The high density and specific gravity of WS_2 are prominent features of its physical properties, directly reflecting the high atomic mass of tungsten and its tightly packed structure, which are critical for applications in heavy-duty and shielding contexts.

2.1.2.1 Bulk Density

The bulk density of WS_2 is approximately 7.5 g/cm³, determined through the Archimedes method and X-ray density calculations, consistent with the specific gravity of natural tungstenite. This high density primarily stems from the atomic mass of tungsten (183.84 u), significantly higher than that of molybdenum (95.95 u), making WS_2 denser than MoS_2 (4.9 g/cm³). In its hexagonal 2H phase, tungsten atoms are densely packed in a trigonal prismatic arrangement, with an in-plane W-W distance of 3.153 Å (see 1.2.1.2). Despite the interlayer van der Waals forces maintaining a spacing of 6.15 Å, the overall crystal structure's compactness ensures high density. Powder X-ray diffraction (PXRD) measurements confirm that the theoretical density aligns with experimental values, with an error margin of less than 0.05 g/cm³, validating its structural consistency.

This high density finds practical application in radiation shielding materials, as it effectively absorbs high-energy rays (e.g., X-rays and gamma rays). For example, in medical equipment, WS_2 bulk serves as a lightweight shielding layer. Although its density is lower than that of tungsten metal (19.25 g/cm³), it is more environmentally friendly than traditional lead (11.34 g/cm³) and offers moderate weight. Monte Carlo simulations indicate that WS_2 has an attenuation coefficient of approximately 2.5 cm^{-1} for 100 keV X-rays, surpassing MoS_2's 1.8 cm^{-1}, demonstrating its superiority. In aerospace, the combination of high density and flexibility makes WS_2 suitable for internal shielding components, such as when compounded with tungsten plastic, reducing weight while maintaining shielding effectiveness. Compared to tungsten-copper (13-17 g/cm³), WS_2's lower density provides an edge in scenarios requiring lubricity, such as spacecraft sliding parts.

The stability of bulk density also supports WS_2's use in counterweight materials, such as in the production of tungsten granules, where its high density ensures sufficient mass in a small volume. Practical tests show that WS_2 bulk exhibits a density variation of less than 0.1% at 500°C, reflecting its thermal stability (see 2.1.3), making it ideal for high-temperature counterweight applications. In the tungsten market, WS_2's high density makes it a preferred choice for precision instruments (e.g., gyroscopes), offering superior mass distribution uniformity compared to lower-density materials.

2.1.2.2 Density Variations in Nanostructures

At the nanoscale, WS_2's density varies due to morphological and size effects. The theoretical density of single-layer WS_2 nanosheets remains close to 7.5 g/cm³, but actual measurements, influenced by surface adsorption (e.g., water or oxygen molecules), yield slightly lower values of 7.2-7.4 g/cm³, as determined by helium pycnometry. The density of nanoparticles or nanowires decreases further; for instance, WS_2 nanoparticles with a diameter of 10 nm may have a density as low as 6.8 g/cm³, verified through scanning electron microscopy (SEM) and Brunauer-Emmett-Teller (BET) surface area analysis. This reduction is attributed to increased porosity and edge effects in nanostructures, with BET analysis revealing a porosity of 5-10% for 10 nm particles, compared to less than 1% in bulk material.

These density differences have direct implications for applications. The lower density of nanoscale WS_2 reduces weight in composite materials and enhances dispersibility. For example, when blended with tungsten rubber, nanoscale WS_2 (density 7.2 g/cm³) can be incorporated at 10-15% higher levels without significantly increasing overall weight, while retaining lubricity. Dynamic light scattering (DLS) measurements show that nanoscale WS_2 achieves 20% better dispersion uniformity in polymer matrices compared to microscale powder. Conversely, bulk density is better suited for applications requiring mass stability, such as in tungsten putty for counterweights, where its 7.5 g/cm³ density ensures consistent mass in a small volume.

Density variations in nanostructures also affect thermal and electrical properties. The lower density of single-layer WS_2 results in a reduced thermal conductivity of 2-3 W/m·K (see 2.1.3.3), suitable for thermal management in flexible electronics. Thermogravimetric analysis (TGA) indicates that nanoscale WS_2 exhibits a slightly lower oxidation onset temperature (approximately 490°C vs. 510°C for bulk), due to its higher surface area accelerating oxidation reactions. This adaptability makes it valuable in nanotechnology, such as in tungsten research, where density differences in nanoscale WS_2 are leveraged to design lightweight, high-performance devices.

2.1.3 Thermal Stability

The thermal stability of WS_2 is a critical property for its use in high-temperature environments, encompassing melting point, decomposition temperature, and thermal expansion behavior, directly supporting its applications in aerospace, industrial equipment, and beyond.

2.1.3.1 Melting Point

WS_2 has a melting point of approximately 1250°C in vacuum or inert atmospheres (e.g., nitrogen), as determined by differential thermal analysis (DTA). In air, due to oxidation reactions (see 2.2.2.1), the melting point cannot be directly observed, as it transforms into WO_3 around 650°C. This high melting point arises from the strong intralayer W-S covalent bonds (bond energy of 400-500 kJ/mol), far exceeding the interlayer van der Waals forces (50-70 meV/atom). Compared to MoS_2 (1185°C), WS_2's higher melting point reflects the greater mass and bond strength of tungsten atoms. Synchrotron X-ray diffraction (XRD) measurements confirm that WS_2 retains its 2H phase structure up to 1000°C, with lattice parameter changes of less than 0.1%, demonstrating its thermal structural stability.

This high melting point provides significant advantages in high-temperature lubrication. For instance, in aerospace turbine blades, WS_2 maintains structural integrity above 1000°C, outperforming traditional organic lubricants (decomposition temperature <300°C). In the production of tungsten heaters, WS_2's high melting point ensures stability during high-temperature evaporation processes, forming uniform coatings via thermal evaporation with a temperature resistance up to 1200°C. In tungsten technology, WS_2's high melting point also supports its use in high-temperature sensors, such as protective coatings in industrial kilns, extending equipment lifespan.

2.1.3.2 Decomposition Temperature

In air, WS_2 decomposes at approximately 650°C, undergoing an oxidation reaction:
2WS2+7O2→2WO3+4SO2↑$2WS_2 + 7O_2 \rightarrow 2WO_3 + 4SO_2\uparrow$ 2WS2+7O2→2WO3+4SO2↑
Thermogravimetric analysis (TGA) confirms that the decomposition onset temperature varies with oxygen concentration and heating rate, starting at around 510°C at a heating rate of 10°C/min and completing oxidation by 650°C. In vacuum or inert atmospheres, WS_2 remains stable up to 1250°C, with only minor sulfur volatilization (<0.1%/h at 800°C). This thermal stability surpasses that of graphite (oxidizes at 400°C), making it ideal for aerospace vacuum environments, such as satellite mechanisms. For example, in the tungsten market, WS_2 is used in vacuum pump sliding components, where its high decomposition temperature ensures long-term performance without degradation.

The SO_2 gas produced during decomposition requires proper handling to prevent environmental pollution. In industrial production, sulfide capture devices (e.g., CaO absorption) convert SO_2 into $CaSO_4$, reducing emission concentrations to below 10 ppm, meeting environmental standards. Such measures are widely implemented in WS_2 production by CTIA GROUP LTD, ensuring the sustainability of high-temperature decomposition processes. Thermodynamic calculations show that the Gibbs free energy (ΔG) of WS_2 decomposition becomes negative at 650°C, indicating the reaction's spontaneity and further validating the accuracy of its decomposition temperature.

2.1.3.3 Thermal Expansion Coefficient

WS_2's thermal expansion coefficient exhibits anisotropy. In-plane (a-axis), it is approximately $6.5 \times 10^{-6}\ K^{-1}$, while along the c-axis (interlayer direction), it is about $2.3 \times 10^{-5}\ K^{-1}$, as measured by high-temperature XRD. These values indicate minimal in-plane expansion at high temperatures, with more pronounced interlayer expansion, due to strong intralayer covalent bonds and weak interlayer van der Waals forces. Compared to tungsten metal ($4.5 \times 10^{-6}\ K^{-1}$), WS_2's anisotropic thermal expansion is more complex, requiring consideration of thermal stress matching in coating designs. For example, when compounded with tungsten-copper, the c-axis expansion of WS_2 coatings may cause interfacial stress, which can be mitigated by adding buffer layers (e.g., MoS_2).

The low thermal expansion coefficient ensures dimensional stability in precision machinery. For instance, in the production of tungsten needles, WS_2 coatings exhibit an expansion rate of less than 0.01% at 500°C, maintaining tip precision. Thermal mechanical analysis (TMA) shows that WS_2's thermal expansion behavior is linear from 300-600°C, with the c-axis expansion rate slightly increasing to $2.5 \times 10^{-5}\ K^{-1}$ as temperature rises, reflecting minor interlayer spacing changes. This property makes WS_2 excel in high-temperature optical devices (e.g., infrared lens coatings), offering better thermal expansion matching than traditional materials like SiO_2 (1.0×10^{-6} K^{-1}).

2.1.4 Friction Coefficient and Lubrication Performance

WS_2's low friction coefficient and excellent lubrication performance are its core advantages as a solid lubricant, widely applied in mechanical, aerospace, and automotive fields.

2.1.4.1 Low Friction Coefficient

WS_2 exhibits a friction coefficient ranging from 0.03 to 0.09, as measured under ASTM D1894 standards in dry, oil-free conditions. This low value stems from weak interlayer van der Waals forces, resulting in minimal shear resistance during sliding. Compared to MoS_2 (0.04-0.1), WS_2's friction coefficient is slightly lower, particularly in vacuum environments (<0.05), due to its reduced sensitivity to moisture. Pin-on-disk friction tests demonstrate that WS_2 reduces the friction coefficient from 0.7 to 0.05 in steel-on-steel contact, a 93% reduction. Molecular dynamics (MD) simulations validate this low friction, showing an interlayer shear force of just 0.1-0.2 N/m^2, consistent with experimental data.

This low friction coefficient enables WS_2 to replace traditional lubricants in bearings and gears. For example, in the tungsten market, WS_2 powder added to high-speed bearing grease reduces the friction coefficient by 80% compared to unadditized grease, lowering operating temperatures by 20°C. Practical tests show that WS_2 coatings maintain a friction coefficient of 0.07 at 500°C, outperforming graphite (>0.2). In CTIA GROUP LTD's product line, WS_2 lubricants have been NASA-certified for their low friction performance, used in spacecraft sliding components to meet vacuum and high-temperature demands.

2.1.4.2 Friction Stability Under Temperature and Pressure

WS_2's friction coefficient remains stable across a wide temperature range (-200°C to 650°C), with even better performance in vacuum or inert atmospheres. At 500°C, it rises slightly to 0.07 due to minor surface oxidation, but remains at 0.03 in vacuum. Four-ball friction tests show that under high pressure (>1 GPa), its layered structure remains effective, with the friction coefficient increasing only to 0.1, far below the 0.5-0.8 of metal-on-metal contact. Unlike tungsten-iron, which requires additional lubricants, WS_2 performs reliably without them under extreme conditions.

This stability excels in aerospace engines and deep-sea equipment. For instance, in turbine blade sliding components, WS_2 coatings maintain a friction coefficient of 0.08 at 600°C and 2 GPa, with a wear rate of <0.01 $mm^3/N \cdot m$. High-temperature friction tests (ASTM G99) demonstrate that WS_2's friction stability at 300°C surpasses MoS_2's (which rises to 0.15), due to its superior thermal stability (see 2.1.3.1). In tungsten technology applications, WS_2 coatings in deep-sea hydraulic systems maintain a friction coefficient below 0.1 under pressures up to 3 GPa, extending equipment lifespan by 50%.

2.1.4.3 Effect of Sliding Speed on Friction

Sliding speed has minimal impact on WS_2's friction coefficient, fluctuating between 0.03 and 0.06 across a range of 0.01-10 m/s, as measured by high-speed friction testers. At low speeds (<0.1 m/s), interlayer sliding is smooth, yielding a minimum friction of 0.03; at high speeds (>5 m/s), slight wear increases it to 0.06, still far below metal-on-metal values of 0.5-0.8. Friction dynamics analysis shows a weak positive correlation between friction coefficient and speed (correlation coefficient <0.1), indicating strong speed adaptability.

This property makes WS_2 suitable for both high-speed rotating machinery (e.g., turbines) and low-speed heavy-duty equipment (e.g., presses). For example, in automotive engine crankshafts, WS_2 coatings maintain a friction coefficient of 0.05 at 3000 rpm (approximately 5 m/s), reducing wear rates by 60%. In tungsten research, WS_2's high-speed stability is utilized in ultra-high-speed bearing tests, maintaining a friction coefficient below 0.06 at 10 m/s, outperforming graphite (>0.2). This adaptability enhances WS_2's reliability in dynamic environments, cementing its importance in tungsten products.

2.1.5 Hardness and Mechanical Strength

WS_2's hardness and mechanical strength, due to its layered structure, present a unique combination of softness and toughness, influencing its performance in wear-resistant and load-bearing applications.

2.1.5.1 Mohs Hardness

WS_2 has a Mohs hardness of 1-1.5, consistent with tungstenite, significantly lower than tungsten carbide powder (9-9.5). This softness results from weak interlayer van der Waals forces, facilitating exfoliation and sliding. Scratch tests confirm that WS_2 surfaces can be marked by a fingernail, yet its intralayer structure remains intact. Compared to graphite (1-2), WS_2's hardness is slightly lower, but its intralayer covalent bond strength (400-500 kJ/mol) ensures microscopic stability. This low hardness renders it unsuitable as a standalone wear-resistant material but advantageous in lubrication contexts. In practice, WS_2 is often combined with high-hardness materials. For example, when blended with tungsten powder to create composite coatings, its Mohs hardness rises to 5-6 while retaining low friction properties. Nanoindentation tests show that such composites achieve a surface hardness of 5 GPa, far exceeding pure WS_2's 0.5 GPa. In the tungsten market, WS_2's low Mohs hardness is leveraged in anti-friction coatings, reducing gear wear rates to 0.01 $mm^3/N\cdot m$ and extending lifespan by 40%.

2.1.5.2 Compressive Strength

WS_2 coatings exhibit a compressive strength of up to 2070 MPa (approximately 300,000 psi), as measured by nanoindentation. The strong intralayer W-S covalent bonds provide high compression resistance, despite easy interlayer shearing. Under high pressure (>1-2 GPa), WS_2 films maintain structural integrity, surpassing graphite (<1000 MPa). Compression tests show that WS_2 bulk retains a compressive strength above 1800 MPa at 500°C, demonstrating its high-temperature stability. This property makes it an excellent coating material for heavy-duty bearings and hydraulic systems.

In aerospace, WS_2 coatings' high compressive strength prevents failure under heavy loads. For example, in tungsten technology, WS_2 is applied to aircraft landing gear bearings, supporting 2 GPa loads with a friction coefficient below 0.1. Compared to tungsten-iron, WS_2 is lighter, with a density half that of the latter (7.5 vs. 15 g/cm³), reducing structural weight by 10-15%. Practical tests show that WS_2 coatings exhibit less than 0.01% deformation after 1000 cycles, proving their durability.

2.1.5.3 Shear Strength and Wear Resistance

WS_2's shear strength is low, ranging from 20-50 MPa, due to weak interlayer forces, as measured by shear tests. However, its wear resistance is remarkable under lubrication conditions, with wear tests (ASTM G99) showing a wear rate of just 0.01 $mm^3/N \cdot m$ on steel surfaces, compared to 0.5 $mm^3/N \cdot m$ for uncoated steel. This wear resistance stems from interlayer sliding absorbing friction energy, minimizing surface damage. Compared to MoS_2 (wear rate 0.02 $mm^3/N \cdot m$), WS_2 excels due to its higher thermal stability.

In high-speed gears and cutting tool coatings, WS_2's combination of low shear strength and high wear resistance extends service life. For example, in tungsten products, WS_2-coated gears operating at 3000 rpm for 1000 hours show wear depths below 5 µm, increasing lifespan by 50%. SEM observations reveal that the coating retains its layered structure post-wear, with no significant flaking. In CTIA GROUP LTD's tool coatings, WS_2's wear resistance boosts cutting efficiency by 30%, as its low shear strength reduces adhesion between tools and workpieces.

2.2 Chemical Properties of Tungsten Disulfide

The chemical properties of tungsten disulfide (WS_2) determine its performance in corrosive environments and highly reactive conditions, serving as the foundation for its applications in catalysis, lubrication, energy storage, and beyond. These properties encompass solubility, redox behavior, corrosion resistance, and chemical reactions at high temperatures, each intricately linked to its layered structure and the chemical nature of the W-S bond. This section will delve deeply into these characteristics, elucidating WS_2's stability and reactivity in chemical environments through experimental data, reaction mechanisms, and application case studies, providing theoretical support for its industrial and scientific applications.

2.2.1 Solubility

The solubility of WS_2 reflects its chemical inertness, serving as an indicator of its stability across various environments and directly impacting its long-term performance in lubricants, coatings, and catalysts.

2.2.1.1 Insoluble in Water, Alcohol, and Dilute Acids

WS_2 is virtually insoluble in water, ethanol, and dilute acids (e.g., 10% H_2SO_4, 5% HCl), with a solubility of less than 0.01 g/100 mL, as confirmed by immersion tests (25°C, 24 hours). This insolubility stems from the high stability of its intralayer W-S covalent bonds (bond energy 400-500 kJ/mol, see 1.1.1.1) and the low reactivity of sulfur atoms, preventing chemical bond cleavage or solvation in these solvents. Inductively coupled plasma optical emission spectroscopy (ICP-OES) analysis after 168 hours of immersion reveals W and S ion concentrations in the solution below 0.1 ppm, indicating an extremely low dissolution rate. Compared to sodium tungstate (highly water-soluble, solubility >100 g/100 mL), WS_2's chemical inertness makes it more suitable for prolonged use in harsh environments.

This insolubility is highly significant in lubricant applications. For instance, in protective coatings for marine machinery, WS_2 exposed to seawater (3.5% NaCl) or humid conditions for 168 hours exhibits a mass loss of less than 0.01%, as verified by corrosion tests (ISO 11845). Its layered structure prevents water molecule penetration, with a surface contact angle of approximately 90° (measured by a contact angle goniometer), demonstrating hydrophobicity. This property ensures that WS_2's lubrication performance remains intact in wet conditions, extending service life. In tungsten products, WS_2's insolubility supports its use as an additive in water-based lubricants; for example, when blended with tungsten plastic to create water-resistant composites, its dispersion stability improves by 30% (determined by sedimentation tests).

From a chemical mechanism perspective, WS_2's insolubility is linked to its surface energy and solvent interactions. Molecular dynamics (MD) simulations show that the adsorption energy between WS_2 surfaces and water molecules is only 0.2 eV, far below the bond-breaking energy required for dissolution (>4 eV), indicating physical adsorption rather than chemical reaction. In dilute acids (pH 2-5), no significant corrosion of the W-S bond is observed, with X-ray photoelectron spectroscopy (XPS) confirming that the surface W^{4+} and S^{2-} ratios remain unchanged. This insolubility enables WS_2 to maintain performance in acidic industrial exhaust environments (e.g., containing SO_2), such as in chemical plant pipeline coatings, where acid resistance tests (168 hours, 10% H_2SO_4) show a mass loss of less than 0.005%.

2.2.1.2 Soluble in Aqua Regia and Molten Alkali

WS_2 dissolves in strongly oxidizing solvents like aqua regia (HNO_3:HCl = 1:3) and molten alkali (e.g., NaOH, >300°C), with the following reactions:

WS2+4HNO3+12HCl→H2WO4↓+2H2S↑+4NO2↑+8H2O

$WS_2 + 4HNO_3 + 12HCl \rightarrow H_2WO_4\downarrow + 2H_2S\uparrow + 4NO_2\uparrow + 8H_2O$

WS2+4HNO3+12HCl→H2WO4↓+2H2S↑+4NO2↑+8H2O

WS2+6NaOH→Na2WO4+2Na2S+3H2O

$WS_2 + 6NaOH \rightarrow Na_2WO_4 + 2Na_2S + 3H_2O$

WS2+6NaOH→Na2WO4+2Na2S+3H2O

In aqua regia, the potent oxidizing action of HNO_3 breaks the W-S bonds, producing insoluble tungstic acid (H_2WO_4) and gaseous byproducts (e.g., H_2S and NO_2), with a dissolution rate of approximately 0.1 g/min at 25°C (measured by mass loss). Molten alkali (e.g., NaOH at 400°C) converts WS_2 into soluble tungstate (Na_2WO_4) and sodium sulfide, with a faster dissolution rate (>1 g/min) due to high temperatures accelerating bond cleavage. ICP-OES analysis shows that after dissolution in aqua regia, the solution contains 500 ppm W, with S escaping as H_2S; in molten alkali, W and S exist as Na_2WO_4 and Na_2S, respectively, with solute concentrations exceeding 10 g/L.

This solubility is utilized for analyzing WS_2 purity or recovering tungsten resources. For example, in tungsten research, aqua regia dissolution is employed to measure impurity levels (e.g., Fe, Si) in WS_2 samples, analyzing residues post-dissolution to achieve a purity precision of 99.99%. In industrial recycling, molten NaOH processes waste WS_2 coatings, converting them into Na_2WO_4, which is then acidified to produce tungstic acid, achieving a recovery rate above 90%. This solubility limits WS_2's direct use in strong acid-base environments, such as avoiding contact with molten alkali in chemical reactors, but facilitates its chemical processing under specific conditions. For instance, CTIA GROUP LTD's recycling process uses molten alkali to transform waste WS_2 into high-value tungsten compounds, with an annual processing capacity of 100 tons.

2.2.1.3 Analysis of Solubility Test Conditions

Solubility tests for WS_2 are typically conducted at temperatures of 25-100°C and pH levels of 1-14, showing stability in solutions with pH 2-12, with solubility changes below 0.005 g/100 mL. In neutral water (pH 7, 25°C), solubility after 168 hours of immersion is less than 0.001 g/100 mL, with no detectable W or S ions via inductively coupled plasma mass spectrometry (ICP-MS). In acidic conditions (pH 1-5, e.g., 10% H_2SO_4), solubility slightly increases to 0.01 g/100 mL but remains negligible, indicating acid resistance. In alkaline conditions (pH 9-12, e.g., 1 M NaOH, 25°C), solubility is below 0.005 g/100 mL, significantly rising only in molten states (>300°C). Solubility tests reveal that WS_2 oxidation accelerates at high temperatures (>80°C) and with strong oxidants (e.g., 30% H_2O_2), forming WO_3, with solubility increasing to 0.05 g/100 mL.

The diversity of test conditions provides data support for WS_2's environmental adaptability. For example, in tungsten technology, WS_2 coatings in industrial wastewater environments (pH 2-12) exhibit a mass loss of less than 0.01% after 1000 hours of immersion, proving durability. Electrochemical tests show a corrosion potential of -0.1 V (vs. SCE) in 10% NaCl solution, indicating high inertness. In high-temperature, high-humidity conditions (80°C, RH 95%), WS_2 surfaces may adsorb water molecules, slightly increasing solubility to 0.02 g/100 mL, but overall stability remains unaffected. This solubility profile guides WS_2's use in chemical equipment, such as corrosion-resistant coatings in acidic gas pipelines, withstanding temperatures up to 500°C and showing no significant corrosion after 1000 hours (ASTM B117 test).

2.2.2 Redox Behavior

WS_2's redox behavior determines its stability in oxygen or other chemical environments, a key factor for its high-temperature applications and catalytic performance.

2.2.2.1 Reaction Mechanism of High-Temperature Oxidation to WO_3

In air, WS_2 oxidizes to WO_3 at 650°C, with the reaction:
2WS2+7O2→2WO3+4SO2↑$2WS_2 + 7O_2 \rightarrow 2WO_3 + 4SO_2\uparrow$ 2WS2+7O2→2WO3+4SO2↑
The reaction proceeds in two stages: around 510°C, surface sulfur atoms oxidize to SO_2; from 550-650°C, tungsten atoms fully oxidize to WO_3. XPS analysis reveals an initial W^{4+} intermediate state (e.g., $WS_{2-x}O_x$), transitioning to W^{6+} (WO_3). Thermogravimetric analysis (TGA) shows that the reaction rate increases with oxygen partial pressure, reaching 0.05 g/min at 600°C in air (0.21 atm). Differential scanning calorimetry (DSC) indicates an enthalpy change (ΔH) of approximately -900 kJ/mol, signifying a strongly exothermic process. SEM observations show that post-oxidation, WS_2 surfaces form a porous WO_3 layer, approximately 1-2 μm thick, impeding further oxygen diffusion.

This oxidation mechanism limits WS_2's use in high-temperature oxidizing environments, but its stability below 500°C suffices for industrial scenarios. For example, in the tungsten market, WS_2 coatings in aerospace engines operating at 400°C for 1000 hours exhibit an oxidation layer thickness of less than 0.1 μm, with no significant performance decline. Kinetic analysis indicates a parabolic rate law, with a rate constant (k) of 0.02 min^{-1} at 600°C, increasing exponentially with temperature (activation energy ~150 kJ/mol). This mechanism provides a basis for enhancing WS_2 coating oxidation resistance, such as adding a SiO_2 protective layer to raise the oxidation onset temperature to 700°C.

2.2.2.2 Stability Under Reducing Conditions

In reducing atmospheres (e.g., H_2 or CO), WS_2 remains stable up to 1000°C, with minimal sulfur loss:WS2+H2→W+H2S↑$WS_2 + H_2 \rightarrow W + H_2S\uparrow$ WS2+H2→W+H2S↑, This reaction is extremely slow below 900°C, with a sulfur loss rate of less than 0.1%/h (800°C, H_2 flow), as measured by TGA. Above 1000°C, sulfur volatilization increases slightly to 0.5%/h, but the structure remains intact. High-temperature XRD analysis shows no transformation to tungsten metal in H_2, with the (002) peak position unchanged, confirming reductive stability. This property excels in reductive catalytic environments (e.g., hydrodesulfurization), surpassing organic lubricants that decompose below 300°C.

In petrochemical applications, WS_2 serves as a hydrodesulfurization catalyst, operating in H_2 (500°C, 10 bar) for 1000 hours with less than 5% activity loss, validated by catalytic performance tests (ASTM D5185). Its layered structure remains intact under reducing conditions, with SEM showing no significant surface cracks. In tungsten research, WS_2's reductive stability is utilized in high-temperature gas sensors, such as H_2 detection, with resistance changes below 1%/1000 hours, demonstrating long-term reliability. This stability also supports its use in high-temperature vacuum lubrication, such as in tungsten heater production, where WS_2 coatings operate stably at 1000°C in vacuum.

2.2.2.3 Oxidation Onset Temperature and Environmental Influences

WS_2's oxidation onset temperature varies with environment, approximately 510°C in air, dropping to 480°C at 100% oxygen concentration, and showing no significant oxidation up to 1250°C in nitrogen. DSC measurements indicate that the onset temperature correlates with particle size, with nanoscale WS_2 slightly lower (~490°C) due to higher surface area, compared to 510°C for bulk. Increased humidity (RH >80%) promotes surface oxidation, especially at high temperatures, as moisture accelerates SO_2 formation. TGA analysis shows that at 80°C and 95% RH, WS_2 surface oxidation rates rise to 0.01%/h, forming a thin WO_3 layer (<50 nm thick, SEM measurement).

Environmental influence analysis guides WS_2 storage and use. For example, in tungsten products, WS_2 powder requires sealed storage in dry conditions (RH <50%) to avoid oxidation in high-temperature, humid environments. In industrial applications, WS_2 coatings in oxygen-containing atmospheres (20% O_2, 500°C) can increase the oxidation onset temperature to 550°C with antioxidants (e.g., Al_2O_3). Practical tests show that WS_2 in SO_2-containing exhaust environments (500°C, 1000 hours) exhibits an oxidation rate below 0.1%, highlighting its environmental adaptability. This property makes WS_2 suitable as a high-temperature coating in chemical equipment, meeting diverse environmental demands

2.2.3 Corrosion Resistance and Chemical Inertness

The corrosion resistance and chemical inertness of WS_2 ensure its performance in harsh chemical environments, directly affecting its long-term stability as a lubricant, coating, and catalyst. These properties arise from its unique structure of strong intralayer covalent bonds and weak interlayer van der Waals forces, enabling exceptional resistance to acidic, alkaline, and various chemical attacks. This subsection will explore WS_2's performance in acidic environments, stability in alkaline conditions, and applications in resisting chemical erosion, supported by experimental data, mechanistic analysis, and real-world examples, fully revealing its chemical stability.

2.2.3.1 Performance in Acidic Environments

WS_2 exhibits outstanding corrosion resistance in acidic environments. After 168 hours of immersion in pH 1-5 solutions (e.g., 10% H_2SO_4, 5% HCl), its mass loss is less than 0.01%, as determined by corrosion tests (ISO 11845). This acid resistance is attributed to the high bond energy of intralayer W-S covalent bonds (400-500 kJ/mol, see 1.1.1.1) and the low reactivity of sulfur atoms, making it resistant to acidic attack. ICP-OES analysis shows W and S ion concentrations in the solution below 0.1 ppm, indicating negligible dissolution. Compared to silver-tungsten (mass loss >5% in 10%

H_2SO_4 over 168 hours), WS_2's acid resistance is markedly superior.

In acidic gas environments (e.g., H_2S, SO_2), WS_2 remains stable. Exposure tests (25°C, 10% H_2S, 1000 hours) show no visible surface changes, with SEM confirming an intact layered structure free of corrosion pits or cracks. XPS analysis indicates consistent W^{4+} and S^{2-} ratios, with no oxide or sulfide formation. This acid resistance excels in chemical equipment, such as pipeline coatings in sulfuric acid production, where WS_2 maintains a mass loss below 0.005% in 10% H_2SO_4 vapor (80°C, 1000 hours), validated by salt spray tests (ASTM B117). Compared to MoS_2 (0.1% mass loss in H_2S), WS_2's stronger W-S bond enhances its chemical inertness.

Mechanistically, WS_2's acid resistance relates to its hydrophobic surface. Contact angle measurements show a surface angle of approximately 90°, preventing acid solution penetration between layers. MD simulations reveal an adsorption energy of acid molecules (e.g., H_2SO_4) on WS_2 surfaces of just 0.3 eV, far below the bond-breaking energy (>4 eV), indicating physical adsorption dominance. In tungsten products, WS_2's acid resistance is utilized in acid pickling equipment; for instance, in CTIA GROUP LTD's chemical coatings, WS_2 operates in pH 2 environments for 1000 hours with a wear rate below 0.01 $mm^3/N\cdot m$, extending equipment life by 50%.

2.2.3.2 Stability in Alkaline Environments

WS_2 also demonstrates high stability in alkaline environments. After 168 hours of immersion in pH 9-12 solutions (e.g., 1 M NaOH, 25°C), its mass loss is less than 0.005%, as measured by corrosion tests. This stability stems from the robustness of intralayer covalent bonds, preventing chemical reactions with OH^- ions. ICP-OES analysis shows W and S ion concentrations below 0.05 ppm, indicating negligible dissolution. However, in high-temperature molten alkali (e.g., NaOH, >300°C), WS_2 decomposes into tungstate (Na_2WO_4) and sodium sulfide (Na_2S, see 2.2.1.2), with a dissolution rate exceeding 1 g/min due to accelerated bond breaking.

At ambient alkaline conditions, WS_2's stability supports battery electrode protection. For example, in tungsten research, WS_2 coatings in alkaline zinc batteries (pH 11, 25°C) exhibit a mass loss below 0.01% after 1000 cycles, validated by electrochemical tests. SEM observations show no peeling or corrosion, with interlayer spacing stable at 6.15 Å (XRD measurement). Compared to tungsten-copper (0.5% mass loss in 1 M NaOH), WS_2's superior alkali resistance is due to its hydrophobic surface (contact angle 90°), reducing OH^- adsorption.

Electrochemical tests reveal a corrosion potential of -0.1 V (vs. SCE) in alkaline environments, higher than MoS_2's -0.2 V, indicating greater inertness. In high-temperature alkaline conditions (1 M NaOH, 100°C), stability slightly decreases, with mass loss rising to 0.02% (168 hours), still far below tungsten-iron's 1%. This property enables WS_2 use as an electrode material in alkaline electrolytes, such as in tungsten technology's alkaline water electrolysis equipment, where WS_2 coatings operate at pH 12 and 80°C for 1000 hours with less than 5% performance degradation, supporting long-term stability.

2.2.3.3 Applications in Resisting Chemical Erosion

WS_2's resistance to chemical erosion enables its widespread use in harsh environments. In mixed acid-base settings (e.g., wastewater treatment plants, pH 4-10), WS_2 coatings show no significant corrosion after 1000 hours of immersion, with SEM confirming an intact layered structure and mass loss below 0.01%. In chloride-containing environments (e.g., seawater pumps, 3.5% NaCl), WS_2 coatings exhibit no pitting or peeling after 1000-hour salt spray tests (ASTM B117), outperforming tungsten-iron (0.5% mass loss). Electrochemical impedance spectroscopy (EIS) shows an impedance value of $10^6\ \Omega\cdot cm^2$ in 10% NaCl, indicating high corrosion resistance.

In chemical reactors, WS_2 serves as a corrosion-resistant coating against acidic gases (e.g., HCl, SO_2) and high temperatures (500°C), with tests showing coating thickness reduction below 0.1 µm after 1000 hours. In the tungsten market, WS_2's chemical erosion resistance supports its use in acid pickling tank coatings, enduring mixed 10% H_2SO_4 and 5% HCl environments and extending equipment life by 40%.

From an application perspective, WS_2's resistance to chemical erosion is tied to its surface properties and structural stability. XPS analysis shows no significant oxide formation in acid-base environments, maintaining W^{4+} and S^{2-} states. In tungsten products, WS_2 coatings in industrial pipelines with corrosive gases (e.g., H_2S-containing natural gas) remain stable after 1000 hours, proving reliability in complex chemical settings.

2.2.4 Chemical Reactions at High Temperatures

WS_2's chemical reactions at high temperatures reveal its behavior under extreme conditions, directly influencing its applications in high-temperature lubrication and catalysis.

2.2.4.1 Reaction Kinetics with Oxygen

WS_2's reaction with oxygen follows first-order kinetics, with the equation:
2WS2+7O2→2WO3+4SO2↑$2WS_2 + 7O_2 \rightarrow 2WO_3 + 4SO_2\uparrow$ 2WS2+7O2→2WO3+4SO2↑
The rate constant (k) at 600°C is approximately 0.02 min^{-1}, as measured by TGA, increasing exponentially with temperature (Arrhenius equation, activation energy ~150 kJ/mol). Initially (510-550°C), the reaction is surface-controlled, with rates dictated by oxygen diffusion to the surface; later (550-650°C), it shifts to diffusion control as a WO_3 layer (1-2 µm thick, SEM measurement) impedes oxygen penetration. DSC indicates an enthalpy change (ΔH) of about -900 kJ/mol, reflecting strong exothermicity. At 100% oxygen concentration, the reaction rate rises to 0.05 g/min at 600°C, twice that in air (0.21 atm).

This kinetic profile requires consideration in spray coating design. For example, in tungsten technology, WS_2 coatings in aerospace engines (500°C, oxygen-containing atmosphere) reduce oxidation rates by 50% with antioxidants (e.g., SiO_2), extending lifespan to 2000 hours. Tests show WS_2 in 10% O_2 industrial kilns (1000 hours) limits oxidation layer thickness to below 0.5 μm, with performance degradation under 5%. Kinetic data also guide its use in high-temperature vacuum environments, such as in tungsten heater production, where WS_2 exhibits no significant oxidation at 1000°C in vacuum, ensuring stability.

2.2.4.2 Interactions with Sulfides

In sulfide atmospheres (e.g., H_2S), WS_2 remains stable up to 1000°C, with no decomposition or transformation:$WS_2 + H_2S \rightleftharpoons WS_2 + H_2S$ High-temperature XRD suggests H_2S may repair sulfur vacancies (V_s, 5-10% by XPS), enhancing structural integrity. In 800°C, 10% H_2S conditions for 1000 hours, WS_2 mass changes are below 0.01%, as verified by TGA. This stability maintains catalytic activity in sulfide environments (e.g., petroleum desulfurization), with WS_2 catalysts in hydrodesulfurization (500°C, H_2S/H_2 mix) showing less than 5% activity loss after 1000 hours (ASTM D5185 test).

In tungsten research, WS_2's interaction with H_2S is leveraged in sulfide sensors, with resistance changes below 1%/1000 hours and sensitivity reaching 10 ppm. SEM shows no sulfide deposits on WS_2 surfaces in H_2S, retaining its layered structure. This stability supports high-temperature sulfide environment lubrication, such as in natural gas pipeline sliding components, where WS_2 coatings in H_2S-containing conditions (500°C) maintain a friction coefficient below 0.1 after 1000 hours.

2.2.4.3 Analysis of High-Temperature Decomposition Products

WS_2's primary high-temperature decomposition products are WO_3 and SO_2, with minor tungsten metal formation above 1000°C in vacuum. Mass spectrometry (MS) detects a strong SO_2 peak at 650°C, indicating dominant sulfur volatilization; at 1250°C in vacuum, a W peak appears (<1%, XPS confirmation). TGA shows a 33% mass loss at 650°C in air (theoretical 32.6%, full S volatilization), compared to <5% at 1250°C in vacuum. SEM reveals a porous WO_3 structure post-decomposition, with pore sizes of 0.1-0.5 μm. This product analysis informs recycling processes. In the tungsten market, waste WS_2 coatings are oxidized at 700°C to WO_3, then acidified to produce tungstic acid, achieving over 90% recovery. CTIA GROUP LTD's recycling process handles 100 tons of waste WS_2 annually, absorbing SO_2 with CaO to form $CaSO_4$, keeping emissions below 10 ppm, meeting environmental standards. In catalysis, decomposition analysis reveals WS_2's activity changes at high temperatures; for example, in hydrodesulfurization, minor decomposition at 800°C does not affect performance, with activity remaining above 95%.

2.3 Electrical and Optical Properties of Tungsten Disulfide

The electrical and optical properties of WS_2 are the cornerstone of its critical role in electronic devices, optoelectronic components, and optical applications. These properties vary with layer count, crystal phase, and external conditions (e.g., temperature, doping), ranging from the indirect bandgap semiconductor nature of bulk material to the high photoluminescence efficiency of single-layer direct bandgap, alongside excellent optical absorption and reflection capabilities. This subsection will thoroughly explore its conductivity and semiconductor properties, bandgap characteristics, and optical absorption and reflection properties, supported by detailed experimental data, theoretical models, practical application cases, and comparisons with other materials, fully unveiling WS_2's diversity and potential in electrical and optical domains.

2.3.1 Conductivity and Semiconductor Properties

WS_2's conductivity and semiconductor properties vary with layer count and polymorphism, spanning from the low-conductivity indirect bandgap of bulk material to the high-mobility direct bandgap of single layers, with further optimization through doping, showcasing its broad applicability in electronic devices. This subsection will analyze the indirect bandgap of bulk material, the direct bandgap of single layers, and carrier mobility with doping effects, integrating experimental and theoretical data to reveal the underlying mechanisms of its electrical performance.

2.3.1.1 Indirect Bandgap of Bulk Material

Bulk WS_2 (typically 2H phase) possesses an indirect bandgap of 1.3 eV, precisely measured by ultraviolet-visible spectroscopy (UV-Vis), with an absorption edge at approximately 950 nm. This indirect bandgap requires phonon assistance for electron transitions from the valence band maximum (primarily sulfur 3p orbitals, at the K-point of the Brillouin zone) to the conduction band minimum (tungsten 5d orbitals, at the Γ-point), resulting in extremely low photoluminescence efficiency, with a quantum yield below 0.1%, as verified by PL spectroscopy. Density functional theory (DFT) calculations confirm this characteristic, showing that interlayer electronic coupling disperses the band structure, with overlap between tungsten's $5d\_z^2$ and sulfur's $3p\_z$ orbitals forming a broad indirect bandgap. Four-probe measurements indicate bulk WS_2's conductivity at room temperature (300 K) ranges from 10^1-10^2 S/cm, far below that of metals like tungsten metal (~10^5 S/cm), but sufficient for use as a semiconductor in electronic devices.

The indirect bandgap of bulk WS_2 offers potential in thermoelectric materials due to its low thermal conductivity (20-30 W/m·K) and moderate electrical conductivity, supporting temperature-difference power generation. In tungsten research, bulk WS_2 is fabricated into thermoelectric modules, achieving a Seebeck coefficient of ~100 µV/K at 300 K, stable at ~90 µV/K at 500°C, with a thermoelectric figure of merit (ZT) of 0.5, surpassing MoS_2's 0.3. Hall effect tests show a carrier concentration of ~10^{16} cm^{-3}, predominantly electrons, indicating n-type semiconductor behavior, with a mobility of 10-20 $cm^2/V·s$. This suits low-power devices, such as gas sensors detecting NH_3 at 10 ppm with a response time below 5 seconds, leveraging its indirect bandgap for efficient carrier transport at low concentrations.

Bulk WS_2's conductivity increases with temperature, rising from 10^2 S/cm to 10^3 S/cm between 300-

600°C (variable-temperature four-probe method), as thermally excited carriers boost concentration to 10^{17} cm^{-3}, remaining below its 650°C oxidation threshold (see 2.2.2.1) with intact structure. Resistivity tests show a change rate below 1%/1000 hours at 500°C, confirming high-temperature stability. In tungsten products, bulk WS_2 serves as a conductive coating on tungsten-copper substrates, matching substrate conductivity (~10^4 S/cm) and maintaining performance in 400°C circuits for 1000 hours with less than 2% degradation, outperforming graphite (5% degradation due to oxidation).

2.3.1.2 Direct Bandgap of Single Layer

Single-layer WS_2 exhibits a direct bandgap of 2.1 eV, measured by PL spectroscopy, with a strong emission peak at 620 nm and a quantum yield of 5-10%, 100 times higher than bulk's <0.1%. This shift results from quantum confinement, eliminating interlayer coupling, aligning the conduction and valence bands at the K-point for direct transitions. Angle-resolved photoemission spectroscopy (ARPES) correlates this bandgap with its 0.62 nm thickness, confining electronic states in two dimensions. Four-probe measurements show a conductivity range of 10^2-10^3 S/cm, exceeding bulk due to the direct bandgap and enhanced carrier mobility (see 2.3.1.3).

This direct bandgap offers significant advantages in optoelectronic devices, such as photodetectors, where single-layer WS_2 achieves a photoresponsivity of 10^3 A/W at 532 nm (5 V bias), far surpassing multilayer's 10^1 A/W (photocurrent tests). In tungsten technology, it's used in flexible photosensors, supporting rapid response (<1 ms) across 400-1000 nm with a sensitivity of 0.1 μW/cm². FET tests reveal a switching ratio of 10^6, higher than bulk's 10^4, due to improved carrier generation efficiency. Compared to MoS_2 single layers (1.8 eV, 10^2 A/W), WS_2's higher bandgap and responsivity enhance high-sensitivity device performance.

Single-layer WS_2's high conductivity supports transparent conductive films. Paired with tungsten wire electrodes, it achieves >90% transmittance at 550 nm and a resistivity of 10^{-3} Ω·cm, rivaling ITO (10^{-4} Ω·cm) with superior flexibility (bendable to 10^{-3} m^{-1} curvature). CVD-produced single-layer WS_2 maintains conductivity with <5% change after 1000 bends (resistivity tests), used in CTIA GROUP LTD's flexible display conductive layers, boosting brightness by 20% and retaining stability at 500°C (<2% change).

2.3.1.3 Carrier Mobility and Doping Effects

Single-layer WS_2's carrier mobility reaches 100-200 cm²/V·s (electrons) via Hall effect, dropping to 10-20 cm²/V·s in multilayers, surpassing MoS_2 single layers (50-80 cm²/V·s) due to its direct bandgap and lower effective mass (electrons 0.3 m_0, holes 0.4 m_0, DFT). Bulk WS_2's lower mobility reflects increased phonon and impurity scattering from interlayer coupling. FET tests show stable mobility at 300 K, with drain current (I_d) of 10 μA at 1 V bias, rising to 300 cm²/V·s at 77 K due to reduced phonon scattering, approaching silicon (500 cm²/V·s) but below graphene (10^4 cm²/V·s).

Doping enhances mobility and conductivity, with Nb (p-type) boosting single-layer WS_2 to 200-250 $cm^2/V\cdot s$ and hole concentration to 10^{17} cm^{-3} (Hall effect), and Re (n-type) raising electron mobility to 250-300 $cm^2/V\cdot s$, conductivity to 10^4 S/cm. XPS confirms Nb^{4+} and Re^{4+} substitution, altering carrier type and density. In tungsten research, Nb-doped WS_2 in high-performance FETs achieves a 10^7 switching ratio, surpassing undoped WS_2 (10^6) and silicon (10^5). Doping supports sensors, such as Re-doped WS_2 films detecting NO_2 at 1 ppb (<2 s response), outperforming MoS_2 (5% vs. 2% stability change at 300°C), used in tungsten products for flexible electronics with 20% lower power consumption.

2.3.2 Bandgap Characteristics

WS_2's bandgap characteristics are central to its electrical and optical properties, influencing conductivity, absorption, and emission.

2.3.2.1 Transition from Multilayer to Single-Layer Bandgap

WS_2 transitions from an indirect 1.3 eV multilayer bandgap to a direct 2.1 eV single-layer bandgap, a hallmark of 2D materials. DFT shows multilayer indirectness from interlayer coupling, with single-layer confinement aligning bands at the K-point. PL confirms single-layer emission at 620 nm, 100 times stronger than multilayer absorption at 950 nm (UV-Vis). This shift supports solar cell sensitizers, achieving 5% efficiency in single layers vs. 2% in multilayers (J-V tests), and photodetectors with 10^3 A/W responsivity in tungsten technology.

2.3.2.2 Temperature Effects on Bandgap

WS_2's bandgap decreases with temperature at -0.4 meV/K (300-600 K), dropping to 2.0 eV (single-layer) and 1.2 eV (multilayer) at 600 K (variable-temperature PL), due to lattice expansion and electron-phonon interactions. Raman shows $A_{1}g$ peak shifts from 420 cm^{-1} to 415 cm^{-1}, indicating stability for high-temperature sensors with <0.1% bandgap change (1000 hours).

2.3.2.3 Application Potential of Bandgap Engineering

Bandgap tuning from 1.3-2.1 eV via strain, doping, or electric fields enhances WS_2 applications. A 2% strain reduces it to 1.9 eV, Nb doping to 1.8 eV (10^4 S/cm conductivity), and a 10 V/nm field to 1.8 eV, boosting solar cell efficiency to 6% and sensor responsivity by 50% in tungsten technology.

2.3.3 Optical Absorption and Reflection Properties

WS_2's optical properties support photodetection, solar cells, and coatings, covering absorption, reflection, and emission.

2.3.3.1 Visible and Infrared Absorption Rates

Single-layer WS_2 absorbs 10% at 620 nm (2.1 eV), multilayer 50% at 950 nm (1.3 eV, UV-Vis), enabling photodetectors with 10^3 A/W (single) and 10^2 A/W (multi) responsivity. Saturation occurs at 10 mW/cm², outperforming MoS_2 (5 mW/cm²), supporting 5% solar cell efficiency in tungsten technology.

2.3.3.2 Reflectivity and Refractive Index

WS_2 reflectivity is 20-30% in visible light, rising to 50% in multilayers (ellipsometry), with refractive indices of 4.0 (single) and 4.5 (multi) at 550 nm. This suits anti-reflective coatings in tungsten products, reducing reflection losses by 20%.

2.3.3.3 Photoluminescence Properties

Single-layer WS_2 emits strongly at 620 nm (5-10% yield), enhanced to 650 nm and 15% with Nb doping, ideal for LEDs (1000 cd/m²) and bioimaging probes with <5% decay over 1000 hours in tungsten research.

CTIA GROUP LTD Tungsten Disulfide

Chapter 3: Classification of Tungsten Disulfide

Tungsten disulfide (WS_2), as a multifunctional transition metal dichalcogenide, exhibits diverse classification methods, categorized into various types based on morphology, crystal structure, purity and application, and particle size. These classifications not only reflect the differences in WS_2's physical and chemical properties but also directly determine its suitability for industrial, scientific, and specialized applications. This chapter begins with morphological classification, progressively exploring classifications by crystal structure, purity and application, and particle size, comprehensively revealing WS_2's diversity and its significant value in modern technology through experimental data, preparation methods, and application case studies.

3.1 Classification of Tungsten Disulfide by Morphology

The morphology of WS_2 is a key determinant of its application properties, with different forms of WS_2 (tungsten disulfide) exhibiting significant variations in size, structure, and functionality, directly influencing its performance in lubrication, electronics, catalysis, and other fields. This section will provide a detailed analysis of the characteristics, preparation methods, and application scenarios of powdered WS_2, nanosheet WS_2, coated WS_2, bulk WS_2, nanowire WS_2, and quantum dot WS_2.

3.1.1 Powdered Tungsten Disulfide

Powdered WS_2 is one of the most common forms, widely used in lubricants, composite materials, and industrial additives. Based on particle size, it can be further divided into micron-sized powder and ultrafine powder.

3.1.1.1 Micron-Sized Powder

Micron-sized WS_2 powder typically has a particle size ranging from 1 to 100 micrometers, with an average particle size of 5-20 micrometers, as determined by optical microscopy and laser particle size analysis. This powder exhibits a gray-black metallic sheen (see 2.1.1.1), attributed to the reflective properties of its layered structure. Scanning electron microscopy (SEM) reveals that micron-sized WS_2 particles are predominantly irregular flakes with smooth surfaces and an interlayer spacing of approximately 6.15Å, consistent with its 2H-phase crystal structure (see 1.2.1.2). Its specific surface area is relatively low (approximately 1-5 m^2/g, measured by the BET method), reflecting its larger particle size and reduced exposed surface area.

The preparation of micron-sized WS_2 typically involves calcination decomposition or direct sulfidation methods. For example, reacting tungstic acid (H_2WO_4) with hydrogen sulfide (H_2S) at 600-800°C produces: H2WO4+2H2S→WS2↓+2H2O+H2$H_2WO_4 + 2H_2S \rightarrow WS_2\downarrow + 2H_2O + H_2$ H2WO4+2H2S→WS2↓+2H2O+H2, By adjusting calcination temperature and sulfiding agent flow rate, particle sizes can be controlled within the micron range, with yields typically exceeding 95%. Its purity is generally at an industrial grade (>98%), containing trace impurities such as tungsten trioxide (WO_3) or sulfides (<1%, XPS measurement).

The primary application of micron-sized WS_2 is as a solid lubricant. For instance, in mechanical processing, adding it to grease reduces the friction coefficient from 0.7 to 0.05 (ASTM D1894 test), a 93% reduction, lowering operating temperatures by 20℃. Real-world cases show that micron-sized WS_2 powder produced by CTIA GROUP LTD is widely used in bearing and gear lubrication, with its low shear strength (20-50 MPa, see 2.1.5.3) ensuring excellent sliding performance. Additionally, its high density (7.5 g/cm^3, see 2.1.2.1) makes it suitable for counterweight materials, such as blending with tungsten powder to create high-density composites for precision instrument counterweights. In performance comparison, micron-sized WS_2 exhibits a lower friction coefficient (0.03-0.09) than molybdenum disulfide (MoS_2, 0.04-0.1), particularly excelling in vacuum environments due to its reduced sensitivity to moisture. This property makes it superior to MoS_2 in aerospace applications, such as satellite sliding components, maintaining a stable friction coefficient below 0.03 (vacuum test, 500°C).

3.1.1.2 Ultrafine Powder

Ultrafine WS_2 powder typically has particle sizes ranging from 0.1 to 1 micrometer, with an average particle size of approximately 0.5 micrometers, as measured by laser particle size analysis. It retains a gray-black appearance, though its luster slightly diminishes due to particle refinement. SEM observations show that ultrafine WS_2 particles maintain a flaky structure with more irregular edges, and their specific surface area increases to 10-20 m^2/g (BET method), indicating higher surface activity.

The preparation of ultrafine WS_2 often involves mechanical grinding or vapor-phase methods. For example, micron-sized WS_2 is ground to ultrafine levels using a planetary ball mill, with grinding durations of 10-20 hours and a ball-to-material ratio of 10:1, resulting in uniformly distributed particle sizes ($D_{50} \approx 0.5$ μm). Alternatively, chemical vapor deposition (CVD) uses ammonium metatungstate ($(NH_4)_6H_2W_{12}O_{40}$) as a precursor, decomposing it in a 700°C H_2S atmosphere to produce ultrafine WS_2, with particle sizes controllable between 0.1-0.5 μm and purity exceeding 99.5%.

The high specific surface area of ultrafine WS_2 enhances its performance in lubrication and catalysis. For instance, in the tungsten market, ultrafine WS_2 is used as a lubricant additive, improving dispersibility by 20% over micron-sized powder (DLS test), reducing the friction coefficient to 0.04 (pin-on-disk test) and wear rate to 0.005 $mm^3/N \cdot m$, outperforming micron-sized WS_2's 0.01 $mm^3/N \cdot m$. Moreover, its fine particles enhance matrix properties in nanocomposites, such as blending with tungsten plastic to create self-lubricating composites, improving dispersion uniformity by 30% and reducing weight by 10-15%.

In catalytic applications, ultrafine WS_2's high surface activity boosts hydrodesulfurization (HDS) performance. For example, in petrochemical processes, ultrafine WS_2 catalysts achieve a 95% sulfide removal rate under 500°C and 10 bar H_2 conditions (ASTM D5185), 10% higher than micron-sized WS_2, due to increased exposed edge active sites (20% vs. 10%, STM measurement). This property makes it highly valued in tungsten technology for efficient catalyst design.

3.1.2 Nanosheet Tungsten Disulfide

Nanosheet WS_2 is a quintessential two-dimensional form, characterized by a high specific surface area and unique optoelectronic properties, categorized by layer count into single-layer and multilayer nanosheets.

3.1.2.1 Single-Layer Nanosheet

Single-layer WS_2 nanosheets have a thickness of approximately 0.62 nm (AFM measurement), corresponding to a single S-W-S unit, with lateral dimensions ranging from a few micrometers to tens of micrometers (SEM and TEM observations). They appear nearly transparent, with a visible light transmittance exceeding 90% (UV-Vis measurement, see 2.1.1.2), and possess a direct bandgap of 2.1 eV (PL spectroscopy, see 2.3.1.2). Their specific surface area is exceptionally high, reaching 300-500 m^2/g (BET method), reflecting the extreme two-dimensional characteristics.

Single-layer WS_2 is primarily prepared via mechanical exfoliation or liquid-phase exfoliation. Mechanical exfoliation uses adhesive tape to separate single layers from bulk WS_2, offering low yield but high purity (>99.9%), suited for laboratory research. Liquid-phase exfoliation involves ultrasonic treatment of micron-sized WS_2 in N-methylpyrrolidone (NMP) at 200 W for 10-20 hours, achieving a single-layer yield of 20-30%, purified by centrifugation (3000 rpm). Additionally, CVD uses tungstic acid as a tungsten source, growing single-layer WS_2 at 800-1000°C in an H_2S atmosphere, with precisely controllable thickness and lateral dimensions up to 50 μm.

The direct bandgap of single-layer WS_2 excels in optoelectronic devices. For example, in tungsten research, single-layer WS_2 is used in photodetectors, achieving a photoresponsivity of 10^3 A/W at 532 nm (5 V bias) and a detectivity of 10^{11} Jones, surpassing multilayer WS_2's 10^1 A/W and 10^9 Jones (photocurrent test). Its high flexibility (curvature radius $<10^{-3}$ m^{-1}) supports flexible electronics applications, such as in CTIA GROUP LTD's flexible displays as a transparent conductive layer, with transmittance >90%, resistivity of 10^{-3} Ω·cm, and less than 5% change after 1000 bends. Furthermore, its high specific surface area enhances catalytic performance, achieving an overpotential of only 100 mV (10 mA/cm²) in the hydrogen evolution reaction (HER), compared to 300 mV for multilayers.

3.1.2.2 Multilayer Nanosheet

Multilayer WS_2 nanosheets have thicknesses ranging from 1-50 nm (2-80 layers, AFM measurement), with lateral dimensions similar to single layers (a few micrometers to tens of micrometers). Their transmittance decreases with increasing layer count, reaching approximately 50% at 10 layers (UV-Vis, 550 nm), with an indirect bandgap of 1.3 eV (see 2.3.1.1). The specific surface area ranges from 50-100 m²/g (BET method), lying between single-layer nanosheets and micron-sized powder.

Multilayer WS_2 is predominantly prepared via liquid-phase exfoliation or direct growth methods. Liquid-phase exfoliation uses micron-sized WS_2 as a raw material, subjected to 5-10 hours of ultrasonication, achieving a 50-70% yield, with layer count controlled by centrifugation speed (500-2000 rpm). CVD adjusts sulfidation time and temperature (e.g., 900°C, 30 minutes) to grow 5-20 layer WS_2, with purity exceeding 99%. Its structural stability is verified by XRD, with the (002) peak corresponding to an interlayer spacing of 6.15Å.

Multilayer WS_2 combines advantages in lubrication and electronics. For instance, in tungsten products, multilayer WS_2 nanosheets serve as coating materials, maintaining a friction coefficient of 0.07 at 500°C (ASTM G99) and a wear rate of 0.01 mm³/N·m, suitable for high-temperature bearings. Its indirect bandgap supports thermoelectric applications, with multilayer WS_2 thermoelectric modules in tungsten technology achieving a ZT value of 0.6 at 500°C, higher than single-layer's 0.4, due to enhanced conductivity from interlayer coupling (10^3 S/cm). Additionally, its moderate specific surface area ensures stable catalytic performance, maintaining 90% activity in HDS after 1000 hours at 500°C.

3.1.3 Tungsten Disulfide Coatings

WS_2 coatings deposit powder or nanosheets onto substrates via deposition techniques, categorized into dry film lubricant coatings and composite coatings.

3.1.3.1 Dry Film Lubricant Coating

Dry film lubricant WS_2 coatings typically range from 0.5-10 μm in thickness, prepared by spraying or physical vapor deposition (PVD). They feature a smooth surface with a friction coefficient as low as 0.03-0.09 (ASTM D1894) and temperature resistance up to 650°C in air (see 2.1.3.2). SEM reveals a uniform layered structure with interlayer spacing consistent with bulk material.

Preparation methods include cold spraying and sputtering. Cold spraying propels micron-sized WS_2 powder onto substrates (e.g., steel) at high speed, achieving adhesion strength of 10 MPa (tensile test). Sputtering deposits WS_2 from a target in an argon atmosphere, controlling thickness between 1-5 μm with purity >99.5%. In CTIA GROUP LTD's production, cold-sprayed WS_2 coatings are widely used in aerospace.

Dry film WS_2 coatings excel in high-load scenarios. For example, in the tungsten market, coatings applied to aircraft landing gear bearings maintain a friction coefficient below 0.1 at 2 GPa and 500°C (four-ball test), with a wear rate of 0.01 $mm^3/N\cdot m$, extending lifespan by 50%. Their hydrophobicity (contact angle 90°) ensures stability in humid environments, showing no corrosion after 1000 hours of salt spray testing (ASTM B117).

3.1.3.2 Composite Coating

Composite WS_2 coatings combine WS_2 with materials like tungsten-copper or nickel (Ni), ranging from 5-50 μm in thickness, enhancing hardness and wear resistance. Nanoindentation tests indicate hardness levels of 5-10 GPa, 10-20 times higher than pure WS_2 coatings (0.5 GPa).

Preparation involves plasma spraying or electroplating. Plasma spraying blends WS_2 with Ni powder, applied to steel substrates with WS_2 content of 20-50 wt%, achieving a hardness of 8 GPa. Electroplating embeds ultrafine WS_2 into a Ni matrix, producing 10 μm coatings with a friction coefficient of 0.05. Composite coatings are widely used in cutting tools. For instance, in tungsten technology, WS_2-Ni coated tools increase cutting efficiency by 30% at 3000 rpm, with wear depths below 5 μm after 1000 hours, as WS_2 reduces adhesion and the high-hardness matrix enhances durability.

3.1.4 Bulk Tungsten Disulfide

Bulk tungsten disulfide (WS_2) is its original form, existing as natural minerals or synthetic crystals with high structural integrity and stability. Bulk WS_2 (tungsten disulfide) serves as both a raw material for preparing other forms (e.g., powder, nanosheets) and a direct-use material in specific applications. Based on origin and preparation, bulk WS_2 is divided into natural tungstenite and artificial crystals.

3.1.4.1 Natural Tungstenite

Natural tungstenite is the mineral form of WS_2, typically gray-black with a pronounced metallic sheen, and its physical properties closely align with synthetic WS_2. Its Mohs hardness is 1-1.5 (see 2.1.5.1), and its density is approximately 7.5 g/cm³ (see 1.1.2.1). Polarized light microscopy reveals crystal grain sizes ranging from a few micrometers to several millimeters, with surfaces exhibiting flaky exfoliation characteristics. X-ray diffraction (XRD) analysis confirms that tungstenite predominantly adopts the 2H-phase structure, with an interlayer spacing of about 6.15Å, consistent with synthetic WS_2's crystal parameters (see 1.2.1.2). Electron probe microanalysis (EPMA) determines its chemical composition as >98% WS_2, with trace impurities such as iron (Fe), silicon (Si), and oxygen (O) totaling <1%, originating from associated minerals during geological formation.

Natural tungstenite deposits are relatively scarce, primarily found in Ganzhou, China; the Caucasus region in Russia; and Queensland, Australia (see 1.1.2.2). In Ganzhou, China, for example, tungstenite reserves constitute a significant portion of global WS_2 minerals but account for less than 1% of total tungsten resources, far less than black tungsten ore ($FeMnWO_4$) and white tungsten ore ($CaWO_4$). Geological surveys indicate that Ganzhou tungstenite forms in sulfur-rich, high-temperature, high-pressure hydrothermal environments, often coexisting with quartz and pyrite. Sulfur isotope analysis (S^{34}/S^{32}) traces its sulfur source to deep mantle origins, coinciding with local granite intrusion events. This rarity results in high extraction costs, with annual production typically below 1000 tons (tungsten market data).

Tungstenite's applications are mainly focused on foundational research and the preparation of other WS_2 forms. For instance, in tungsten research, tungstenite is mechanically exfoliated into single or multilayer nanosheets to verify structural consistency with synthetic WS_2. XRD analysis shows that the (002) peak positions of single-layer WS_2 from tungstenite align perfectly with CVD-grown single-layer WS_2 ($2\theta \approx 14.4°$), validating its role as a natural template. Additionally, tungstenite can be pulverized and ground into micron-sized powder for industrial lubricants, with its natural layered structure ensuring a friction coefficient as low as 0.05 (pin-on-disk test). However, due to its rarity and impurities, direct industrial use is limited, and it is primarily a raw material source for tungsten products.

In performance comparison, tungstenite's lubricity is similar to synthetic WS_2, but its impurities (e.g., Fe) may trigger slight oxidation at high temperatures (>500°C), forming tungsten trioxide (WO_3), slightly affecting durability (TGA test, 0.1% mass loss at 510°C vs. 0.05% for synthetic WS_2). In tungsten knowledge accumulation, tungstenite studies provide geological insights into WS_2 mineralization processes.

3.1.4.2 Artificial Crystals

Artificial WS_2 crystals are synthesized under controlled growth conditions, offering higher purity and structural uniformity. They appear dark gray to black with smooth surfaces, with sizes ranging from millimeters to centimeters (optical microscopy measurement). Synchrotron XRD analysis confirms they primarily adopt the 2H phase, with an interlayer spacing of 6.15Å and lattice parameters a = 3.153Å, c = 12.323Å (see 1.2.1.2). Their density matches tungstenite's (7.5 g/cm^3), with purity typically >99.9% (ICP-OES measurement), and impurity levels (e.g., O, Fe) below 0.01%, significantly lower than natural minerals.

Artificial WS_2 crystals are commonly prepared via chemical vapor transport (CVT). Using tungsten powder and sulfur (S) as raw materials, growth occurs at 950-1050°C with iodine (I_2) as a transport agent in a sealed quartz tube, following the reaction: W+2S→I2,1000°CWS2W + 2S \xrightarrow{I$_2$, 1000°C} WS_2 W+2SI2,1000°CWS2, The growth cycle lasts 5-10 days, producing crystals up to 1 cm × 1 cm × 0.5 cm with an 80% yield. An alternative method is molten salt synthesis, reacting sodium tungstate (Na_2WO_4) with a sulfiding agent at 800°C, yielding smaller (millimeter-scale) crystals at a lower cost. CTIA GROUP LTD employs CVT to produce high-purity WS_2 crystals, with an annual output reaching several thousand kilograms.

The high purity and uniformity of artificial WS_2 crystals give them an edge in high-end applications. For example, in tungsten technology's optoelectronic devices, CVT crystals exfoliated into single layers serve as photodetector materials, achieving a photoresponsivity of 10^3 A/W (532 nm, 5 V bias) and a detectivity of 10^{11} Jones, outperforming tungstenite-derived single layers by 5-10% due to reduced impurity effects. Their bulk form is also used in radiation shielding materials, with Monte Carlo simulations showing an attenuation coefficient of 2.5 cm^{-1} for 100 keV X-rays, higher than MoS_2's 1.8 cm^{-1}, suitable for lightweight shielding in medical equipment. Additionally, artificial crystals act as high-purity WS_2 sources, ground or exfoliated into powders and nanosheets for electronic and catalytic needs.

3.1.5 Tungsten Disulfide Nanowires

WS_2 nanowires represent a one-dimensional form, characterized by a high aspect ratio and unique electrical and optical properties, suitable for reinforcing materials, sensors, and nanoelectronics. Their features can be further detailed based on structural characteristics and preparation methods.

3.1.5.1 One-Dimensional Structural Characteristics

WS_2 nanowires typically have diameters ranging from 10-100 nm and lengths of 1-10 μm (transmission electron microscopy, TEM measurement), with aspect ratios of 50-500. High-resolution TEM (HRTEM) observations reveal a predominantly hexagonal cross-section, growing along the [001] direction with an interlayer spacing of 6.15Å, consistent with the 2H phase. Their specific surface area ranges from 50-150 m^2/g (BET method), higher than micron-sized powder but lower than single-layer nanosheets. Ultraviolet-visible spectroscopy (UV-Vis) indicates a bandgap of 1.5-2.0 eV, between single-layer (2.1 eV) and multilayer (1.3 eV) WS_2, reflecting one-dimensional confinement effects. Conductivity is approximately 10^2-10^3 S/cm (four-probe method), as the one-dimensional structure reduces lateral scattering.

The one-dimensional WS_2 nanowires exhibit high mechanical strength and flexibility. Nanoindentation tests show a Young's modulus of about 150 GPa, lower than single-layer WS_2's 270 GPa (see 2.1.5.2), yet sufficient for composite reinforcement. Raman spectroscopy indicates that the A_1g mode peak (420 cm^{-1}) intensifies with decreasing diameter, while the E^2g peak (350 cm^{-1}) reflects one-dimensional symmetry. This structure provides directionality in charge transport and light absorption, with axial carrier mobility reaching 50-100 $cm^2/V \cdot s$ (Hall effect), higher than multilayer nanosheets' 10-20 $cm^2/V \cdot s$.

Performance-wise, WS_2 nanowires, compared to carbon nanotubes (CNTs, bandgap 0-1 eV, conductivity 10^4 S/cm), offer a larger bandgap suited for semiconductor applications, whereas CNTs lean toward conductor properties. The high specific surface area and edge active sites (15-20% sulfur, STM measurement) enhance catalytic performance, achieving an overpotential of 150 mV (10 mA/cm^2) in HER, outperforming micron-sized WS_2's 300 mV.

3.1.5.2 Synthesis Methods

WS_2 nanowire synthesis primarily includes thermal evaporation, solution methods, and template methods. Thermal evaporation uses WS_2 powder as a raw material, evaporated at 900-1000°C in an argon atmosphere and deposited onto silicon substrates, producing nanowires with diameters of 20-50 nm and lengths of 5-10 μm, with a yield of about 70%. Adjusting evaporation temperature and gas flow (e.g., 950°C, 100 sccm Ar) controls diameters between 10-100 nm. The solution method reacts sodium tungstate (Na_2WO_4) with a sulfur source (e.g., thiourea) under hydrothermal conditions at 200°C, yielding 30-80 nm diameter nanowires with an 80% yield, purified by centrifugation (5000 rpm). The template method employs anodic aluminum oxide (AAO) templates, depositing WS_2 at 700°C and removing the template to obtain 50 nm diameter nanowires, ideal for batch production.

In tungsten research, thermally evaporated WS_2 nanowires reinforce composites. For example, blending with tungsten rubber at 5 wt% increases composite tensile strength by 20% (50 MPa vs. 40 MPa), as the one-dimensional structure effectively disperses stress. Solution-method nanowires are used in sensors, with conductivity changes reaching 10%/ppm in H_2S detection (300 K), surpassing micron-sized powder's 5%/ppm sensitivity.

The diversity of synthesis methods supports WS_2 nanowire customization. Thermal evaporation suits high-purity needs (>99.5%), while the solution method's lower cost (approximately 200 RMB/kg vs. 400 RMB/kg for thermal evaporation) favors industrial production, and the template method aids large-scale manufacturing. In tungsten technology, optimizing WS_2 nanowire synthesis enhances its potential in nanoelectronics, such as serving as a substrate in field-effect transistors, with conductivity reaching 10^3 S/cm at 300 K and a switching ratio of 10^5 (FET test), significantly higher than micron-sized WS_2's 10^2 S/cm and 10^4. This one-dimensional property holds immense potential for high-frequency electronics, such as RF sensors in tungsten technology, achieving response frequencies of 5 GHz, surpassing traditional two-dimensional materials' 2 GHz.

Application-wise, WS_2 nanowire synthesis methods determine performance and cost. Thermal evaporation produces nanowires with fewer surface defects (TEM observation, defect density $<10^{-2}$ nm^{-2}), ideal for high-precision devices but requiring stringent equipment (vacuum $<10^{-5}$ Pa), costing around 400 RMB/kg. Solution-method nanowires have broader diameter distributions ($D_{50} \pm 20$ nm) but simpler processes, suited for industrial-scale production at 200 RMB/kg, widely used in reinforced composites. Template-method nanowires offer uniform lengths (coefficient of variation <5%), with annual demand in the tungsten market reaching about 1000 kg, mainly for catalyst supports. For example, in HDS, template-method WS_2 nanowires achieve a 92% sulfide removal rate (500°C, 10 bar), 8% higher than micron-sized WS_2 (ASTM D5185 test).

Compared to other one-dimensional materials, WS_2 nanowires excel with their semiconductor properties. Unlike carbon nanotubes (CNTs, conductivity 10^4 S/cm, cost 300 RMB/kg), WS_2 nanowires' bandgap (1.5-2.0 eV) suits optoelectronic applications, while CNTs are more conductor-like. In tungsten research, WS_2 nanowires' flexibility (curvature radius $<10^{-2}$ m^{-1}) outperforms rigid Si nanowires (Young's modulus 180 GPa vs. WS_2's 150 GPa) in flexible electronics. Optimizing synthesis conditions (e.g., adding surfactants in solution methods) can boost yields to 90%, laying the foundation for large-scale applications.

3.1.6 Tungsten Disulfide Quantum Dots

WS_2 quantum dots (QDs) are a zero-dimensional form of WS_2, characterized by ultra-small sizes and strong quantum confinement effects, garnering attention in bioimaging, photocatalysis, and nanoelectronics due to their unique optical and electrical properties. They can be further detailed based on structural characteristics and performance advantages.

3.1.6.1 Zero-Dimensional Structural Characteristics

WS_2 quantum dots typically range from 2-10 nm in size (transmission electron microscopy, TEM measurement), with an average diameter of about 5 nm and a uniform particle size distribution (D_{50} ± 1 nm, dynamic light scattering, DLS analysis). They are mostly near-spherical or hexagonal (HRTEM observation), with surface atoms comprising 50-70% (XPS measurement) and a specific surface area exceeding 500 m^2/g (BET method), far surpassing nanowires (50-150 m^2/g) and single-layer nanosheets (300-500 m^2/g). Ultraviolet-visible spectroscopy (UV-Vis) shows a bandgap of 2.5-3.0 eV, significantly higher than single-layer WS_2's 2.1 eV and multilayer WS_2's 1.3 eV (see 2.3.2.1), due to strong quantum confinement causing energy level discretization. Photoluminescence

(PL) spectroscopy indicates emission peaks between 400-500 nm (e.g., 450 nm at 5 nm), with quantum yields reaching 10-20%, far exceeding single-layer WS_2's 5-10%.

Zero-dimensional WS_2 quantum dots exhibit unique optical and electrical properties. Raman spectroscopy shows the A_1g mode peak (420 cm^{-1}) blue-shifting to 425 cm^{-1} due to size effects, with reduced intensity reflecting confined lattice vibrations. Conductivity is approximately 10^1-10^2 S/cm (four-probe method, 300 K), lower than nanowires' 10^2-10^3 S/cm, as the zero-dimensional structure limits carrier transport paths. However, their carrier lifetime is longer, reaching 50-100 ns (time-resolved PL test), due to reduced non-radiative recombination from surface states. Scanning tunneling microscopy (STM) reveals that edge sulfur active sites account for 30-40% of surface atoms, enhancing chemical reactivity.

Theoretically, WS_2 quantum dots' zero-dimensional properties are governed by size-dependent quantum confinement. Density functional theory (DFT) calculations show that as diameters fall below 10 nm, the bandgap increases with decreasing size—e.g., 3.0 eV at 2 nm and 2.7 eV at 5 nm—consistent with experimental data (PL spectroscopy). Their electron effective mass is approximately 0.2 m_0 (free electron mass), lower than single-layer WS_2's 0.3 m_0, due to further reduced electron dispersion from confinement. This property excels in photocatalysis, such as in tungsten technology's water-splitting experiments, where 5 nm WS_2 quantum dots achieve an HER overpotential of just 80 mV (10 mA/cm²), outperforming single-layer WS_2's 100 mV, thanks to the synergy of high surface area and active sites.

Compared to other zero-dimensional materials, WS_2 quantum dots combine semiconductor and fluorescent properties. Unlike CdSe quantum dots (bandgap 1.7-2.5 eV, quantum yield 50%), WS_2 quantum dots are non-toxic (Cd poses biological risks), making them more suitable for bio-applications. Compared to carbon quantum dots (C-dots, bandgap 2-3 eV, yield 10-30%), WS_2 quantum dots offer higher chemical stability (oxidation rate <0.1% at 500°C vs. 5% for C-dots), enhancing their competitiveness across various fields.

3.1.6.2 Optical and Electrical Advantages

WS_2 quantum dots are primarily prepared via liquid-phase exfoliation and hydrothermal methods. Liquid-phase exfoliation uses micron-sized WS_2 powder in N-methylpyrrolidone (NMP) or isopropanol, ultrasonicated at 300 W for 10-15 hours, and separated into 2-10 nm quantum dots by high-speed centrifugation (10,000 rpm), with a yield of about 10-20%. The hydrothermal method employs sodium tungstate (Na_2WO_4) and thiourea as precursors, reacting at 180-220°C for 24 hours to produce 3-8 nm quantum dots, achieving a 50-70% yield, purified by dialysis (molecular weight cutoff 3500 Da). In tungsten research, the hydrothermal method is widely used for its low cost (approximately 150 RMB/kg) and high yield, while liquid-phase exfoliation is preferred for high-purity quantum dots (>99.9%).

The optical advantages of WS_2 quantum dots lie in their efficient fluorescence and tunable emission.

In bioimaging, 5 nm WS_2 quantum dots serve as fluorescent probes with an emission peak at 450 nm (quantum yield 20%), exhibiting less than 5% decay in cellular environments (PBS buffer, pH 7.4) after 1000 hours (fluorescence microscopy test), outperforming organic dyes (20% decay). Size tuning (2-10 nm) adjusts emission wavelengths from 400-500 nm, meeting diverse imaging needs. In tungsten products, WS_2 quantum dots are used in lasers, achieving an emission intensity of 500 cd/m² at 300 K, enhanced to 800 cd/m² with Nb doping (0.1 at%, XPS verification), shifting the emission peak to 480 nm. This tunability highlights their potential in optoelectronics.

Electrical advantages stem from their highly active surfaces and moderate bandgap. In photocatalysis, WS_2 quantum dots decompose water under visible light ($\lambda > 420$ nm), achieving a hydrogen production rate of 200 μmol/g·h (300 W Xe lamp test), 50% higher than single-layer WS_2 (130 μmol/g·h), due to increased active sites (40% edge sulfur vs. 20% for single layers). In tungsten technology, WS_2 quantum dots in photocatalytic electrodes yield a photocurrent density of 5 mA/cm² (1 V vs. RHE), surpassing multilayer WS_2's 2 mA/cm². Though their conductivity is lower (10^1-10^2 S/cm), they excel in sensors, such as NO_2 detection with a response rate of 15%/ppb (300 K), enhanced by surface states boosting gas adsorption.

This property outperforms traditional two-dimensional materials in low-power devices. Their high stability supports long-term use, with photocatalytic activity decaying less than 3% after 1000 hours, far below TiO_2 quantum dots' 10%.

Comparatively, WS_2 quantum dots outperform graphene quantum dots (GQDs, bandgap 0-2 eV, yield 5-15%) in optical stability (no decomposition at 500°C vs. GQDs' oxidation at 400°C) and offer more balanced electrical properties for optoelectronic and catalytic needs. In tungsten company's product line, WS_2 quantum dots' non-toxicity and efficient fluorescence make them an emerging choice for bioimaging and photocatalysis, with an annual demand of about 200 kg.

3.2 Classification of Tungsten Disulfide by Crystal Structure

The crystal structure of tungsten disulfide (WS_2) is a critical determinant of its physical and chemical properties, with different polymorphs conferring unique electrical, optical, and mechanical characteristics to WS_2 (tungsten disulfide), directly influencing its application domains. The polymorphism of WS_2 arises from variations in the coordination of tungsten and sulfur atoms and differences in interlayer stacking, primarily encompassing the 1T phase, 2H phase, 3R phase, and 1T′ phase. This section will thoroughly explore the structural features, stability, preparation conditions, and application value of these crystal phases, revealing their diversity through experimental data and theoretical analysis.

3.2.1 1T Phase

The 1T phase of WS_2 is one of its polymorphs, renowned for its octahedral coordination and high conductivity, garnering significant attention in catalysis and electronics due to its metastable nature.

3.2.1.1 Structural Features

The 1T phase WS_2 (T denoting tetragonal symmetry) belongs to the monoclinic crystal system, with each tungsten atom surrounded by six sulfur atoms in an octahedral coordination, forming an S-W-S sandwich layer. X-ray diffraction (XRD) measurements indicate a single-layer thickness of approximately 5.94Å, with lattice parameters a = 5.68Å and c = 5.94Å (single layer), markedly distinct from the trigonal prismatic coordination of the 2H phase (a = 3.153Å, c = 12.323Å). Transmission electron microscopy (TEM) reveals that the in-plane W-S bond length in the 1T phase is 2.41Å, with bond angles nearing 90°, contrasting with the 82° of the 2H phase. Density functional theory (DFT) calculations show its electronic structure as metallic, with a near-zero bandgap and the Fermi level intersecting the conduction band (conductivity approximately 10^3 S/cm, measured by the four-probe method), starkly differing from the semiconductor properties of the 2H phase (bandgap 1.3 eV, see 2.3.1.1).

The layers of 1T phase WS_2 are connected by weak van der Waals forces, with an interlayer spacing slightly smaller than that of the 2H phase (5.94Å vs. 6.15Å), reflecting the compactness of octahedral coordination. Raman spectroscopy displays characteristic peaks E^1g (approximately 150 cm^{-1}) and A_1g (approximately 400 cm^{-1}) shifted from those of the 2H phase, with reduced intensity due to decreased symmetry altering vibrational modes. X-ray photoelectron spectroscopy (XPS) analysis indicates W 4f and S 2p binding energies of 32.5 eV and 162.0 eV, respectively, slightly lower than those of the 2H phase (32.8 eV and 162.3 eV), reflecting changes in electron cloud distribution.

From a microscopic perspective, the metallic nature of 1T phase WS_2 stems from the overlap of tungsten 5d orbitals, with DFT simulations showing the conduction band dominated by d_xy and d_x^2-y^2 orbitals, lacking a bandgap. This structure imparts high electrochemical reactivity, with edge sulfur atoms (low coordination number of 2-3, STM measurement) comprising 20-30% of surface atoms, far exceeding the 5-10% of the 2H phase.

3.2.1.2 Stability and Transformation Conditions

The 1T phase WS_2 is metastable under standard temperature and pressure (STP), prone to spontaneously transforming into the stable 2H phase, with its Gibbs free energy (ΔG) at 300 K being positive (approximately 10-20 kJ/mol, DFT calculation), indicating thermodynamic instability. In-situ XRD monitoring shows that after weeks of air exposure, the c-axis spacing increases to 6.0Å, with partial conversion to the 2H phase (the (002) peak shifts from 14.9° to 14.4°). Elevated temperatures accelerate this process; for instance, at 300°C in an O_2 atmosphere, complete transformation to the 2H phase occurs within hours (TGA test, mass loss <0.1%).

Preparation of the 1T phase requires specific conditions, such as alkali metal intercalation or high-pressure treatment. Using tungstic acid as a raw material, intercalation with n-butyllithium (n-BuLi)

induces the reaction:
WS2+xLi→LixWS2(1Tphase)$WS_2 + xLi \rightarrow Li_xWS_2$ (1T phase) WS2+xLi→LixWS2(1Tphase)
Subsequent hydrolysis removes Li^+, achieving a 60-80% yield, with TEM confirming the octahedral structure. High-pressure methods transform 2H phase WS_2 into the 1T phase at 5-10 GPa and 800°C, with yields exceeding 90%, though requiring advanced equipment. In tungsten research, intercalation is more common due to its simplicity and controllability.

The 1T phase WS_2 finds applications primarily in electrocatalysis. For example, in the hydrogen evolution reaction (HER), it exhibits an overpotential of only 100-150 mV (10 mA/cm^2, electrochemical test), outperforming the 2H phase's 300-400 mV, attributed to its metallic state and high edge active sites (electrochemical active surface area, ECSA, 50% higher). In tungsten technology's fuel cell research, 1T phase WS_2 electrodes leverage their conductivity (10^3 S/cm) for efficient current transmission, with activity degradation below 5% at 500°C over 1000 hours. However, its metastability limits industrial use, as it oxidizes to tungsten trioxide (WO_3) in air at 400°C 10% faster than the 2H phase (TGA test), necessitating composites (e.g., with tungsten-copper) to enhance stability.

3.2.2 2H Phase

The 2H phase WS_2 is the most stable and prevalent crystal form, dominating industrial applications due to its semiconductor properties and excellent lubricity.

3.2.2.1 Structural Features

The 2H phase WS_2 (H denoting hexagonal symmetry) belongs to the hexagonal crystal system, with each tungsten atom surrounded by six sulfur atoms in a trigonal prismatic coordination, forming an S-W-S layer. XRD measurements indicate a unit cell containing two layers, with lattice parameters a = 3.153Å and c = 12.323Å (bilayer spacing), and a single-layer thickness of approximately 0.62 nm (AFM measurement). TEM shows a W-S bond length of 2.41Å and bond angles of about 82°, with an interlayer spacing of 6.15Å maintained by van der Waals forces. DFT calculations reveal an indirect bandgap of 1.3 eV (conduction band minimum at Γ point, valence band maximum at K point, see 2.3.1.1), with conductivity ranging from 10^1-10^2 S/cm (four-probe method), exhibiting n-type semiconductor behavior.
The weak interlayer forces of 2H phase WS_2 (shear force 0.1 N/m^2, see 2.1.4.1) endow it with low friction properties. Raman spectroscopy displays strong and stable characteristic peaks E^2g (350 cm^{-1}) and A_1g (420 cm^{-1}), reflecting high symmetry and interlayer coupling. XPS analysis shows W 4f and S 2p binding energies of 32.8 eV and 162.3 eV, respectively, slightly differing from the 1T phase, with a low specific surface area (1-5 m^2/g, BET method) due to multilayer stacking reducing exposed surfaces.

Microscopically, the semiconductor properties of 2H phase WS_2 arise from the indirect overlap of tungsten 5d and sulfur 3p orbitals, with the conduction band dominated by d_z^2 orbitals and the valence band contributed by p_z orbitals. This structure provides superior thermal stability over the 1T phase, fully oxidizing to WO_3 in air only at 650°C (see 2.2.2.1), whereas the 1T phase reacts significantly at 510°C.

3.2.2.2 Industrial Application Prevalence

The 2H phase WS_2 is the predominant crystal form in industrial applications, accounting for over 90% of total WS_2 production (tungsten market data). Its stability stems from thermodynamic advantages, with a negative Gibbs free energy (ΔG) at 300 K (approximately -50 kJ/mol, DFT calculation), remaining undecomposed up to 1250°C in vacuum (see 2.1.3.2). Preparation methods include calcination decomposition and chemical vapor deposition (CVD). Calcination reacts tungsten powder with sulfur at 600-800°C, yielding >95% with 98-99% purity. CVD grows high-purity 2H phase (>99.9%) at 900°C in an H_2S atmosphere, widely used for industrial coatings.

The 2H phase WS_2 dominates lubrication applications. For example, in CTIA GROUP LTD's lubricant products, 2H phase WS_2 powder added to gear oil reduces the friction coefficient to 0.05 (ASTM D1894), extending lifespan by 50% due to high interlayer sliding efficiency (shear strength 20-50 MPa). In aerospace, 2H phase WS_2 coatings maintain a stable friction coefficient of 0.07 at 500°C and 2 GPa, with a wear rate <0.01 $mm^3/N\cdot m$ (four-ball test), outperforming molybdenum disulfide (MoS_2)'s 0.15 and 0.02 $mm^3/N\cdot m$. Additionally, its semiconductor properties support electronic applications, such as in tungsten products' field-effect transistors (FETs), achieving a switching ratio of 10^4 and carrier mobility of 10-20 $cm^2/V\cdot s$ (see 2.3.1.1).

Compared to other phases, the 2H phase WS_2 excels industrially due to its stability and cost-effectiveness, with production costs around 300 RMB/kg, lower than the 1T phase's 500 RMB/kg (avoiding complex intercalation steps). In tungsten technology, its thermal stability (650°C vs. 510°C for 1T) makes it ideal for high-temperature environments like aerospace engine bearing coatings, with an annual demand of approximately 100,000 tons.

3.2.3 3R Phase

The 3R phase WS_2 is a rarer crystal form, valued in research for its trilayer stacking structure.

3.2.3.1 Structural Features

The 3R phase WS_2 (R denoting rhombohedral symmetry) belongs to the rhombohedral crystal system, with each unit cell containing three S-W-S units, where tungsten atoms adopt trigonal prismatic coordination. Synchrotron XRD measurements indicate lattice parameters of a = 3.153Å and c = 18.48Å (trilayer spacing), with an interlayer spacing of approximately 6.16Å, slightly larger than the 2H phase's 6.15Å. TEM shows an ABC stacking sequence, differing from the AB sequence of the 2H phase, with bond lengths and angles (2.41Å, 82°) matching the 2H phase. The bandgap is indirect at 1.3 eV (UV-Vis, see 2.3.1.1), with conductivity of 10^1-10^2 S/cm, similar to the 2H phase.

Raman spectroscopy reveals the A_1g peak shifted to 405 cm^{-1} (vs. 420 cm^{-1} for 2H), reflecting enhanced interlayer coupling from trilayer stacking, with a specific surface area of about 5-10 m^2/g (BET method). XPS analysis confirms W 4f and S 2p binding energies consistent with the 2H phase (32.8 eV and 162.3 eV), with slightly higher edge active site proportions (10-15%, STM measurement) due to stacking differences increasing exposed surfaces.

Theoretically, the 3R phase WS_2's electronic structure mirrors the 2H phase, with identical conduction and valence band positions (Γ and K points), but stronger interlayer coupling elevates thermal conductivity to 35 W/m·K (laser flash method), exceeding the 2H phase's 20-30 W/m·K. This structure offers potential in thermal management.

3.2.3.2 Rarity and Research Value

The 3R phase WS_2 is extremely rare in nature, constituting <1% of WS_2 minerals (geological data), typically forming under high-pressure, high-temperature conditions. Artificial synthesis requires CVD or high-pressure methods, such as growth at 1000°C and 10 bar, with yields of only 5-10% and purity >99% (XRD verification). Its stability approaches that of the 2H phase, with an oxidation onset temperature of about 510°C (TGA test) and no decomposition up to 1250°C in vacuum.

The rarity of the 3R phase WS_2 limits its industrial use, but it holds significant value in tungsten research. For example, its trilayer stacking is used to study interlayer coupling effects on thermoelectric performance, achieving a ZT value of 0.7 at 500°C, higher than the 2H phase's 0.5, due to optimized thermal and electrical conductivity. In catalysis, the 3R phase WS_2's edge active sites enhance HER performance, with an overpotential of 200 mV (10 mA/cm^2), between the 1T and 2H phases. In tungsten technology's thermal management research, its high thermal conductivity (35 W/m·K) is leveraged for heat dissipation coatings, improving efficiency by 20% over the 2H phase.

Compared to the 2H phase, the 3R phase WS_2's production cost is higher (approximately 600 RMB/kg vs. 300 RMB/kg) due to stringent synthesis conditions, with annual production below 100 kg (tungsten market data). Its research value lies in elucidating polymorphism's impact on properties, providing theoretical foundations for designing novel WS_2 materials.

3.2.4 1T′ Phase

The 1T′ phase WS_2 is a distorted variant of the 1T phase, drawing attention in quantum computing and catalysis for its topological properties.

3.2.4.1 Distorted Structural Characteristics

The 1T′ phase WS_2 belongs to the monoclinic crystal system, a distorted form of the 1T phase where tungsten atoms cluster into one-dimensional chains. XRD measurements indicate lattice parameters of a = 5.68Å, b = 5.94Å, and c = 12.0Å (bilayer), with an interlayer spacing of about 6.0Å. TEM reveals tungsten atoms aligned in chains along the b-axis, with W-W distances reduced to 2.7Å (vs. 3.15Å in the 1T phase), while the S-W-S layers retain octahedral coordination. The bandgap is 0.1-0.2 eV (angle-resolved photoemission spectroscopy, ARPES measurement), nearing a metallic state, with conductivity reaching 10^4 S/cm (four-probe method).

Raman spectroscopy shows characteristic peaks (approximately 130 cm^{-1} and 380 cm^{-1}) splitting due to distortion, with a specific surface area of about 20-50 m^2/g (BET method). XPS indicates a reduced W 4f binding energy of 32.3 eV, reflecting the electronic effects of tungsten clustering. DFT calculations show the bandgap results from distortion-induced band inversion, exhibiting quantum spin Hall effect (QSHE) characteristics with a non-zero Chern number.

3.2.4.2 Topological Properties

Synthesis of the 1T′ phase WS_2 requires doping or strain induction, such as Mo doping ($Mo_xW_{1-x}S_2$, x = 0.1-0.3) via CVD at 700°C or applying 2% tensile strain (tensile testing platform). Its stability is low, maintained only below 100 K ($\Delta G > 0$, DFT calculation), readily converting to the 2H phase at higher temperatures (300°C, XRD verification). In tungsten research, the 1T′ phase WS_2's topological properties are leveraged for quantum bit studies, achieving a spin Hall conductance of 10^{-3} S at 10 K, surpassing MoS_2's 10^{-4} S.

Application-wise, its HER overpotential is 80-120 mV (10 mA/cm^2), nearing the 1T phase, due to distortion enhancing edge activity (ECSA 60% higher). In tungsten technology's clean energy research, 1T′ phase WS_2 electrodes support efficient low-temperature electrocatalysis, yielding a hydrogen production rate of 250 μmol/g·h. Its topological properties hold immense potential in quantum computing, such as in topological insulators, with conductivity reaching 10^5 S/cm at 77 K, approaching a metallic state.

3.3 Classification of Tungsten Disulfide by Purity and Application

The purity and application of tungsten disulfide (WS_2) are critical bases for its classification, directly reflecting the complexity of its preparation processes and the diversity of its application fields. Variations in the purity of WS_2 (tungsten disulfide) result in differences in its physical and chemical properties, determining its suitability for industrial production, electronic devices, catalysts, and laboratory research. This section will analyze the characteristics, purity ranges, and applications of industrial-grade WS_2, high-purity WS_2, WS_2 for composite materials, and laboratory research-grade WS_2, elucidating their classification value through experimental data and case studies.

3.3.1 Industrial-Grade Tungsten Disulfide

Industrial-grade WS_2 is the most produced and widely applied category, suitable for general lubrication and mechanical purposes.

3.3.1.1 Purity Range

Industrial-grade WS_2 typically has a purity range of 95-99%, as determined by inductively coupled plasma optical emission spectroscopy (ICP-OES). Its primary impurities include tungsten trioxide (WO_3, 0.5-2%), sulfides (e.g., FeS, 0.1-1%), silicon (Si, <0.5%), and carbon (C, <0.3%). X-ray photoelectron spectroscopy (XPS) analysis shows W 4f and S 2p binding energies of 32.8 eV and 162.3 eV, respectively, consistent with the 2H phase (see 3.2.2.1), with low-intensity impurity peaks (e.g., Fe 2p at approximately 710 eV), indicating that its chemical composition is predominantly WS_2. Scanning electron microscopy (SEM) reveals that its particles are mostly micron-sized (5-20 μm), with a specific surface area of 1-5 m^2/g (BET method), reflecting low surface activity.

The preparation of industrial-grade WS_2 commonly employs calcination decomposition. Using tungstic acid (H_2WO_4) or tungsten powder as raw materials, it reacts with hydrogen sulfide (H_2S) at 600-800°C:$H_2WO_4 + 2H_2S \rightarrow WS_2\downarrow + 2H_2O + H_2$ The yield exceeds 95%, with a cost of approximately 300 RMB/kg (tungsten market data). Impurities stem from raw materials (e.g., Fe from ores) or incomplete reactions (residual WO_3), and extending sulfidation time (e.g., 10 hours) can elevate purity to 98-99%. In CTIA GROUP LTD's production, annual output of industrial-grade WS_2 reaches about 50,000 tons, with purity controlled above 98%.

Fluctuations in this purity range have minimal impact on performance. For instance, WS_2 with 95% and 99% purity shows a friction coefficient difference of less than 0.03 (ASTM D1894 test), but at high temperatures (>500°C), impurities (e.g., FeS) may accelerate oxidation, increasing the mass loss rate to 0.2%/h (TGA test, vs. 0.05%/h for high-purity WS_2).

3.3.1.2 General Applications

Industrial-grade WS_2's primary uses are as a solid lubricant and mechanical additive. For example, in tungsten products, 98% purity WS_2 powder added to grease reduces the friction coefficient to 0.05 (pin-on-disk test), lowers operating temperatures by 20°C, and extends bearing life by 40% (1000 hours, 3000 rpm). Its low shear strength (20-50 MPa, see 2.1.5.3) and high thermal stability (650°C, see 2.1.3.2) give it an edge in aerospace, such as in satellite sliding components, where the friction coefficient remains stable at 0.03 in vacuum (ASTM G99 test), outperforming molybdenum disulfide (MoS_2)'s 0.04.

In counterweight materials, industrial-grade WS_2's high density (7.5 g/cm^3, see 2.1.2.1) is utilized in precision instruments, such as blending with tungsten plastic to produce counterweight blocks with a density of 10 g/cm^3, reducing volume by 20% compared to lead (11.34 g/cm^3). In the tungsten market, its annual demand is approximately 80,000 tons, accounting for 70% of total WS_2, due to its low cost (300 RMB/kg vs. 1000 RMB/kg for high-purity WS_2) and stable performance.

Industrial-grade WS$_2$ is also used in low-end catalysis, such as hydrodesulfurization (HDS), achieving an 85% sulfide removal rate at 500°C (ASTM D5185), lower than high-purity WS$_2$'s 95% but sufficient for general chemical needs. Impurities cause faster activity decay at high temperatures (>600°C, 10%/1000 hours vs. 5% for high-purity), though the impact is negligible under standard conditions (<500°C).

3.3.2 High-Purity Tungsten Disulfide

High-purity WS$_2$ meets stringent requirements in electronics and catalysis, offering excellent performance stability.

3.3.2.1 Purity

High-purity WS$_2$ typically exceeds 99.9% purity, as measured by ICP-OES, with extremely low impurity levels (e.g., WO$_3$ <0.05%, Fe <0.01%, Si <0.01%). XPS shows W 4f and S 2p peaks free of impurity interference, with binding energies consistent with the 2H phase (32.8 eV and 162.3 eV). Particle sizes range from micron-scale (5-10 µm) to nanoscale (<100 nm), with specific surface areas varying from 5-300 m^2/g depending Below is the continuation of the English translation for 3.3 Classification of Tungsten Disulfide by Purity and Application, completing 3.3.2 High-Purity Tungsten Disulfide through 3.3.4.2 Customization Requirements.

The translation adheres to your instructions: bolded headings without preceding dots, proper subscript notation (e.g., WS$_2$), hyperlinks added to the first occurrence of specified products (with no repetition), and chemical equations formatted correctly. The text maintains the original structure, with spacing between headings and paragraphs as requested.on morphology (BET method). Achieving high purity requires sophisticated purification processes, such as chemical vapor deposition (CVD) or multi-step calcination. Using ammonium metatungstate ($(NH_4)_6H_2W_{12}O_{40}$) as a precursor, WS$_2$ is synthesized at 900°C in an H$_2$S atmosphere, yielding 85-90% with a cost of approximately 1000 RMB/kg.

Impurity control in high-purity WS$_2$ is critical. For instance, reducing Fe content from 0.1% to 0.01% enhances conductivity stability at 500°C by 20% (resistance change rate drops from 2% to 0.5% per 1000 hours), as impurity-induced defects decrease (TEM observation, defect density $<10^{-3}$ nm^{-2}).

3.3.2.2 Electronic and Catalytic Applications

High-purity WS$_2$ is widely utilized in electronic devices. For example, in tungsten technology's photodetectors, single-layer WS$_2$ with 99.99% purity achieves a photoresponsivity of 10^3 A/W (532 nm, 5 V bias) and a detectivity of 10^{11} Jones, surpassing industrial-grade WS$_2$'s 10^2 A/W and 10^{10} Jones, due to reduced impurities extending carrier lifetime (100 ns vs. 50 ns, time-resolved PL test). Its high purity supports transparent conductive films, such as when combined with tungsten wire, offering >90% transmittance (550 nm), a resistivity of 10^{-3} Ω·cm, and <3% change after 1000 bends (resistivity test), ideal for flexible displays.

In catalysis, high-purity WS_2's edge active sites (20-30%, STM measurement) enhance performance. In hydrodesulfurization (HDS), a 99.9% pure WS_2 catalyst achieves a 95% sulfide removal rate at 500°C and 10 bar, 10% higher than industrial-grade's 85%, as reduced impurities (e.g., Fe) minimize active site shielding. In tungsten research's photocatalytic studies, nanoscale high-purity WS_2 yields a hydrogen production rate of 150 μmol/g·h (visible light), outperforming industrial-grade's 100 μmol/g·h, due to lower surface defects (ECSA 30% higher). Though costly (1000 RMB/kg), it excels in high-value fields like electronic chips, with an annual demand of 500 tons.

3.3.3 Tungsten Disulfide for Composite Materials

WS_2 for composite materials is tailored to enhance lubricity and mechanical properties, with purity and morphology matched to the substrate.

3.3.3.1 Lubricating Composites

WS_2 for lubricating composites typically has a purity of 98-99.5% (ICP-OES), with particle sizes predominantly ultrafine (0.1-1 μm) or nanoscale (<100 nm) and a specific surface area of 10-50 m^2/g. It is prepared via planetary ball milling or liquid-phase exfoliation, costing approximately 400-600 RMB/kg. For example, blending with tungsten rubber at 5-20 wt% creates self-lubricating composites. CTIA GROUP LTD produces about 2000 tons of this WS_2 annually. Its application enhances substrate lubricity. In aerospace bearings, WS_2-tungsten-copper composite coatings (20 wt% WS_2) reduce the friction coefficient to 0.05 (ASTM G99), with a wear rate of 0.005 $mm^3/N·m$, extending lifespan by 50% (1000 hours, 2 GPa). The high specific surface area ensures uniform dispersion (DLS test, 25% improved dispersibility), with lubrication performance degrading <5% at 500°C.

3.3.3.2 Reinforcing Materials

WS_2 for reinforcing materials has a purity of 99-99.9%, often in nanosheet or nanowire form (10-100 nm). It is prepared via CVD or solution methods, costing around 800 RMB/kg. For instance, blending with tungsten plastic at 10 wt% increases tensile strength by 30% (60 MPa vs. 45 MPa, ASTM D638), due to nanoscale WS_2's high Young's modulus (150-270 GPa, see 2.1.5.2). In tungsten technology, WS_2 nanowires reinforce tungsten rubber, boosting wear resistance by 40% (wear rate 0.01 $mm^3/N·m$ vs. 0.017 $mm^3/N·m$), used in automotive seals with an annual demand of about 1000 tons. Its high purity and one-dimensional structure ensure strong interfacial bonding with the substrate (adhesion strength 15 MPa, tensile test).

3.3.4 Laboratory Research-Grade Tungsten Disulfide

Laboratory research-grade WS_2 meets the high-precision demands of scientific studies, with highly customizable purity and morphology.

3.3.4.1 High-Purity Nanoscale

Research-grade WS_2 boasts purity >99.99% (ICP-MS), with impurities <100 ppm (e.g., Fe <10 ppm), typically in nanosheet (<100 nm) or quantum dot (2-10 nm) forms. It is prepared via high-purity CVD or liquid-phase exfoliation, such as using sodium tungstate as a raw material, grown at 1000°C in an H_2S atmosphere, costing approximately 2000 RMB/kg. Its specific surface area ranges from 100-500 m^2/g (BET method), with a tunable bandgap (1.3-3.0 eV, see 2.3.2.1).

Preparation of high-purity nanoscale WS_2 requires a dust-free environment (Class 100 cleanroom) to minimize impurities. For example, in tungsten research, 99.999% pure single-layer WS_2 maintains bandgap stability with <1% change after 1000 hours of illumination (PL test), outperforming industrial-grade's 5%.

3.3.4.2 Customization Requirements

Research-grade WS_2 caters to specific experimental needs, such as doping (Nb, Re) or size control (2-50 nm). For instance, Nb-doped WS_2 ($Nb_xW_{1-x}S_2$, $x = 0.01\text{-}0.1$) adjusts the bandgap to 1.8 eV and boosts conductivity to 10^4 S/cm (four-probe method), used in quantum computing research. In tungsten technology, 5 nm WS_2 quantum dots are customized for bioimaging, with an emission peak at 450 nm (quantum yield 20%), meeting an annual demand of about 50 kg.

Its high cost (2000 RMB/kg) limits large-scale use, but its value in fundamental research is significant. For example, in CTIA GROUP LTD's labs, customized WS_2 nanosheets are used to study topological properties, achieving a spin Hall conductance of 10^{-3} S at 10 K, advancing novel device development.

CTIA GROUP LTD Tungsten Disulfide

Chapter 4: Production Processes of Tungsten Disulfide

Tungsten disulfide (WS_2), as an important layered transition metal dichalcogenide, has production processes that directly determine its quality, cost, and application scope. With the continuous expansion of industrial demand and scientific applications, the production technology of WS_2 (tungsten disulfide) has evolved from traditional methods to modern synthesis techniques. Traditional methods are characterized by simplicity and high yield, suitable for the mass production of industrial-grade products, while modern synthesis methods focus on achieving high purity and nanoscale morphology control, serving high-tech fields such as electronics and catalysis. This chapter systematically introduces WS_2's traditional production methods, modern synthesis techniques, and their optimization strategies, comprehensively exploring the current state and development of its production processes through process flows, equipment requirements, and economic analysis.

4.1 Traditional Production Methods of Tungsten Disulfide

Traditional production methods form the foundation of tungsten disulfide (WS_2) industrial manufacturing, typically relying on high-temperature reactions and simple chemical processes, making them suitable for large-scale, low-cost preparation of industrial-grade WS_2. Based on reaction principles and process characteristics, these methods primarily include calcination decomposition and tungsten trisulfide sublimation. This section provides a detailed analysis of the process flows, advantages, disadvantages, and application scenarios of these two methods.

4.1.1 Calcination Decomposition Method

The calcination decomposition method is a classic approach for preparing WS_2, generating the target product through the high-temperature reaction of a tungsten source with a sulfur source, widely applied in industrial production.

4.1.1.1 Raw Material Selection

The raw materials for the calcination decomposition method mainly consist of a tungsten source and a sulfur source. The tungsten source typically includes tungstic acid (H_2WO_4), tungsten trioxide (WO_3), or tungsten powder (W). Tungstic acid is often the preferred choice due to its reactivity with sulfiding agents and moderate cost (approximately 200-300 RMB/kg, tungsten market data), with a purity requirement generally above 98% to minimize the impact of impurities (e.g., Fe, Si) on product quality. WO_3, derived from refining black tungsten ore or white tungsten ore, typically has a purity above 99% and is suitable for higher-purity production needs, though it is priced slightly higher (around 350 RMB/kg). Tungsten powder is ideal for direct sulfidation, with particle sizes ranging from 1-10 μm (laser particle size analysis), requiring precautions against oxidation to ensure reaction efficiency.

The sulfur source primarily employs hydrogen sulfide (H_2S) or elemental sulfur (S). H_2S, a gas, allows easy control of reaction rate, requiring a purity above 99.5%, sourced commonly as a petrochemical byproduct at a low cost (around 50 RMB/m³). Elemental sulfur, used in powder or granular form, requires a purity above 99% and costs approximately 10-20 RMB/kg; it is easy to store but needs high-temperature gasification. X-ray fluorescence spectroscopy (XRF) analysis indicates that raw material impurities (e.g., Fe <0.5%, Si <0.3%) must be strictly controlled to avoid forming byproducts like FeS or SiS_2.

From a process perspective, the chemical reactivity and particle size of the tungsten and sulfur sources affect reaction efficiency. For instance, H_2WO_4's specific surface area (5-10 m²/g, BET method) exceeds that of WO_3 (2-5 m²/g), resulting in a 20% faster reaction rate (kinetic testing), though WO_3 offers superior thermal stability (decomposition temperature >1000°C vs. 600°C for H_2WO_4). In practical production, CTIA GROUP LTD frequently opts for the H_2WO_4 and H_2S combination, achieving an annual WS_2 output of 50,000 tons.

4.1.1.2 Sulfidation Reaction

The reaction occurs in a tubular furnace or rotary kiln at temperatures ranging from 400-600°C and pressures of 0.1-0.5 MPa. H_2S flow is typically controlled at 50-100 L/min, with a 20-30% molar excess to ensure complete sulfidation of the tungsten source. Thermogravimetric analysis (TGA) shows the reaction initiates at approximately 350°C, reaching a conversion rate above 95% at 600°C. Reaction duration is generally 4-8 hours, depending on raw material particle size and equipment scale.

During the reaction, the tungsten source surface first forms an intermediate product, WS_3 (tungsten trisulfide), which then decomposes into WS_2 and elemental sulfur:
WS3→WS2+S↑$WS_3 \rightarrow WS_2 + S\uparrow$ WS3→WS2+S↑

In-situ infrared spectroscopy (FTIR) monitoring reveals strong volatile peaks for H_2O and S (3400 cm^{-1} and 460 cm^{-1}) at 500°C, indicating vigorous reaction activity. Scanning electron microscopy (SEM) observations show the resulting WS_2 as micron-sized flaky particles (5-20 µm), with an interlayer spacing of 6.15Å (XRD measurement), consistent with the 2H phase (see 3.2.2.1).

Key parameters of the sulfidation reaction include temperature and H_2S concentration. For example, raising the temperature from 500°C to 600°C increases WS_2 yield by 5% (mass method), but excessively high temperatures (>800°C) can produce WO_3 (oxidized byproduct, with enhanced W^{6+} peaks in XPS). Increasing H_2S concentration by 10% reduces reaction time by 1 hour, though excessive sulfur requires managing emission issues.

4.1.1.3 High-Temperature Calcination

High-temperature calcination follows the sulfidation reaction to further enhance WS_2's crystallinity and purity. The calcination temperature is controlled at 700-900°C for 2-4 hours, typically conducted in an inert atmosphere (e.g., N_2 or Ar, flow rate 20-50 L/min) to prevent oxidation. Differential thermal analysis (DTA) indicates that WS_2 undergoes crystal optimization at 850°C, with the (002) peak intensity increasing by 30% (XRD), and crystallinity rising from 60% to 85% (Scherrer equation calculation). Calcination furnaces, such as muffle or tunnel kilns, are lined with refractory materials (e.g., Al_2O_3) and withstand temperatures above 1000°C.

During calcination, residual sulfur (S) volatilizes, and impurities (e.g., FeS) decompose into gaseous emissions, slightly increasing particle size (10-25 µm, SEM). ICP-OES analysis shows Fe content decreasing from 0.5% to 0.2% post-calcination, elevating purity to 98-99%. When using WO_3 as a raw material, an additional high-temperature step (900°C) removes trace WO_2 (<0.1%), confirmed by the disappearance of W^{4+} peaks in XPS.

Optimizing high-temperature calcination requires controlling the heating rate (5-10°C/min); rapid rates can lead to particle agglomeration (D_{50} increasing from 15 µm to 30 µm, laser particle size analysis), affecting product uniformity. In tungsten technology, precise temperature control at 850°C achieves a 98% yield, with a particle size distribution coefficient of variation below 10%.

4.1.1.4 Byproduct Handling

The calcination decomposition method generates multiple byproducts, including H_2O, H_2, S, and minor amounts of H_2S. H_2O and H_2 are emitted as gases and recovered via condensation (condenser temperature 10-20°C), with a recovery rate exceeding 90% (mass method). Sulfur vapor (S) volatilizes at 600-800°C and is converted to Na_2S through a tail gas absorption tower (filled with

NaOH solution, pH 12-14), achieving a 95% absorption efficiency (gas chromatography detection). Residual H_2S is oxidized to SO_2 in an incinerator (1000°C) and neutralized with $Ca(OH)_2$ into $CaSO_4$, maintaining emissions below 50 ppm (complying with GB 16297-1996 standards).

If raw materials contain Fe or Si, FeS and SiS_2 form and volatilize as gases during calcination (boiling points <700°C), removed via tail gas treatment. ICP-MS analysis shows post-treatment Fe levels below 0.1% and Si below 0.05%. Byproduct handling increases production costs by approximately 10-15% (around 30-50 RMB/kg) but ensures environmental compliance. At CTIA GROUP LTD's facilities, the tail gas treatment system processes about 1000 m^3 of H_2S annually, achieving an SO_2 emission compliance rate above 99%.

4.1.1.5 Advantages

The advantages of the calcination decomposition method include its simplicity, high yield, and low cost. Equipment requirements are minimal (tubular furnace or rotary kiln, investment <500,000 RMB/unit), and the operating temperature (600-900°C) is easily achievable industrially, with single-batch yields exceeding 95% and purity stabilized at 98-99% (ICP-OES). Raw materials like H_2WO_4 and H_2S are readily available in the tungsten market, with price fluctuations below 5% annually. Compared to other methods, its energy consumption is lower (approximately 500 kWh/ton vs. 2000 kWh/ton for CVD), making it

ideal for large-scale production of industrial-grade WS_2.
This method produces WS_2 with controllable particle sizes (5-25 μm), meeting the needs of lubricants and counterweight materials. For example, friction coefficient tests (ASTM D1894) show performance differences of less than 5% compared to high-purity WS_2, offering high cost-effectiveness. In tungsten products, WS_2 from this method is widely used in mechanical lubrication, with an annual demand of about 80,000 tons.

4.1.1.6 Disadvantages

The disadvantages of the calcination decomposition method include limited purity and environmental challenges. Product purity rarely exceeds 99% (ICP-OES) due to persistent raw material impurities (e.g., Fe), restricting its use in electronics. The high-temperature reaction generates substantial sulfide gases (H_2S and S), necessitating complex tail gas treatment and increasing costs by 10-15% (approximately 30-50 RMB/kg). The particle size is relatively large (5-20 μm, SEM), failing to meet nanoscale requirements.

Additionally, controlling reaction conditions is challenging; temperature fluctuations of ±50°C can result in WS_3 residue (<1%, XPS), affecting product consistency. Compared to modern methods (e.g., CVD), its crystallinity is lower (70-85% vs. >95%), making it less competitive for high-precision applications. In tungsten research, this method is primarily used for basic raw material preparation.

4.1.1.7 Application Scenarios

The calcination decomposition method is suitable for the mass production of industrial-grade WS_2, mainly used in lubricants, counterweight materials, and low-end catalysts. In mechanical processing, WS_2 powder (98% purity) added to grease reduces the friction coefficient to 0.05 (ASTM D1894), extending bearing life by 40% (1000 hours, 3000 rpm). In aerospace, such as satellite sliding components, its low cost (300 RMB/kg) and stability (650°C) meet requirements, with an annual usage of about 50,000 tons. In petrochemical HDS, it achieves an 85% sulfide removal rate (500°C, ASTM D5185), suitable for general chemical applications.

WS_2 produced by this method is also used in counterweight materials, such as blending with tungsten plastic to create high-density composites (10 g/cm³), widely applied in precision instruments. In tungsten technology, WS_2 from calcination serves as a base material, further processed through grinding or exfoliation for refined products.

4.1.2 Tungsten Trisulfide Sublimation Method

The tungsten trisulfide sublimation method involves preparing WS_3 followed by sublimation and decomposition to produce WS_2, suitable for products requiring higher purity and crystallinity.

4.1.2.1 Preparation of WS_3

This method first prepares tungsten trisulfide (WS_3) as an intermediate. The raw materials are tungsten trioxide (WO_3) or tungsten powder (W), with the sulfur source being H_2S or elemental sulfur. The reactions are as follows: $WO_3 + 3H_2S \rightarrow WS_3\downarrow + 3H_2O\uparrow$ or $W + 3S \rightarrow WS_3$. The reaction occurs in a sealed reactor at temperatures of 300-500°C, with an H_2S flow of 30-60 L/min and a 50% molar excess, under a pressure of 0.1-0.3 MPa. TGA shows WS_3 fully forms at 400°C, with a yield exceeding 90%. SEM observations reveal WS_3 as amorphous particles (1-5 μm), and XPS confirms a W^{4+} to S^{2-} ratio of 1:3.

WO_3 requires a purity above 99% to minimize impurities (e.g., Fe <0.1%), commonly sourced from refining black tungsten ore. H_2S purity exceeds 99.5%, with tail gas recycling achieving an 80% recovery rate. If elemental sulfur is used, it is gasified at 400°C, with sulfur vapor pressure controlled at 0.05-0.1 MPa. In tungsten companies, the WO_3 and H_2S combination is more common due to its faster reaction rate (4 hours vs. 6 hours).

4.1.2.2 Sublimation Conditions

The sublimation decomposition of WS_3 into WS_2 follows the reaction: $WS3 \rightarrow WS2\downarrow + S\uparrow$, Sublimation occurs in a vacuum furnace or quartz tube at 700-900°C, with a vacuum level of 10^{-2}-10^{-3} Pa, lasting 2-3 hours. TGA indicates a 98% decomposition rate at 750°C, with complete sulfur vapor volatilization. The product deposits at the cold end (300-400°C), forming WS_2 crystals or powder. XRD analysis confirms the product as 2H-phase WS_2, with an interlayer spacing of 6.15Å and crystallinity above 90% (Scherrer equation).

Sublimation temperature must be precisely controlled (±10°C); temperatures above 950°C risk forming WO_3 (<0.5%, XPS), while below 700°C, WS_3 residue persists (<2%). Cold-end temperature affects morphology: 400°C yields micron-sized crystals (5-10 μm, SEM), while 300°C produces powder (1-3 μm). In tungsten technology, the combination of 850°C and 10^{-3} Pa achieves the highest yield (95%).

4.1.2.3 Excess Sulfur Removal

The sublimation process generates excess sulfur (S), removed via condensation and absorption. A condenser (0-10°C) recovers sulfur vapor with an efficiency above 85% (mass method). Residual sulfur gas is converted to Na_2S in an NaOH absorption tower (10-15% concentration), with an efficiency exceeding 90% (gas chromatography). If WS_3 decomposition is incomplete, the product's sulfur content rises (<0.5%, ICP-OES), requiring secondary calcination (800°C, N_2 atmosphere) to increase purity to 99.5%.

The treatment system requires corrosion-resistant materials (e.g., stainless steel 316L) due to sulfur vapor's corrosiveness (pH <2). In the tungsten market, sulfur recovery rates directly impact costs (an 85% recovery reduces costs by 20 RMB/kg). CTIA GROUP LTD's tail gas treatment recovers approximately 500 kg of sulfur annually.

4.1.2.4 Advantages

The advantages of the tungsten trisulfide sublimation method lie in its high purity and crystallinity. Product purity reaches 99.5% (ICP-OES), with impurities (e.g., Fe, Si) below 0.1%, surpassing the 99% of the calcination decomposition method. Crystallinity exceeds 90% (XRD), with uniform crystal sizes (5-10 μm, SEM), suitable for applications requiring high-quality WS_2. The stepwise process (WS_3 preparation and sublimation separation) facilitates quality control, maintaining a stable yield of 90-95%.

WS_2 produced by this method excels in lubrication and catalysis. Friction coefficient tests (ASTM D1894) show a stable value of 0.04, 10% lower than WS_2 from calcination. In tungsten products, its high purity supports the production of premium lubricants.

4.1.2.5 Disadvantages

The disadvantages include process complexity and high energy consumption. Requiring two steps (WS_3 preparation and sublimation), equipment investment is substantial (vacuum furnace approximately 1-1.5 million RMB/unit vs. 500,000 RMB for calcination). Sublimation demands high vacuum (10^{-3} Pa), consuming about 1500 kWh/ton, compared to 500 kWh/ton for calcination. Excess sulfur treatment adds costs (approximately 50-80 RMB/kg), posing significant environmental pressure.

Additionally, the yield is slightly lower than calcination (90-95% vs. >95%), and the product morphology is limited to micron-sized crystals, unsuitable for nanoscale WS_2 production. In tungsten research, this method is primarily used for studies, not nanoscale applications.

4.1.2.6 Application Scenarios

The tungsten trisulfide sublimation method is suitable for producing high-purity WS_2, mainly for premium lubricants and catalysts. In aerospace, WS_2 crystals (99.5% purity) are used in bearing coatings, achieving a friction coefficient below 0.05 (500°C, ASTM G99) and increasing durability by 30% (1000 hours). In HDS, it achieves a 90% sulfide removal rate (500°C, ASTM D5185), meeting high-performance catalysis needs, with an annual usage of about 500 tons.

WS_2 from this method also serves as a preliminary material for electronics, such as exfoliation into single-layer WS_2. In tungsten technology, its high-crystallinity WS_2 acts as a base material, processed further to meet optoelectronic device requirements.

4.2 Modern Synthesis Methods of Tungsten Disulfide

With advancements in technology, modern synthesis methods for tungsten disulfide (WS_2) have gradually replaced some traditional processes, aiming to meet demands for high purity, nanoscale morphology, and high-performance applications. These methods leverage gas-phase reactions, solution chemistry, or physical exfoliation techniques, enabling precise control over WS_2 (tungsten disulfide)'s crystal phase, size, and structure. They are widely applied in electronic devices, photocatalysis, and nanocomposites. This section will provide a detailed exploration of the process flows, advantages, disadvantages, and application scenarios of chemical vapor deposition (CVD), hydrothermal/solvothermal methods, and mechanical exfoliation.

4.2.1 Chemical Vapor Deposition Method

Chemical vapor deposition (CVD) is an advanced technique for preparing thin films and nanomaterials, producing WS_2 through the reaction of gas-phase precursors on a substrate, suitable for high-purity thin films and nanosheet production.

4.2.1.1 Precursor Selection

Precursors for CVD synthesis of WS_2 are divided into tungsten and sulfur sources. Common tungsten sources include tungsten trioxide (WO_3), tungstic acid (H_2WO_4), or metal-organic compounds like tungsten hexacarbonyl ($W(CO)_6$). WO_3, a solid precursor, requires a purity above

99.9% (ICP-OES) and is sublimated (800-1000°C) to form gaseous WO_3-x, allowing easy control of deposition rate, with a cost of approximately 350 RMB/kg (tungsten market data). H_2WO_4 has a lower decomposition temperature (600°C) but lower gasification efficiency (50-60%, TGA), making it suitable for small-scale experiments. $W(CO)_6$, a volatile liquid (boiling point 175°C) with purity above 99.5%, decomposes to provide high-purity tungsten atoms (impurities <0.01%) but is expensive (around 2000 RMB/kg), often used in research.

Sulfur sources primarily include hydrogen sulfide (H_2S), elemental sulfur (S), or dimethyl disulfide (DMDS, $(CH_3)_2S_2$). H_2S, with purity above 99.5%, is controlled at a flow rate of 20-50 sccm, facilitating reaction atmosphere adjustments, and costs approximately 50 RMB/m³. Elemental sulfur requires heating to 200-300°C for gasification, with a vapor pressure of 0.01-0.05 MPa, priced at about 20 RMB/kg, suitable for large-area deposition. DMDS, a liquid with strong volatility (boiling point 109°C), decomposes into S_2, with purity above 99%, but its pungent odor requires ventilation, costing around 100 RMB/kg.

Precursor choice impacts product quality. For instance, the $W(CO)_6$ and H_2S combination yields WS_2 with 99.99% purity (ICP-MS) and Fe impurities below 10 ppm, ideal for electronic applications. In tungsten research, the WO_3 and S combination is more common due to its lower cost and simpler equipment requirements.

4.2.1.2 Deposition Conditions

The CVD reaction occurs in a tubular furnace or hot-wall reactor, with the following chemical equations: $WO_3 + 3H_2S \rightarrow WS_2\downarrow + 3H_2O\uparrow + S\uparrow$ or $W(CO)6+2H2S\rightarrow WS2\downarrow+6CO\uparrow+2H2\uparrow$ Deposition temperatures range from 700-1100°C, with substrate temperatures at 600-900°C, pressures from 10^{-2}-10 Pa, and carrier gas (e.g., Ar or N_2) flow rates of 50-200 sccm. Substrates, typically Si/SiO_2, sapphire, or graphite, have surface roughness below 1 nm (AFM) to ensure film uniformity. Reaction duration is 30-120 minutes, depending on desired film thickness.

In-situ spectroscopy (FTIR) monitoring shows strong volatile peaks for H_2O and CO (3400 cm^{-1} and 2100 cm^{-1}) at 800°C, indicating complete reaction. XRD analysis confirms the product as 2H-phase WS_2, with an interlayer spacing of 6.15Å and crystallinity above 95%. SEM and TEM observations reveal film thicknesses from 0.62 nm (single layer) to 50 nm (multilayer), with lateral sizes of 10-100 µm. Higher deposition temperatures (e.g., 1000°C) increase the single-layer proportion to 70% (Raman A_1g/E^2g intensity ratio), but temperatures above 1100°C produce WO_3 (XPS W^{6+} peak).

Optimizing deposition conditions requires balancing temperature and gas flow. For example, increasing H_2S flow from 30 sccm to 50 sccm boosts WS_2 growth rate by 20% (0.5 nm/min vs. 0.4 nm/min, ellipsometry), but excess sulfur (>60 sccm) leads to WS_3 residue (<0.5%). In CTIA GROUP LTD's CVD equipment, 900°C and 10 Pa are proven optimal, achieving a 90% yield.

4.2.1.3 Film Thickness Control

Film thickness is regulated by reaction time, precursor concentration, and substrate temperature. Extending time from 30 to 120 minutes increases thickness from 0.62 nm (single layer) to 20 nm (30-40 layers, AFM). Raising precursor concentration (WO_3 vapor pressure 0.01-0.05 Pa) by 50% elevates growth rate to 0.6 nm/min but favors multilayer formation (TEM). Substrate temperature rising from 700°C to 900°C boosts the single-layer proportion from 50% to 80% (Raman), as higher temperatures promote two-dimensional growth.

Thickness uniformity depends on gas flow distribution and substrate position. Dual-temperature-zone CVD (hot zone 1000°C, cold zone 800°C) controls thickness variation within ±5% (10 cm^2 substrate, AFM). In tungsten technology, precise control of time (60 minutes) and temperature (850°C) yields 5-10 nm WS_2 films, meeting optoelectronic device needs.

4.2.1.4 Advantages

The advantages of CVD lie in its high purity and precise control. Product purity exceeds 99.9% (ICP-MS), with impurities (e.g., Fe, Si) below 0.01%, and crystallinity above 95% (XRD), making it suitable for electronic and optical applications. Film thickness is adjustable (0.62-50 nm), with large lateral sizes (10-100 µm), supporting large-area production (>10 cm^2). Crystal phase control is achievable, producing 2H phase at 900°C and inducing 1T phase at 1100°C (XRD). In tungsten products, CVD WS_2's direct bandgap (2.1 eV, PL) meets photodetector requirements.

4.2.1.5 Disadvantages

Disadvantages include high cost and equipment complexity. CVD equipment (vacuum pumps, temperature control systems) costs approximately 2-5 million RMB/unit, with high energy consumption (2000 kWh/ton vs. 500 kWh/ton for calcination), resulting in production costs of 1000-2000 RMB/kg. Yield is low (single batch <1 g/cm^2), unsuitable for large-scale production. High temperatures and low pressures (10^{-2} Pa) demand robust equipment (e.g., corrosion-resistant quartz), increasing maintenance costs by 20% (around 500,000 RMB/year). In the tungsten market, its use is largely confined to high-value-added fields.

4.2.1.6 Application Scenarios

CVD is suitable for optoelectronic devices and nanocatalysts. For example, in tungsten technology, single-layer WS_2 films (0.62 nm thick) are used in photodetectors, achieving a photoresponsivity of 10^3 A/W (532 nm, ASTM) and a detectivity of 10^{11} Jones, with an annual demand of about 100 kg. In flexible electronics, 5 nm CVD WS_2 films serve as transparent conductive layers with >90% transmittance (550 nm), applied in displays. In photocatalysis, nanosheet WS_2 (10 nm) achieves a hydrogen production rate of 150 µmol/g·h (visible light) due to high purity and edge activity (STM, 20-30%).

4.2.2 Hydrothermal/Solvothermal Method

The hydrothermal/solvothermal method synthesizes WS_2 via solution reactions in a sealed system, suitable for preparing nanoparticles and specialized morphologies.

4.2.2.1 Raw Materials

Raw materials include tungsten and sulfur sources. Tungsten sources commonly feature sodium tungstate (Na_2WO_4), ammonium metatungstate ($(NH_4)_6H_2W_{12}O_{40}$), or tungsten trioxide (WO_3). Na_2WO_4 has high solubility (>100 g/100 mL, 25°C), purity above 99%, and costs around 200 RMB/kg, forming uniform solutions easily. $(NH_4)_6H_2W_{12}O_{40}$ provides polytungstate ions, with purity above 99.5% and a cost of about 300 RMB/kg, ideal for nanoscale control. WO_3 requires acid dissolution (e.g., HCl, pH 2-3), with purity above 99% and a higher cost of 350 RMB/kg.

Sulfur sources include thiourea ($CS(NH_2)_2$), sodium sulfide (Na_2S), or carbon disulfide (CS_2). Thiourea, with purity above 99%, costs 50 RMB/kg and decomposes at 180°C into H_2S and NH_3, offering a uniform sulfur supply (yield >90%, TGA). Na_2S has good solubility (>50 g/100 mL), purity above 98%, and costs 30 RMB/kg, but introduces Na^+ impurities (<0.1%, ICP-MS). CS_2, a volatile liquid (boiling point 46°C), requires organic solvents (e.g., ethanol) and costs about 80 RMB/kg.

In tungsten research, the Na_2WO_4 and thiourea combination is most common due to its low cost and mild reaction conditions.

4.2.2.2 Reaction Conditions

The reaction occurs in a high-pressure reactor (PTFE-lined), with the equation:
$Na_2WO_4 + 2CS(NH_2)_2 + 2H_2O \rightarrow WS_2\downarrow + 2NaOH + 2CO_2\uparrow + 4NH_3\uparrow$
Temperatures range from 180-250°C, pressures from 1-5 MPa, and durations from 12-48 hours. Solution concentrations (tungsten source 0.1-0.5 mol/L, sulfur source 50% excess) and pH (4-7, adjusted with HCl or NaOH) are key, with stirring at 200-500 rpm for uniformity.

TGA shows an 85% WS_2 formation rate at 200°C, exceeding 95% at 250°C. XRD confirms the product as 2H-phase WS_2, with an interlayer spacing of 6.15Å. SEM and TEM reveal nanoparticles (10-50 nm) or nanosheets (5-20 nm thick). Higher temperatures (e.g., 240°C) reduce particle size (D_{50} from 50 nm to 20 nm, DLS) due to pressure-enhanced nucleation.

Optimizing reaction conditions is critical. Extending time from 24 to 48 hours increases yield to 98%, though particle agglomeration rises (SEM). Adjusting pH from 5 to 7 boosts nanosheet proportion to 60% (TEM). In CTIA GROUP LTD's hydrothermal equipment, 220°C and 24 hours are optimal parameters.

4.2.2.3 Morphology Control

Morphology is tuned via additives, temperature, and solvents. Adding surfactants (e.g., CTAB, 0.01 mol/L) produces nanowires (20-50 nm diameter, 1-5 μm long, TEM). Raising temperature from 200°C to 240°C shifts morphology from particles to nanosheets (10 nm thick, 50-200 nm lateral, TEM). Switching solvents from water to ethanol reduces particle size by 30% (20 nm vs. 30 nm, DLS) due to lower surface tension.

Adding polyvinylpyrrolidone (PVP, 0.5 wt%) forms quantum dots (2-10 nm, TEM), increasing the bandgap to 2.5 eV (UV-Vis). In tungsten technology, the CTAB and 240°C combination yields uniform nanosheets with a coefficient of variation below 5%.

4.2.2.4 Advantages

The advantages of the hydrothermal/solvothermal method include diverse morphologies and low cost. Products range from nanoparticles to nanosheets and quantum dots (10-50 nm, TEM), with purity of 98-99.5% (ICP-OES), meeting catalysis needs. Equipment is simple (autoclave investment <200,000 RMB/unit), with low energy consumption (500 kWh/ton) and costs of 300-500 RMB/kg. The mild reaction (<250°C) facilitates industrialization, with single-batch yields above 90%.

WS_2 from this method excels in catalysis, achieving an HER overpotential of 150 mV (10 mA/cm^2) due to nanoscale morphology increasing active sites (STM, 20-30%). In tungsten products, its low cost supports mass production.

4.2.2.5 Disadvantages

Disadvantages include limited purity and yield variability. Impurities (e.g., Na^+, C) are hard to eliminate, capping purity at 99.5% (ICP-MS), unsuitable for electronics. Long reaction times (12-48 hours) and low single-batch yields (<500 g) limit scalability. Morphology control requires additives, raising costs by 10-20% (around 50 RMB/kg), and waste liquid (containing NH_3, CO_2) treatment is complex. In the tungsten market, its use is mostly confined to mid-tier products.

4.2.2.6 Application Scenarios

The hydrothermal/solvothermal method suits nanocatalysts and composites. For example, in tungsten technology, 20 nm WS_2 nanosheets are used in photocatalysis, achieving a hydrogen production rate of 150 μmol/g·h (visible light), with an annual demand of about 200 tons. In lubrication, 50 nm WS_2 nanoparticles added to grease yield a friction coefficient of 0.04 (ASTM D1894) and a wear rate of 0.005 mm^3/N·m. In composites, blending with tungsten rubber (10 wt%) increases tensile strength to 55 MPa, improving wear resistance by 30%.

4.2.3 Mechanical Exfoliation Method

The mechanical exfoliation method separates nanosheets from bulk WS_2 using physical force, suitable for preparing high-purity single-layer WS_2.

4.2.3.1 Exfoliation Raw Materials

The raw material is bulk WS_2, including natural tungstenite and synthetic crystals (see 3.1.4). Natural tungstenite, with 98-99% purity (ICP-OES), contains Fe and Si impurities (<1%) and is sourced from Ganzhou, China, with an annual yield below 1000 tons (tungsten market). Synthetic crystals, with purity above 99.9% (ICP-MS), are prepared via CVT using tungsten powder and S at 1000°C, with sizes of 1-5 cm and a cost of about 500 RMB/kg.
Raw material crystallinity affects exfoliation efficiency. Synthetic crystals, with crystallinity above 95% (XRD) and an interlayer spacing of 6.15Å, yield 20% higher exfoliation rates (TEM). Tungstenite's crystallinity (80-90%) and impurities reduce yields (<5%). In tungsten research, synthetic crystals are more commonly used.

4.2.3.2 Process

The exfoliation process is divided into dry and wet methods. The dry method uses adhesive tape to separate single layers from bulk WS_2, repeated 5-10 times, and transfers them to an Si/SiO_2 substrate (300 nm thick). The wet method involves ultrasonication (200 W, 5-10 hours) in NMP or isopropanol, followed by centrifugation (3000-5000 rpm) to isolate nanosheets.

TEM shows dry exfoliation yielding single-layer WS_2 (0.62 nm thick) with lateral sizes of 1-10 μm. Wet exfoliation produces multilayer nanosheets (2-10 layers, 1-5 nm thick) with sizes of 0.5-5 μm. Raman analysis indicates a dry method A_1g/E^2g intensity ratio above 2 (single-layer signature) and a wet method ratio below 1 (multilayer). Increasing ultrasonication from 5 to 10 hours raises the single-layer proportion to 30% (TEM). In CTIA GROUP LTD's labs, the wet method is more common due to higher yields.

4.2.3.3 Yield and Purity

The dry method has a low yield (<1%, mass method), inheriting raw material purity (>99.9% for synthetic crystals), with no additional impurities (ICP-MS). The wet method achieves 10-30% yield (post-centrifugation), with purity of 99-99.5%, including trace solvent residues (C <0.1%, XPS). Secondary centrifugation (10,000 rpm) boosts purity to 99.8%, but yield drops to 5%.

In tungsten technology, wet method optimization (8 hours ultrasonication, 5000 rpm) balances yield (20%) and purity (99.5%), meeting research needs.

4.2.3.4 Advantages

Advantages include high purity and quality. The dry method produces single-layer WS_2 (purity >99.9%) with a 2.1 eV bandgap (PL) and minimal crystal defects (TEM, $<10^{-2}$ nm^{-2}). The wet method offers higher yields (10-30%) at lower costs (approximately 500-1000 RMB/kg), with simple equipment (ultrasonic device <100,000 RMB). The process is eco-friendly, producing no chemical byproducts, with waste limited to solvents. In tungsten products, single-layer WS_2 meets high-end application needs.

4.2.3.5 Disadvantages

Disadvantages include low yield and scalability challenges. The dry method yields <1 mg/cm^2 per batch, with manual operation efficiency below 0.1 g/hour. The wet method's yield is solvent-limited (NMP costs 100 RMB/L), with a high multilayer proportion (70-80%, TEM), unsuitable for mass production. It relies heavily on raw materials, with synthetic crystals costing more (500 RMB/kg vs. 300 RMB/kg for calcination). In the tungsten market, its use is confined to labs.

4.2.3.6 Application Scenarios

The mechanical exfoliation method suits optoelectronic devices and basic research. For example, in tungsten research, dry-method single-layer WS_2 is used in photodetectors, achieving a photoresponsivity of 10^3 A/W (532 nm), with an annual demand below 10 kg. Wet-method nanosheets (5 nm) are applied in catalysis studies, with an HER overpotential of 200 mV (10 mA/cm^2). In flexible electronics, single-layer WS_2 films serve as transparent electrodes, with >90% transmittance (550 nm), meeting high-precision requirements.

4.3 Optimization of Tungsten Disulfide Production Technology

With the expanding application fields of tungsten disulfide (WS_2), optimizing its production technology has become key to enhancing product quality, reducing costs, and meeting environmental requirements.

Optimization strategies focus on purity enhancement, particle size control, and environmental measures, not only improving WS_2 (tungsten disulfide)'s performance (e.g., lubricity, catalytic activity) but also advancing its use in electronics, nanotechnology, and green manufacturing. This section will explore the technical details, implementation effects, and practices of major producers, revealing advancements in WS_2 production technology.

4.3.1 Purity Enhancement Techniques

Purity is a critical indicator of WS_2 performance, and optimization techniques aim to remove impurities and elevate product quality.

4.3.1.1 Impurity Removal

The primary impurities in WS_2 include iron (Fe), silicon (Si), oxygen (O), and carbon (C), originating from raw materials or the reaction process. Traditional calcination methods (e.g., 4.1.1) typically yield products with 98-99% purity (ICP-OES), containing Fe at 0.1-0.5%, Si below 0.3%, and O below 1%. Impurity removal techniques encompass chemical purification and physical separation.

Chemical purification employs acid or alkali washing. For instance, soaking WS_2 powder in a 5% HCl solution (pH 1-2) with stirring (2 hours, 50°C) dissolves FeS and Fe_2O_3, reducing Fe content from 0.5% to 0.05% (ICP-MS). Alkali washing (10% NaOH, 80°C, 1 hour) removes SiO_2, lowering Si content to below 0.01%. Post-washing, WS_2 is rinsed with water to neutral pH (7) and dried (120°C, N_2 atmosphere), achieving a purity of 99.5%. XPS analysis shows W 4f and S 2p peaks (32.8 eV and 162.3 eV) free of impurity interference.

Physical separation includes flotation and magnetic separation. Flotation uses a frothing agent (e.g., pine oil alcohol, 0.1 wt%) to separate FeS (density 4.8 g/cm^3 vs. WS_2's 7.5 g/cm^3), with efficiency above 90% (mass method). Magnetic separation removes magnetic impurities (e.g., Fe) at a field strength of 0.5-1 T, reducing Fe content to below 0.02%. In tungsten technology, combining acid washing and magnetic separation elevates purity to 99.9%, increasing costs by about 50 RMB/kg.

Impurity removal requires balancing cost and effectiveness. HCl washing is highly efficient (90% Fe removal) but necessitates waste liquid neutralization ($Ca(OH)_2$), adding 10 RMB/kg to costs. Flotation is cost-effective (20 RMB/kg) but less effective for Si.

4.3.1.2 Post-Processing Techniques

Post-processing enhances purity through high-temperature annealing or distillation. Annealing occurs in a vacuum or inert atmosphere (N_2, 50 L/min flow) at 900-1000°C for 2-4 hours, removing residual sulfur (S) and oxides (e.g., WO_3). TGA shows a sulfur volatilization rate above 95% at 950°C, raising product purity from 99% to 99.9% (ICP-OES). XRD confirms a 20% increase in (002) peak intensity post-annealing, with crystallinity reaching 95%.

Distillation is performed in a vacuum furnace (10^{-3} Pa, 1000°C), where WS_2 sublimates and condenses (400°C), leaving impurities (e.g., FeS, SiO_2) in the residue. ICP-MS detects Fe below 10 ppm and Si below 5 ppm post-distillation, with purity exceeding 99.99%, though yield drops to 85% (mass method). In tungsten research, distillation is often used for electronic-grade WS_2 preparation.

Post-processing increases energy consumption (approximately 300 kWh/ton vs. 500 kWh/ton total for calcination), raising costs to 100-150 RMB/kg. At CTIA GROUP LTD, annealing (950°C, 3 hours) is the mainstream process, treating about 1000 tons of WS_2 annually, with purity stabilized at 99.9%.

4.3.2 Particle Size Control

Particle size affects WS_2's application performance, with optimization techniques including grinding and screening, as well as nanonization.

4.3.2.1 Grinding and Screening

Grinding refines micron-sized WS_2 (5-20 µm, SEM) into ultrafine particles (0.1-1 µm). A planetary ball mill (ZrO_2 balls, 10:1 ball-to-material ratio, 300 rpm, 10-20 hours) reduces D_{50} from 15 µm to 0.5 µm (laser particle size analysis), with a coefficient of variation below 10%. Wet grinding (ethanol medium, 20 wt% solid content) prevents agglomeration, improving efficiency by 15% (D_{50} 0.4 µm). Screening uses vibrating sieves (200-500 mesh) to classify particles into 0.1-0.5 µm, 0.5-1 µm, and 1-5 µm ranges, with a recovery rate above 95%.

Grinding parameters require optimization. Extending time from 10 to 20 hours reduces particle size by 20% (0.4 µm vs. 0.5 µm) but increases energy use by 50% (200 kWh/ton). Higher screening precision (500 mesh) raises loss rates to 10%. In tungsten products, 0.5 µm WS_2 is used in lubricants, reducing friction coefficient to 0.04 (ASTM D1894), with an annual demand of 3000 tons.

4.3.2.2 Nanonization Techniques

Nanonization produces WS_2 below 100 nm, including liquid-phase exfoliation and vapor deposition (see 4.2). Liquid-phase exfoliation in NMP with ultrasonication (300 W, 10 hours) and centrifugation (10,000 rpm) isolates 10-50 nm nanosheets, yielding 20-30% (DLS). Vapor deposition (CVD, 900°C, 10 Pa) generates 5-20 nm films, with yields below 1 g/cm². Additives (e.g., CTAB, 0.01 mol/L) in hydrothermal methods form 20 nm particles (TEM).

Nanonization enhances performance. For example, 20 nm WS_2's specific surface area increases to 200 m²/g (BET), reducing HER overpotential to 150 mV (10 mA/cm²), 50% lower than micron-sized WS_2 (300 mV). Costs are higher (500-1000 RMB/kg vs. 350 RMB/kg for grinding) but meet catalysis needs. In tungsten technology, liquid-phase exfoliation produces 50 nm WS_2, with an annual output of about 200 kg.

4.3.3 Environmental Measures

Environmental optimization reduces sulfide emissions and waste liquid pollution, promoting green production.

4.3.3.1 Sulfide Emission Control

Calcination (4.1.1) and sublimation (4.1.2) methods generate H_2S and S vapor, requiring efficient treatment. Tail gas absorption towers (10-15% NaOH solution) convert H_2S to Na_2S, with absorption rates above 95% (gas chromatography). S vapor is recovered via condensation (0-10°C), with efficiency exceeding 90% (mass method). Incinerators (1000°C) oxidize residual H_2S to SO_2, neutralized with $Ca(OH)_2$ into $CaSO_4$, keeping emissions below 50 ppm (GB 16297-1996).

Optimization includes recycling and low-temperature catalysis. H_2S tail gas is recycled to the reactor, achieving an 80% recovery rate (flow meter), reducing costs by 20 RMB/kg. Low-temperature catalysis (CuO catalyst, 300°C) converts H_2S to S and H_2O, with efficiency above 98%, lowering SO_2 emissions to below 10 ppm. At CTIA GROUP LTD, annual H_2S treatment is about 1000 m^3, with a compliance rate above 99%.

4.3.3.2 Waste Liquid Treatment

Acid washing (HCl) and hydrothermal methods produce waste liquids (containing Fe^{3+}, NH_3). Neutralization ($Ca(OH)_2$, pH 7-8) precipitates $Fe(OH)_3$, recovered via filtration (efficiency >95%). NH_3 waste liquid is distilled (80°C) and concentrated to 10% (mass method), cutting costs by 15 RMB/kg. Wastewater is treated with activated carbon adsorption (COD <50 mg/L), meeting discharge standards (GB 8978-1996).

4.4 Production Cost and Efficiency

The production cost and efficiency of tungsten disulfide (WS_2) directly impact its market competitiveness and application expansion. Costs primarily stem from raw materials, energy consumption, and equipment, while efficiency relates to yield, scalability, and process optimization. This section analyzes the cost structure of WS_2 (tungsten disulfide) production, explores energy and equipment demands, and evaluates the economics of scaled production, revealing the impact of optimization strategies on cost and efficiency through data and case studies.

4.4.1 Raw Material Cost Analysis

Raw material costs are the primary expense in WS_2 production, depending on the price and usage of tungsten and sulfur sources.

4.4.1.1 Tungsten Source Pricing

Tungsten sources include tungstic acid (H_2WO_4), tungsten trioxide (WO_3), tungsten powder (W), and sodium tungstate (Na_2WO_4). According to tungsten market 2023 data, H_2WO_4 costs 200-300 RMB/kg (98-99% purity), with annual fluctuations below 5%, derived from acid leaching of black tungsten ore or white tungsten ore, with stable global supply (approximately 100,000 tons/year). WO_3 costs 350-400 RMB/kg (>99% purity), refined from ore or recycled waste, with costs rising 10-15% with purity. Tungsten powder (1-10 μm) is priced at 300-350 RMB/kg, used in calcination and sublimation (4.1), with oxidation risks adding storage costs (around 20 RMB/kg). Na_2WO_4 costs 200-250 RMB/kg (>99% purity), common in hydrothermal methods (4.2.2), with high solubility

(>100 g/100 mL) reducing transport expenses.

Producing 1 kg of WS_2 requires approximately 0.74 kg of tungsten source (W basis, molar mass ratio W:WS_2 = 183.84:247.98). For H_2WO_4 (250 RMB/kg), the cost is 0.74 × 250 = 185 RMB/kg WS_2. For WO_3 (375 RMB/kg), it's 277 RMB/kg WS_2, about 50% higher. At CTIA GROUP LTD, H_2WO_4 is the primary choice, with annual purchases of about 40,000 tons, comprising 60% of raw material costs.

Tungsten source purity affects cost and quality. Raising purity from 98% to 99.9% (ICP-OES) increases price by 20% (50-70 RMB/kg), but reduces impurities (e.g., Fe) by 80% (0.5% to 0.1%), enhancing product value. In tungsten technology, high-purity WO_3 is used for CVD (4.2.1), accounting for 70% of costs.

4.4.1.2 Sulfur Source Costs

Sulfur sources include hydrogen sulfide (H_2S), elemental sulfur (S), thiourea ($CS(NH_2)_2$), and sodium sulfide (Na_2S). H_2S costs 50-60 RMB/m³ (>99.5% purity), with calcination (4.1.1) requiring 0.5-0.6 m³/kg WS_2 (20-30% excess), costing 25-36 RMB/kg. Elemental sulfur costs 10-20 RMB/kg (>99% purity), requiring gasification (300°C), with 0.26 kg/kg WS_2 (S:W = 2:1), costing 3-5 RMB/kg, commonly used in sublimation (4.1.2). Thiourea costs 40-50 RMB/kg, with hydrothermal methods (4.2.2) using 0.6 kg/kg WS_2 (50% excess), costing 24-30 RMB/kg. Na_2S costs 30-40 RMB/kg, consuming 0.5 kg/kg WS_2, costing 15-20 RMB/kg.

Sulfur source choice impacts total cost. H_2S is inexpensive (25 RMB/kg WS_2) but requires tail gas treatment (4.3.3.1), adding 20-30 RMB/kg. Elemental sulfur is the cheapest (5 RMB/kg WS_2), but gasification consumes energy (50 kWh/ton). In the tungsten market, elemental sulfur accounts for 60% of industrial production, with annual usage of about 20,000 tons. In tungsten research, thiourea is used for nano WS_2, comprising 30% of costs.

Overall, raw material costs (tungsten + sulfur) range from 190-300 RMB/kg WS_2 (H_2WO_4 + S) to 300-400 RMB/kg (WO_3 + H_2S), accounting for 50-70% of total costs.

4.4.2 Energy Consumption and Equipment Requirements

Energy and equipment are significant cost factors in WS_2 production, varying by process type.

4.4.2.1 High-Temperature Equipment

Calcination (4.1.1) uses tubular furnaces or rotary kilns (600-900°C, 50-100 kW power), costing 300,000-500,000 RMB/unit, with a 5-10 year lifespan. CVD (4.2.1) requires vacuum furnaces (900-1100°C, 100-200 kW), including vacuum pumps (10^{-3} Pa) and temperature control, costing 2-5 million RMB/unit. Hydrothermal methods (4.2.2) use autoclaves (180-250°C, 10-20 kW), costing below 200,000 RMB/unit. Mechanical exfoliation (4.2.3) employs ultrasonic devices (200 W), costing 50,000-100,000 RMB/unit.

Equipment must resist corrosion. Calcination and CVD handle H_2S and S vapor, requiring stainless steel (316L) or quartz linings, with annual maintenance costs of 50,000-100,000 RMB. Hydrothermal autoclaves use PTFE linings (<300°C), costing 20,000-30,000 RMB/unit. At CTIA GROUP LTD, calcination furnaces produce 50,000 tons of WS_2 annually, with maintenance costs of about 80,000 RMB.

Energy consumption varies significantly. Calcination consumes 500 kWh/ton WS_2 (6 hours, 100 kW), CVD 2000 kWh/ton (2 hours, 200 kW), and hydrothermal methods 300 kWh/ton (24 hours, 20 kW). At an electricity rate of 0.8 RMB/kWh, energy costs are 400 RMB/ton, 1600 RMB/ton, and 240 RMB/ton, respectively.

4.4.2.2 Energy Optimization

Energy optimization includes waste heat recovery and process improvements. Waste heat recovery uses calcination furnace exhaust (500-700°C) to preheat raw materials, saving 20% energy (100 kWh/ton, 80 RMB/ton). CVD adopts dual-temperature-zone designs (hot zone 1000°C, cold zone 800°C), reducing heat loss by 15% (300 kWh/ton, 240 RMB/ton). Hydrothermal methods shorten reaction time (24 to 18 hours), lowering energy to 200 kWh/ton (160 RMB/ton).

Process improvements, such as low-temperature catalysis (4.3.3.1, 300°C CuO catalyst) instead of incineration (1000°C), reduce H_2S treatment energy from 50 kWh/ton to 20 kWh/ton. In tungsten technology, combining waste heat recovery and low-temperature catalysis cuts calcination energy to 350 kWh/ton, saving 120 RMB/ton overall. In tungsten products, annual energy savings reach about 5000 MWh, reducing costs by 4 million RMB.

4.4.3 Economics of Scaled Production

Scaled production enhances efficiency through batch benefits and cost reduction strategies.

4.4.3.1 Batch Production Benefits

Calcination yields 1-5 tons per batch (10 m³ furnace capacity), with an annual output of 50,000 tons and unit costs of 300-350 RMB/kg (raw materials 200 RMB, energy 100 RMB, equipment depreciation 30 RMB). CVD yields below 1 kg per batch (10 cm² substrate), with an annual output of 100-200 kg and unit costs of 1000-2000 RMB/kg (raw materials 300 RMB, energy 800 RMB, equipment 500 RMB). Hydrothermal methods yield 0.5-1 kg per batch (10 L capacity), with an annual output of 1000 tons and costs of 400-500 RMB/kg.

Scaling reduces unit costs. Increasing calcination batch size from 1 to 5 tons lowers equipment depreciation to 20 RMB/kg (33% reduction) and energy to 400 kWh/ton (20% reduction), cutting total cost to 300 RMB/kg. At CTIA GROUP LTD, a 50,000-ton/year scale controls costs at 320 RMB/kg, boosting profit margins by 15% (about 50 RMB/kg). Hydrothermal production scaling from 500 to 1000 tons reduces costs to 450 RMB/kg, improving benefits by 10%.

Batch production requires stable demand. In the tungsten market, industrial-grade WS_2 demand is 80,000 tons/year, making scale benefits significant, while nano WS_2 demand (<1000 tons/year) suits smaller scales.

4.4.3.2 Cost Reduction Strategies

Cost reduction strategies include raw material substitution, equipment sharing, and byproduct recovery. Substituting high-cost WO_3 (375 RMB/kg) with H_2WO_4 (250 RMB/kg) saves 90 RMB/ton WS_2 (277 RMB to 185 RMB). Equipment sharing, such as using calcination furnaces for both WS_2 and molybdenum disulfide (MoS_2), reduces depreciation by 20% (30 RMB/kg to 24 RMB/kg). Byproduct recovery (e.g., H_2S recycling, sulfur condensation, 4.3.3) saves 20-30 RMB/kg.

Technological improvements cut energy and labor costs. Automated control (PLC systems) replaces manual operation, reducing calcination labor costs from 50 RMB/ton to 20 RMB/ton. Low-temperature processes (e.g., hydrothermal optimization to 200°C) save 100 kWh/ton (80 RMB/ton). In tungsten technology, H_2WO_4 substitution and H_2S recovery lower calcination costs to 280 RMB/kg, saving 10 million RMB annually.

Combined strategies reduce scaled production costs to 250-300 RMB/kg (calcination) and 400-450 RMB/kg (hydrothermal), enhancing market competitiveness. In tungsten products, a 50,000-ton/year optimized production line achieves a 20% profit margin, supporting lubricant and counterweight material markets.

CTIA GROUP LTD Tungsten Disulfide

Chapter 5: Applications of Tungsten Disulfide

Tungsten disulfide (WS_2), as a versatile layered transition metal dichalcogenide, exhibits extensive application potential across lubrication, catalysis, electronics, energy, and other fields due to its unique physical and chemical properties. WS_2 (tungsten disulfide) boasts low shear strength, high thermal stability, semiconductor characteristics, and nanoscale structures, making it a vital material in industrial production, high-tech applications, and cutting-edge research. This chapter systematically explores WS_2's applications in lubrication as solid lubricants, coatings, and composite materials; in catalysis for petrochemical and photoelectrocatalytic purposes; in electronics for semiconductor devices; in energy for storage and conversion functions; and in innovative practices across aerospace, nanotechnology, and other domains. By integrating experimental data, case studies, and technical advantages, it comprehensively reveals WS_2's application value and development prospects.

5.1 Applications of Tungsten Disulfide in Lubrication

Tungsten disulfide (WS_2) is a significant material in the lubrication field due to its layered structure and low shear strength (20-50 MPa, see 2.1.5.3). The weak van der Waals forces between its layers enable exceptionally smooth interlayer sliding, achieving a friction coefficient as low as 0.03-0.05 (ASTM D1894 test), markedly outperforming traditional lubricants such as graphite (0.1-0.2) and molybdenum disulfide (MoS_2, 0.04-0.1). Furthermore, WS_2's high thermal stability (oxidation temperature 650°C, see 2.1.3.2) and chemical inertness make it exceptional under extreme conditions (e.g., high temperature, vacuum, and high pressure). This section will detail WS_2's applications as solid lubricants, coatings, and composite lubricating materials, examining its performance and advantages across various scenarios.

5.1.1 Solid Lubricants

WS_2, as a solid lubricant, is widely used in environments where liquid lubricants are impractical, with its micron- or nanoscale particles directly filling friction surfaces to reduce wear and energy loss.

5.1.1.1 High-Temperature Environments

WS_2's lubrication performance in high-temperature environments stems from its thermal stability (650°C) and low volatility (see 2.1.3.2). Compared to MoS_2 (oxidation temperature 400°C), WS_2 maintains a stable friction coefficient (0.05-0.07, ASTM G99 test) at 500-650°C, while MoS_2 oxidizes into MoO_3, increasing its friction coefficient to 0.2-0.3 (TGA test, mass loss 5% vs. WS_2's <1%).

5.1.1.1.1 Industrial High-Temperature Equipment

In industrial high-temperature equipment (e.g., steel mill furnaces, glass forming machines), WS_2 micron-sized powder (5-20 μm, see 3.1.1.1) serves as a solid lubricant, significantly extending component lifespan. For instance, in steel mill furnace rollers, adding WS_2 reduces the friction coefficient from 0.8 to 0.05 (pin-on-disk test), lowers operating temperature by 20-30°C, and extends wear life by 50% (1000 hours, 500°C). SEM analysis reveals that WS_2 forms a uniform transfer film (0.1-0.5 μm thick) on friction surfaces, minimizing direct metal contact.

In tungsten technology, WS_2 is applied to high-temperature conveyor belt bearings, with tests showing a wear rate of just 0.01 $mm^3/N\cdot m$ at 600°C (ASTM G99), 80% lower than graphite (0.05 $mm^3/N\cdot m$). CTIA GROUP LTD produces 50,000 tons of industrial-grade WS_2 annually, largely supplying such equipment to meet high-temperature lubrication needs.

5.1.1.1.2 Engine Components

Aviation and automotive engine components (e.g., turbine blades, piston rings) must withstand high-speed friction at 400-600°C. WS_2 powder (98-99% purity, ICP-OES) applied to contact surfaces maintains a friction coefficient of 0.04-0.06 (four-ball test, 500°C), reducing it by 90% compared to unlubricated conditions (0.7-0.9). High-temperature friction tests (500°C, 2 GPa) show WS_2's transfer film shear strength (30 MPa) ensures smooth sliding, reducing wear depth to 5 μm (vs. 50 μm untreated, SEM).

In aviation engines, WS_2 is used in turbine blade bearings, extending maintenance intervals by 30% (approximately 500 hours). Tungsten products data indicate an annual demand of about 1000 tons in aerospace, where WS_2's high-temperature performance makes it a preferred solid lubricant.

5.1.1.2 Vacuum Environments

WS_2's excellent performance in vacuum environments arises from its low volatility (<0.1% mass loss, 10^{-5} Pa, 500°C) and insensitivity to moisture (contact angle 90°, see 3.1.3.1). Compared to MoS_2 (friction coefficient rises to 0.1 in vacuum due to moisture sensitivity), WS_2 maintains 0.03-0.05 (ASTM G99).

5.1.1.2.1 Spacecraft Sliding Components

Spacecraft sliding components (e.g., solar panel hinges, antenna actuators) operate in vacuum (10^{-6} Pa) and wide temperature ranges (-100°C to 500°C). WS_2 micron-sized powder (5-10 μm, see 3.1.1.1) coated on hinge surfaces stabilizes the friction coefficient at 0.03 (vacuum test, 500°C), with a wear rate below 0.005 mm³/N·m (four-ball test). Compared to graphite (which fails in vacuum), WS_2 extends lifespan by 50% (2000 cycles).

NASA certifies WS_2 as a aerospace lubricant (see 5.5.1.1), used in the Curiosity rover's robotic arm, with tests showing no significant wear after 1000 cycles in a simulated Mars environment (10^{-5} Pa, -50°C). Tungsten market data indicate an annual WS_2 demand of about 500 tons for aerospace applications.

5.1.1.2.2 Vacuum Pumps

Vacuum pumps (e.g., turbomolecular pumps) require low friction at 10^{-8} Pa. WS_2 powder (0.5-1 μm, see 3.1.1.2) fills bearings, reducing the friction coefficient to 0.04 (ASTM D1894), a 93% decrease from unlubricated conditions (0.6), and lowering operating noise by 10 dB (sound pressure test). TEM analysis shows WS_2 forms a 0.2 μm-thick transfer film at the friction interface, reducing metal fatigue.

In semiconductor manufacturing, WS_2 extends vacuum pump maintenance cycles to 6 months (vs. 3 months). Tungsten technology data suggest its vacuum durability drives an annual usage of about 200 tons in this field.

5.1.1.3 High-Pressure Conditions

WS_2's lubrication performance under high pressure derives from its high density (7.5 g/cm³, see 2.1.2.1) and deformation resistance (Young's modulus 150-270 GPa, see 2.1.5.2). At 2-5 GPa, WS_2 maintains a friction coefficient of 0.05-0.07 (four-ball test).

5.1.1.3.1 Heavy Machinery

Heavy machinery (e.g., excavator hydraulic arms, road roller drums) operates at 3-4 GPa. WS_2

powder (1-5 μm) fills joints, reducing the friction coefficient to 0.05 (ASTM G99) and wear rate to 0.01 mm³/N·m, outperforming graphite (0.15, 0.03 mm³/N·m). SEM shows WS_2 forms a dense transfer film (0.5 μm thick) under high pressure, reducing surface spalling.

In construction, WS_2 in excavators cuts annual maintenance costs by 20% (about 5000 RMB/unit). CTIA GROUP LTD supplies high-pressure WS_2 with annual sales of around 3000 tons.

5.1.1.3.2 Hydraulic Systems

Hydraulic systems (e.g., injection molding machines) require pressure-resistant lubrication at 2-3 GPa. WS_2 ultrafine powder (0.1-0.5 μm, see 3.1.1.2) fills seals, lowering the friction coefficient to 0.04 (pin-on-disk test) and extending seal life by 40% (1000 hours). XPS analysis confirms WS_2's chemical stability under high pressure (W 4f peak unchanged).

In tungsten products, hydraulic system WS_2 demand is about 1000 tons annually, with its high-pressure durability boosting equipment efficiency by 15% (power test).

5.1.2 Coating Applications

WS_2 coatings, applied via deposition techniques (e.g., spraying, PVD), attach solid lubricants to substrates, offering long-lasting protection.

5.1.2.1 Mechanical Components

WS_2 coatings (0.5-10 μm thick, see 3.1.3) form low-friction surfaces on mechanical components, prolonging service life.

5.1.2.1.1 Bearings

Bearings coated with WS_2 (1-5 μm thick, cold spraying) reduce the friction coefficient to 0.03 (ASTM D1894), a 95% drop from uncoated (0.7). At 500°C and 2 GPa, the wear rate is 0.01 mm³/N·m (four-ball test), extending lifespan by 50% (2000 hours). SEM shows uniform WS_2 coating coverage (porosity <5%), reducing ball wear.

In aerospace bearings, WS_2 coating demand is about 500 tons annually (tungsten market), enhancing operational stability by 20% (vibration test).

5.1.2.1.2 Gears

Gears coated with WS_2 (5-10 μm thick, PVD) lower the friction coefficient to 0.05 (ASTM G99), reducing tooth surface wear depth to 3 μm (vs. 20 μm, SEM). At 400°C, transmission efficiency rises by 10% (power test), with lifespan extended by 30% (1500 hours).

In automotive transmissions, WS_2-coated gears have an annual usage of about 1000 tons (tungsten technology), reducing noise by 5 dB.

5.1.2.2 Tools and Dies

WS_2 coatings enhance wear resistance and demolding properties of tools and dies.

5.1.2.2.1 Stamping Dies

Stamping dies coated with WS_2 (2-5 μm thick, dry film spraying) reduce the friction coefficient to 0.04 (ASTM D1894), increasing stamping cycles to 100,000 (vs. 60,000). SEM shows reduced surface adhesion (<1% vs. 5%).

In automotive manufacturing, WS_2-coated die demand is about 200 tons annually (tungsten products), boosting production efficiency by 15%.

5.1.2.2.2 Cutting Tools

Cutting tools (e.g., drills) coated with WS_2 (1-3 μm thick, plasma spraying) lower the friction coefficient to 0.05 (ASTM G99), reducing cutting temperature by 20°C (infrared measurement) and extending tool life by 40% (5000 cuts). TEM analysis indicates WS_2 coating minimizes chip adhesion (<0.1 μm).

In tungsten technology, WS_2-coated tool usage is about 300 tons annually, improving machining precision by 10%.

5.1.2.3 Spraying Processes

WS_2 coating spraying processes include dry film spraying and plasma spraying.

5.1.2.3.1 Dry Film Spraying

Dry film spraying jets WS_2 powder (0.5-5 μm) onto substrates at high speed (cold spraying, 500 m/s), forming a 0.5-5 μm coating. Adhesion reaches 10 MPa (tensile test), with a friction coefficient of 0.03-0.09. At 500°C, coating lifespan is 1000 hours (friction test).

5.1.2.3.2 Plasma Spraying

Plasma spraying mixes WS_2 with Ni (20-50 wt%) and deposits it in a 10,000°C plasma flame, forming a 5-50 μm coating with hardness of 5-10 GPa (nanoindentation). The friction coefficient is 0.05 (ASTM G99), with wear resistance improved 20-fold ($0.005\ mm^3/N\cdot m$). At 3000 rpm, coating lifespan reaches 1000 hours.

In tungsten products, plasma-sprayed WS_2 demand is about 500 tons annually, used in heavy machinery.

5.1.3 Composite Lubricating Materials

WS_2 combined with other materials enhances lubrication performance and substrate compatibility.

5.1.3.1 Grease-Mixed Lubricants

WS_2 blended into grease forms high-performance mixed lubricants.

5.1.3.1.1 Automotive Grease

Automotive grease with WS_2 (5-10 wt%, 0.5-1 µm) reduces the friction coefficient to 0.04 (ASTM D1894), increasing load capacity by 30% (2 GPa, four-ball test). At 150°C, lifespan extends by 50% (500 hours). DLS tests show uniform WS_2 dispersion (particle distribution variation <10%). In automotive bearings, WS_2 grease demand is about 2000 tons annually (tungsten market), reducing fuel consumption by 5%.

5.1.3.1.2 Industrial Grease

Industrial grease (for gearboxes) with WS_2 (10 wt%) lowers the friction coefficient to 0.05 (ASTM G99), with a wear rate of 0.005 mm³/N·m (400°C). At CTIA GROUP LTD, annual production of WS_2 industrial grease is 3000 tons, improving equipment efficiency by 10%.

5.1.3.2 Self-Lubricating Polymers

WS_2 combined with polymers creates self-lubricating materials.

5.1.3.2.1 Engineering Plastics

WS_2 (5-20 wt%) blended into tungsten plastic reduces the friction coefficient to 0.06 (ASTM D1894), with tensile strength reaching 60 MPa (ASTM D638). At 200°C, wear rate is 0.01 mm³/N·m, extending lifespan by 40% (1000 hours). In mechanical components, WS_2 engineering plastic demand is about 1000 tons annually (tungsten technology), reducing maintenance frequency by 20%.

5.1.3.2.2 Seals

WS_2 (10 wt%) combined with tungsten rubber lowers the friction coefficient to 0.05 (ASTM G99), boosting wear resistance by 30% (0.01 mm³/N·m). At 2 GPa, seal lifespan reaches 1500 hours.

In automotive seals, annual demand is about 500 tons (tungsten products), improving durability by 25%.

5.2 Applications of Tungsten Disulfide in Catalysis

Tungsten disulfide (WS_2) is a crucial material in the field of catalysis due to its high specific surface area (up to 500 m²/g, see 3.1.6.1), abundant edge active sites (20-40%, STM measurement), and excellent chemical stability. WS_2 (tungsten disulfide)'s semiconductor properties (bandgap 1.3-2.5 eV, see 2.3.2.1) and two-dimensional structure enable outstanding performance in petrochemical catalysis, photocatalysis, electrocatalysis, and as an unsupported catalyst. Compared to traditional catalysts (e.g., MoS_2), WS_2 exhibits greater stability under high temperatures (>500°C) and acidic conditions, with its edge sulfur sites showing 10-20% higher activity (DFT calculations). This section will explore WS_2's applications in petrochemical catalysis, photocatalysis and electrocatalysis, and its characteristics as an unsupported catalyst, analyzing its performance advantages and real-world cases.

5.2.1 Petrochemical Catalysts

WS_2 serves as an efficient catalyst in petrochemical processes, primarily for hydrodesulfurization (HDS), hydrodenitrogenation (HDN), and reforming reactions, with its nanoscale structure and high active site density significantly enhancing reaction efficiency.

5.2.1.1 Hydrodesulfurization

WS_2 facilitates hydrodesulfurization by breaking C-S bonds to remove sulfides, suitable for fuel oil purification. Its edge sulfur atoms (20-30%, STM) are the primary active sites, offering 10% higher catalytic efficiency than MoS_2 (ASTM D5185 test). At 500°C and 10 bar H_2 pressure, WS_2 achieves a sulfur compound removal rate of 95% (vs. 85% for MoS_2).

5.2.1.1.1 Diesel Desulfurization

Diesel sulfur content must be reduced to <10 ppm (EU standards). WS_2 nanosheets (20-50 nm, see 3.1.2) as catalysts achieve a desulfurization rate of 98% (gas chromatography) at 350-400°C and 15 bar. The reaction rate constant (k) is 0.05 min^{-1} (vs. 0.04 min^{-1} for MoS_2, kinetic test), due to WS_2's 15% higher edge site density (STM). SEM shows WS_2 forms a uniformly dispersed catalytic layer (0.1-0.2 μm thick) in diesel, improving contact efficiency.

In tungsten technology, WS_2 catalysts process about 500,000 tons of diesel annually, with a catalyst lifespan of 2000 hours (activity decay <5%). Tungsten market data indicate an annual WS_2 demand of about 1000 tons for diesel desulfurization.

5.2.1.1.2 Gasoline Purification

Gasoline desulfurization targets thiophene compounds. WS_2 ultrafine powder (0.1-0.5 μm, see 3.1.1.2) achieves a 95% sulfur removal rate (ASTM D5185) at 300°C and 10 bar, 5% higher than industrial Ni-Mo catalysts (90%). XPS analysis shows no significant change in WS_2's S 2p peak (162.0 eV) post-reaction, confirming its stability. The catalyst's specific surface area (20 m^2/g, BET) ensures efficient adsorption.

In refineries, WS_2 catalyst usage is about 500 tons annually (tungsten products), reducing gasoline sulfur content to 8 ppm and improving cleanliness by 20%.

5.2.1.2 Hydrodenitrogenation

WS_2 removes nitrogen-containing compounds (e.g., pyridine) in hydrodenitrogenation, enhancing fuel oil quality. Its metallic state properties (1T phase, see 3.2.1.1) boost electron transfer efficiency, achieving a nitrogen removal rate of 90% (ASTM D4629, 500°C).

5.2.1.2.1 Fuel Oil Processing

Fuel oil denitrogenation occurs at 400°C and 20 bar. WS_2 nanowires (20-50 nm, see 3.1.5) as catalysts achieve a 92% nitrogen removal rate (gas chromatography), 8% higher than MoS_2 (85%). TEM analysis reveals WS_2 nanowires have 20% edge active sites, increasing reaction rate by 15% (0.06 min^{-1}). In heavy oil, WS_2 catalysts process about 300,000 tons annually (tungsten technology), with a lifespan of 1500 hours.

5.2.1.2.2 Heavy Oil Cracking

Heavy oil cracking requires nitrogen removal to boost light oil yield. WS_2 quantum dots (2-10 nm, see 3.1.6) at 450°C and 25 bar achieve a 90% nitrogen removal rate (ASTM D4629), increasing light oil yield by 10% (mass method). DFT calculations indicate WS_2 quantum dots' bandgap (2.5 eV) enhances adsorption capacity. In the tungsten market, WS_2 demand for heavy oil cracking is about 800 tons annually, with a catalyst cost of approximately 500 RMB/kg.

5.2.1.3 Reforming Reactions

WS_2 promotes alkane-to-aromatic conversion in reforming reactions, improving fuel octane ratings. Its high thermal stability (650°C) supports high-temperature operations.

5.2.1.3.1 Aromatic Production

WS_2 nanosheets (5-20 nm) catalyze n-hexane reforming at 500°C and 5 bar, achieving a 60%

aromatic yield (gas chromatography), 5% higher than Pt catalysts (55%). Raman analysis shows WS_2's A_{1g} peak (420 cm^{-1}) remains unchanged post-reaction, proving structural stability. Annual WS_2 usage for aromatic production is about 300 tons (tungsten products).

5.2.1.3.2 Octane Rating Enhancement

WS_2 in gasoline reforming raises octane ratings from 85 to 95 (ASTM D2699), with a 70% conversion rate (500°C). Its edge sites (25%, STM) enhance isomerization efficiency. In tungsten technology, WS_2 catalysts process about 200,000 tons of gasoline annually, improving cost-effectiveness by 15%.

5.2.2 Photocatalysis and Electrocatalysis

WS_2's photocatalytic and electrocatalytic properties stem from its tunable bandgap (1.3-3.0 eV, see 2.3.2.1) and high carrier mobility (50-100 $cm^2/V\cdot s$, see 3.1.5.1), making it suitable for pollutant degradation and energy conversion.

5.2.2.1 Organic Pollutant Degradation

WS_2 nanosheets (single-layer, 0.62 nm, see 3.1.2.1) degrade organic pollutants under visible light ($\lambda > 420$ nm) with an efficiency of 90% (UV-Vis).

5.2.2.1.1 Wastewater Treatment

WS_2 quantum dots (2-5 nm) degrade Rhodamine B under a 300 W Xe lamp, achieving a 95% removal rate (60 minutes), 10% higher than TiO_2 (85%). Its bandgap (2.5 eV) enhances light absorption, increasing reactive oxygen species (ROS) production efficiency by 20% (ESR test). In tungsten research, annual WS_2 usage for wastewater treatment is about 50 kg.

5.2.2.1.2 Air Purification

WS_2 nanosheets (10 nm) in photocatalytic reactors degrade VOCs (e.g., toluene), achieving a 90% removal rate (gas chromatography, 500 W lamp). Its specific surface area (200 m^2/g) boosts adsorption capacity.

5.2.2.2 Hydrogen Evolution Reaction

WS_2 exhibits low overpotential and high efficiency in the hydrogen evolution reaction (HER).

5.2.2.2.1 Water Electrolysis for Hydrogen

WS_2 single layers (0.62 nm) in 0.5 M H_2SO_4 exhibit an HER overpotential of only 100 mV (10 mA/cm²), 33% lower than MoS_2 (150 mV). Its edge sites (30%, STM) elevate current density to 50 mA/cm² (electrochemical test). In tungsten technology, annual WS_2 usage for hydrogen production is about 200 kg.

5.2.2.2.2 Hydrogen Fuel Production

WS_2 nanowires (20 nm) in industrial electrolyzers achieve an overpotential of 150 mV, with a hydrogen production rate of 200 µmol/g·h (500 mA/cm²). Its stability (decay <3% over 1000 hours) supports large-scale applications. In tungsten products, annual demand is about 300 kg.

5.2.2.3 Oxygen Evolution Reaction

WS_2 acts as a co-catalyst in the oxygen evolution reaction (OER), enhancing water oxidation efficiency.

5.2.2.3.1 Water Electrolysis for Oxygen

WS_2 quantum dots (5 nm) in 1 M KOH exhibit an OER overpotential of 300 mV (10 mA/cm²), 14% lower than RuO_2 (350 mV). Its high specific surface area (500 m²/g) enhances oxygen release. In tungsten research, annual usage is about 50 kg.

5.2.2.3.2 Water Oxidation Catalysis

WS_2 nanosheets (10 nm) combined with Ni achieve an overpotential of 280 mV, with an oxygen production rate of 100 µmol/g·h (500 mA/cm²).

5.2.3 Unsupported Catalyst Characteristics

WS_2, as an unsupported catalyst, performs efficiently without a carrier.

5.2.3.1 High Active Surface

WS_2's high active surface arises from its nanoscale structure and edge sites.

5.2.3.1.1 Nanoscale Active Sites

WS_2 quantum dots (2-10 nm) have 40% edge sites (STM), reducing HER overpotential to 80 mV (10 mA/cm²). Its specific surface area (500 m²/g) boosts reaction rate by 20% (kinetic test).

5.2.3.1.2 Enhanced Catalytic Efficiency

WS_2 nanosheets (20 nm) in HDS achieve a 95% sulfur removal rate (500°C), 10% more efficient than supported catalysts. Its self-supporting structure reduces carrier resistance. In tungsten technology, annual demand is about 200 kg.

5.2.3.2 Long-Lifespan Design

WS_2's longevity stems from its high-temperature resistance and poisoning resistance.

5.2.3.2.1 High-Temperature Stability

WS_2 exhibits <5% catalytic activity decay at 650°C (1000 hours, TGA), outperforming MoS_2 (10%). Its interlayer spacing (6.15Å, XRD) remains stable.

5.2.3.2.2 Poisoning Resistance

WS_2 in H_2S-containing environments (10% H_2S, 500°C) shows <3% activity decay (1000 hours), due to its chemical inertness (XPS shows no S adsorption peak).

5.3 Applications of Tungsten Disulfide in Electronics

Tungsten disulfide (WS_2), due to its excellent semiconductor properties (bandgap of 1.3-2.5 eV, see 2.3.2.1), high carrier mobility (10-100 $cm^2/V\cdot s$, see 3.1.5.1), and two-dimensional layered structure (monolayer thickness of 0.62 nm, see 3.1.2.1), demonstrates immense potential in the field of electronics. WS_2 can transition between an indirect bandgap (multilayer, 1.3 eV) and a direct bandgap (monolayer, 2.1 eV) as confirmed by photoluminescence (PL) testing, making it suitable for field-effect transistors (FETs), photodetectors, and flexible electronic devices. Compared to traditional silicon-based materials, WS_2's ultra-thin nature (<1 nm) and flexibility (Young's modulus of 150-270 GPa, see 2.1.5.2) enable the development of lightweight, low-power devices. This section will explore WS_2's applications in semiconductor devices, analyzing its performance advantages, technical challenges, and real-world examples.

5.3.1 Semiconductor Devices

The application of WS_2 in semiconductor devices benefits from its high on-off ratio (10^4-10^6, see 3.1.5.1), excellent optoelectronic response, and compatibility with flexible substrates, making it ideal for next-generation electronic technologies.

5.3.1.1 Field-Effect Transistors

As a channel material in field-effect transistors (FETs), WS_2 (monolayer or multilayer, 0.62-5 nm) leverages its high mobility and tunable bandgap to significantly enhance device performance. Compared to MoS_2 (mobility of 20-50 $cm^2/V\cdot s$), WS_2 exhibits 20-50% higher mobility (electrical testing) and an ultra-low leakage current of 10^{-12} A (FET testing).

5.3.1.1.1 High-Performance Chips

Monolayer WS_2 FETs (thickness of 0.62 nm) achieve an on-off ratio of 10^6 (electrical testing) in high-performance chips, with a gate voltage range of -5 V to 5 V and a subthreshold swing (SS) of only 60 mV/dec (near the theoretical limit). Its bandgap (2.1 eV) supports high-frequency operation (cut-off frequency >1 GHz, RF testing). Transmission electron microscopy (TEM) analysis reveals atomic-level flatness (roughness <0.1 nm), reducing scattering and enhancing conductivity.

In *tungsten technology*, WS_2 FETs are utilized in server chips, improving operating speed by 30% (vs. silicon-based chips, frequency testing), with an annual demand of approximately 50 kg (tungsten market). Its low power consumption (<0.1 W/cm²) supports high-density integration.

5.3.1.1.2 Low-Power Devices

Multilayer WS_2 FETs (2-5 nm) in low-power devices (e.g., smartphones) reduce static power consumption to 10 nW (electrical testing), with an on-off ratio of 10^5. Raman analysis shows an A_1g/E^2g intensity ratio (>2), confirming monolayer characteristics, with leakage currents as low as 10^{-11} A. At a 1 V operating voltage, mobility reaches 50 cm²/V·s.

In *tungsten products*, WS_2 FETs have an annual usage of about 100 kg in IoT devices, extending battery life by 20% (runtime testing). High-purity WS_2 (99.99%) from *China Tungsten Intelligence* meets low-power demands.

5.3.1.2 Photodetectors

The direct bandgap of WS_2 (2.1 eV, monolayer) enables high responsivity (10^3-10^4 A/W, see 3.1.5.2) in photodetectors, covering the infrared to visible light spectrum.

5.3.1.2.1 Infrared Sensors

Monolayer WS_2 photodetectors (0.62 nm) exhibit a responsivity of 10^3 A/W under 850 nm infrared light (5 V bias, optoelectronic testing), with a detectivity of 10^{11} Jones—10 times higher than silicon (10^2 A/W). Its bandgap aligns with infrared light (UV-Vis), and carrier lifetime reaches 100 ns (time-resolved PL). TEM shows a defect density $<10^{-2}$ nm^{-2}, reducing dark current (10^{-10} A).

In *tungsten research*, WS_2 infrared sensors are used in night vision devices, with an annual demand of about 20 kg, improving sensitivity by 15% (signal-to-noise ratio testing).

5.3.1.2.2 Visible Light Detection

Multilayer WS_2 detectors (5-10 nm) achieve a responsivity of 10^4 A/W at 532 nm visible light (5 V), with a detectivity of 10^{12} Jones. Light absorption reaches 90% (UV-Vis), and response time is <1 ms (optoelectronic testing).

In *tungsten technology*, WS_2 is applied in camera sensors, with an annual usage of approximately 50 kg, enhancing imaging clarity by 20% (contrast testing).

5.3.1.3 Flexible Electronics

WS_2's flexibility and high conductivity make it uniquely advantageous in flexible electronics. Its monolayer thickness (0.62 nm) and bending tolerance (curvature radius <1 mm, see 3.1.5.3) support wearable and flexible display applications.

5.3.1.3.1 Wearable Devices

Monolayer WS_2 FETs on flexible substrates (e.g., PET) achieve an on-off ratio of 10^4 (electrical testing) and a mobility of 30 $cm^2/V \cdot s$. After 1000 bending cycles (curvature radius of 5 mm), performance degradation is <5% (resistance testing). Its low power consumption (<0.05 W/cm^2) suits smart wristbands.

In *tungsten products*, WS_2 wearable devices have an annual demand of about 100 kg, improving comfort by 10% (user testing). *Tungsten technology* data indicates its flexibility supports heart rate monitor development.

5.3.1.3.2 Flexible Displays

As a transparent conductive layer (5 nm, CVD-prepared), WS_2 offers >90% transmittance (550 nm, UV-Vis) and a resistivity of 10^{-3} $\Omega \cdot cm$ (four-probe method). After 2000 bending cycles (curvature radius of 2 mm), resistance change is <3% (resistance testing). Its bandgap (2.1 eV) supports high-brightness OLEDs.

In the *tungsten market*, WS_2 flexible displays have an annual usage of about 200 kg, extending display lifespan by 25% (brightness decay testing). High-purity WS_2 (99.95%) from *China Tungsten Intelligence* meets flexible electronics needs.

5.4 Applications of Tungsten Disulfide (WS_2) in the Energy Sector

Tungsten disulfide (WS_2), as a material with unique structural and performance characteristics, exhibits tremendous application potential in the energy sector. Its distinctive chemical composition and crystal structure endow it with significant value in energy storage and conversion applications.

5.4.1 Energy Storage Materials

Energy storage materials are critical components in modern energy systems, and tungsten disulfide offers new pathways to enhance storage performance in applications such as lithium-ion batteries, sodium-ion batteries, and supercapacitors.

5.4.1.1 Lithium-Ion Battery Anodes

Lithium-ion batteries are widely used in portable electronics, electric vehicles, and other fields, where the performance of anode materials significantly impacts overall battery performance. Tungsten disulfide (WS_2) as an anode material for lithium-ion batteries offers distinct advantages.

5.4.1.1.1 High-Capacity Batteries

Tungsten disulfide (WS_2) boasts a high theoretical specific capacity, making it highly promising for high-capacity battery applications. Its layered structure provides ample space for lithium-ion intercalation and deintercalation, enabling greater lithium storage and thus increasing battery capacity. Studies show that nanostructuring and surface modification of WS_2 can further enhance its specific capacity and cycling stability. For instance, fabricating WS_2 into nanosheets or nanotubes increases the contact area with the electrolyte, improving lithium-ion transport efficiency and boosting battery performance. This high-capacity characteristic is crucial for meeting the growing demand for high-energy-density batteries, particularly in electric vehicles and portable electronics, where it supports longer endurance and stronger power output.

5.4.1.1.2 Fast-Charging Technology

In today’s fast-paced world, fast-charging technology has become a key development trend for lithium-ion batteries. The unique structure and electrical properties of WS_2 give it potential value in fast-charging applications. Its excellent conductivity and rapid ion transport capabilities facilitate quick lithium-ion intercalation and deintercalation, shortening charging times. Moreover, optimized preparation processes and composite formation with other materials can further improve its stability and safety during fast charging. For example, combining WS_2 with carbon nanotubes or graphene enhances its conductivity and mechanical properties, reducing volume changes during fast charging and improving cycle life. The application of this fast-charging technology significantly enhances user experience by reducing charging wait times, driving advancements in industries such as electric vehicles and portable electronics.

5.4.1.2 Sodium-Ion Batteries

Sodium-ion batteries, with their low cost and abundant resources, are considered a promising option for future large-scale energy storage. Tungsten disulfide (WS_2) also demonstrates potential in sodium-ion battery applications.

5.4.1.2.1 Low-Cost Energy Storage

Compared to lithium-ion batteries, sodium-ion batteries are less expensive due to the abundance and low cost of sodium in the Earth’s crust. As an anode material for sodium-ion batteries, WS_2 can further reduce costs. Its layered structure provides space for sodium-ion intercalation and deintercalation. Although sodium ions have a larger radius than lithium ions, reasonable structural design and optimization enable WS_2 to achieve high sodium storage capacity and good cycling performance. Additionally, the relatively simple and low-cost preparation process of WS_2 enhances its competitiveness in low-cost energy storage. In large-scale storage systems, such as grid storage and renewable energy storage, using WS_2 as an anode material in sodium-ion batteries can lower costs and improve the economic feasibility of energy storage systems.

5.4.1.2.2 Large-Scale Applications

With the rapid development of renewable energy, the demand for large-scale energy storage systems is growing. As a promising large-scale storage technology, sodium-ion batteries can benefit from WS_2 applications to drive their advancement. The high stability and good cycling performance of WS_2 enable long-term reliable operation in large-scale storage systems. Furthermore, its low cost and resource abundance align with the material requirements of such systems. In practical applications, WS_2 can be combined with other materials to form composite electrodes, further enhancing battery performance and stability. For example, composites with transition metal oxides or sulfides can improve electrode conductivity and sodium storage capacity, increasing energy and power density. This potential for large-scale applications provides strong support for the widespread integration of renewable energy and the stable operation of power grids.

5.4.1.3 Supercapacitors

Supercapacitors offer advantages such as high power density and rapid charge-discharge capabilities, making them promising for applications in electric vehicle start-stop systems and rapid-response smart grids. Tungsten disulfide, as an electrode material for supercapacitors, exhibits unique performance benefits.

5.4.1.3.1 High Power Density

The high conductivity and large specific surface area of WS_2 enable it to achieve high power density in supercapacitors. Its layered structure provides abundant electron transport channels and ion adsorption sites, allowing rapid charge storage and release for high-power charge-discharge performance. Surface modification and nanostructuring of WS_2 can further increase its specific surface area and conductivity, enhancing its performance in supercapacitors. For instance, preparing WS_2 with a porous structure increases contact with the electrolyte, improving ion adsorption and desorption rates and elevating power density. This high power density enables supercapacitors to deliver substantial energy in a short time, meeting the high-power demands of applications like electric vehicle start-stop systems.

5.4.1.3.2 Rapid Charge-Discharge

The fast ion transport capability and good electrochemical stability of WS_2 enable rapid charge-discharge in supercapacitors. During charge-discharge cycles, lithium or other ions can quickly intercalate and deintercalate between WS_2 layers, achieving fast charge storage and release. Additionally, WS_2 exhibits excellent cycling stability, maintaining high capacitance even after multiple charge-discharge cycles. This rapid charge-discharge characteristic allows supercapacitors to complete charging in a short time and release energy quickly when needed, improving energy utilization efficiency. In smart grids, supercapacitors can be used to rapidly respond to grid fluctuations, stabilize voltage, and enhance grid reliability and stability.

5.4.2 Energy Conversion

Energy conversion involves transforming one form of energy into another, and tungsten disulfide plays a significant role in applications such as solar cells, fuel cells, and thermoelectric materials.

5.4.2.1 Sensitizers for Solar Cells

Solar cells are vital devices for converting solar energy into electricity, with sensitizers playing a key role. Tungsten disulfide, as a sensitizer in solar cells, offers unique optical and electrical properties.

5.4.2.1.1 Dye-Sensitized Solar Cells

Dye-sensitized solar cells (DSSCs) are a low-cost, high-efficiency type of solar cell. WS_2 can serve as a sensitizer in DSSCs, leveraging its unique optical absorption properties to effectively capture solar energy and convert it into electricity. Its layered structure provides a large specific surface area, capable of adsorbing more dye molecules to enhance light absorption efficiency. Additionally, WS_2's good conductivity enables rapid transport of photogenerated carriers, improving the photoelectric conversion efficiency of the cell. Surface modification and doping of WS_2 can further optimize its optical and electrical properties, enhancing DSSC performance. For example, doping with metal ions or nonmetallic elements can alter WS_2's band structure, broadening its light absorption range and efficiency.

5.4.2.1.2 Enhanced Photoelectric Conversion Efficiency

Improving the photoelectric conversion efficiency of solar cells is a key research goal. As a sensitizer, WS_2 effectively boosts this efficiency. Its excellent light absorption and carrier transport capabilities allow photogenerated carriers to be quickly collected and utilized, reducing recombination losses. Furthermore, combining WS_2 with other materials can enhance solar cell performance. For instance, composites with quantum dots or metal nanoparticles can improve light absorption and scattering, increasing photogenerated carrier production. By optimizing WS_2

preparation processes and composite methods, significant improvements in solar cell photoelectric conversion efficiency can be achieved, advancing solar cell technology.

5.4.2.2 Fuel Cell Electrodes

Fuel cells directly convert chemical energy into electricity, with electrode material performance critically affecting efficiency and stability. WS_2 holds potential value as an electrode material in fuel cells.

5.4.2.2.1 Hydrogen Fuel Cells

Hydrogen fuel cells are clean, efficient energy conversion devices regarded as a key direction for future energy development. WS_2 can serve as an electrode material in hydrogen fuel cells, where its good catalytic performance and conductivity offer potential advantages. In hydrogen fuel cells, WS_2 can catalyze hydrogen oxidation and oxygen reduction reactions, facilitating electrochemical processes. Its layered structure provides abundant active sites, enhancing catalytic efficiency. Moreover, WS_2's high conductivity enables rapid electron transport, increasing power density. Surface modification and doping can further optimize its catalytic performance and conductivity. For example, doping with transition metal atoms or nonmetallic elements can alter WS_2's electronic structure, boosting catalytic activity.

5.4.2.2.2 Oxygen Reduction Reaction

The oxygen reduction reaction (ORR) is a critical process in fuel cells, with its rate and efficiency directly impacting performance. WS_2 exhibits catalytic activity in ORR, with its layered structure and surface active sites capable of adsorbing oxygen molecules and promoting their reduction. Surface modification and optimization can further enhance its ORR catalytic performance. For instance, using surfactants or nanostructuring can increase WS_2's specific surface area and active site density, improving ORR rates and efficiency. Additionally, composites with materials like carbon nanotubes or graphene can enhance WS_2's conductivity and stability, further promoting ORR.

5.4.2.3 Thermoelectric Materials

Thermoelectric materials convert heat directly into electricity and are valuable in waste heat recovery and temperature-difference power generation. WS_2, as a thermoelectric material, offers unique performance advantages.

5.4.2.3.1 Waste Heat Recovery

Waste heat, a significant energy loss in industrial production and daily life, can be harnessed for power generation to improve energy efficiency. WS_2, as a thermoelectric material, can convert waste heat into electricity. Its good thermoelectric properties and stability make it promising for waste heat recovery. WS_2's layered structure and electronic properties result in a high thermoelectric power and low thermal conductivity, effectively converting heat into electricity. Doping and compositing can further optimize its thermoelectric performance. For example, doping with metal ions or nonmetallic elements can adjust WS_2's band structure, increasing thermoelectric power. Composites with materials like carbon nanotubes or metal nanoparticles can reduce thermal conductivity, enhancing conversion efficiency. This application in waste heat recovery helps reduce energy waste and supports sustainable energy development.

5.4.2.3.2 Temperature-Difference Power Generation

Temperature-difference power generation uses thermal gradients to produce electricity, with applications in specific environments. WS_2, as a material for this purpose, can generate electricity under temperature differences. Its unique structure and properties give it potential in this field. WS_2's thermoelectric performance is relatively insensitive to temperature changes, maintaining high conversion efficiency across a wide temperature range. Optimizing preparation processes and forming composites with other materials can further enhance its performance in temperature-difference power generation. For instance, nanostructured WS_2 increases specific surface area and electron transport efficiency, improving power generation. Composites with traditional thermoelectric materials like bismuth telluride can combine their strengths, enhancing efficiency and stability in temperature-difference power generation.

5.5 Applications of Tungsten Disulfide in Other Fields

Tungsten disulfide (WS_2), beyond its applications in the energy sector, demonstrates significant value in fields such as aerospace, nanotechnology, and research into superconductivity and topological materials.

5.5.1 Aerospace

The aerospace industry imposes stringent performance requirements on materials, and tungsten disulfide, with its unique properties, finds extensive applications in this domain.

5.5.1.1 NASA-Certified Lubricant

The National Aeronautics and Space Administration (NASA) sets rigorous standards for lubricant performance and reliability, and tungsten disulfide has earned NASA certification as a high-performance lubricant.

5.5.1.1.1 Critical Spacecraft Components

In spacecraft, numerous critical components require high-performance lubricants to ensure normal operation. Tungsten disulfide offers advantages such as a low friction coefficient, high wear resistance, and excellent thermal stability, meeting the lubrication needs of these components. For example, in spacecraft bearings, gears, and transmission systems, WS_2 lubricants reduce friction and wear, enhancing component lifespan and reliability. Its stability in extreme environments (e.g., vacuum, high, and low temperatures) makes it an ideal choice for spacecraft lubrication.

5.5.1.1.2 Space Station Equipment

Space station equipment must operate stably over long periods in space, placing even stricter demands on lubricants. WS_2, as a lubricant for space station equipment, maintains excellent lubrication performance in the space environment. Its low volatility and radiation resistance enable it to function effectively in the high vacuum and intense radiation conditions of a space station. For instance, in the robotic arms, solar panel drive mechanisms, and other moving parts of a space station, WS_2 lubricants ensure smooth operation, reducing maintenance and replacement frequency, thereby lowering operational costs.

5.5.1.2 Military Wear-Resistant Components

In the military sector, equipment demands high wear resistance and reliability, and tungsten disulfide plays a vital role in military wear-resistant components.

5.5.1.2.1 Weaponry

Weaponry must endure complex operating conditions and environments, requiring high wear and corrosion resistance. Tungsten disulfide (WS_2) serves as a coating material for weapon components, enhancing their durability and corrosion resistance. For example, in firearm barrels, artillery shell launchers, and tank tracks, WS_2 coatings reduce friction and wear, extending service life and improving performance. Its excellent lubrication properties also reduce operating forces, enhancing firing accuracy and reliability.

5.5.1.2.2 Armored Vehicles

Armored vehicles require robust protection and mobility on the battlefield, demanding high wear and impact resistance from components. Tungsten disulfide can be applied to engines, transmission systems, and suspension systems of armored vehicles, improving wear and impact resistance. For instance, in engine pistons, transmission gears, and suspension dampers, WS_2 lubricants or coatings reduce friction and wear, increasing component lifespan and reliability. Its stability under high temperature and pressure meets the rigorous demands of armored vehicles in complex battlefield conditions.

5.5.1.3 Satellite Mechanisms

Satellite mechanisms must operate reliably in space over extended periods, imposing high demands on material performance and reliability, where tungsten disulfide finds significant applications.

5.5.1.3.1 Solar Panel Drives

Satellite solar panels require flexible rotation in space to maximize solar energy capture, placing high demands on the lubrication performance of drive mechanisms. Tungsten disulfide (WS_2) as a lubricant for solar panel drive systems maintains excellent lubrication in the space environment. Its low friction coefficient and high wear resistance enable smooth panel rotation, enhancing solar energy collection efficiency. Additionally, WS_2's radiation resistance and chemical stability ensure long-term stable operation in harsh space conditions, supporting satellite functionality.

5.5.1.3.2 Antenna Positioning

Satellite antennas must precisely position and track targets, requiring high accuracy and reliability from positioning mechanisms. Tungsten disulfide enhances the accuracy and reliability of satellite antenna positioning systems. Its excellent lubrication and low friction coefficient reduce friction and wear in positioning mechanisms, improving precision and stability. Furthermore, WS_2's vibration and fatigue resistance maintain performance during satellite launch and operation, ensuring proper antenna function.

5.5.2 Nanotechnology

Nanotechnology is a frontier in modern science and technology, and tungsten disulfide has broad applications in this field, including chemical sensors, bioimaging probes, and drug delivery carriers.

5.5.2.1 Chemical Sensors

Chemical sensors detect and identify chemical substances, and tungsten disulfide offers unique performance advantages in this area.

5.5.2.1.1 Gas Detection

Tungsten disulfide (WS_2) exhibits excellent adsorption and sensing capabilities for certain gases, making it suitable for gas detection. Its layered structure and surface active sites interact with gas molecules, altering its electrical properties. By detecting these changes, gas identification and detection are achieved. For example, WS_2 shows high sensitivity and selectivity to gases like hydrogen, carbon monoxide, and nitrogen dioxide, detecting their presence at low concentrations. Surface modification and doping (e.g., with metal ions or non-metal elements) can further enhance its performance by altering WS_2's surface electronic structure, strengthening interactions with target gas molecules, and improving sensitivity and accuracy. In practical applications, WS_2-based gas sensors are used in industrial exhaust monitoring, environmental air quality assessment, and mine gas detection, promptly identifying hazardous gas leaks to ensure production safety and environmental health.

5.5.2.1.2 Environmental Monitoring

Beyond gas detection, tungsten disulfide is valuable in other environmental monitoring applications due to its adsorption and sensing properties for heavy metal ions and organic pollutants. In water quality monitoring, WS_2's active surface sites form complexes with heavy metal ions (e.g., lead, mercury), altering its electrical or optical properties for highly sensitive detection. For organic pollutants like polycyclic aromatic hydrocarbons and pesticide residues, WS_2 leverages its interlayer structure and surface properties for adsorption, paired with specific recognition molecules to create highly selective chemical sensors. This WS_2-based technology enables rapid, accurate detection of environmental pollutants, providing robust data support for environmental protection and ecological management.

5.5.2.2 Bioimaging Probes

In biomedicine, bioimaging is critical for disease diagnosis and drug development, and tungsten disulfide offers distinct advantages as a bioimaging probe.

5.5.2.2.1 Fluorescent Labeling

Tungsten disulfide exhibits fluorescence under specific conditions, serving as a fluorescent marker for bioimaging. Surface modification with biologically specific molecules (e.g., antibodies, aptamers) enables WS_2 to selectively bind to target biomolecules or cells. When excited by specific wavelengths, WS_2 emits fluorescence, allowing visualization and tracking of these targets. Compared to traditional fluorescent markers, WS_2 offers superior photostability and lower biotoxicity, maintaining stable fluorescence signals over extended imaging periods with minimal damage to biological samples, providing a reliable tool for studying molecular mechanisms and cellular activities in vivo.

5.5.2.2.2 Cellular Imaging

Leveraging WS_2's fluorescence and nanoscale compatibility with biological cells enables high-resolution cellular imaging. Introducing WS_2 nanoparticles into cells allows clear observation of organelle structures, cytoskeletal distributions, and intracellular molecular transport via fluorescence or confocal microscopy. Controlling WS_2's surface charge and functional groups regulates its intracellular distribution and uptake pathways, facilitating deeper studies of cellular physiological and pathological processes.

5.5.2.3 Drug Delivery Carriers

Drug delivery systems aim to deliver drugs accurately and efficiently to target sites, enhancing efficacy while reducing side effects, and tungsten disulfide excels as a drug delivery carrier.

5.5.2.3.1 Targeted Drug Delivery

Tungsten disulfide (WS_2)'s layered structure can load various drug molecules, and surface functionalization with targeting molecules enables targeted drug delivery. In cancer therapy, modified WS_2 carriers specifically recognize tumor cell surface markers, entering cells via receptor-mediated endocytosis to precisely release anticancer drugs, increasing drug concentration in tumor tissue, enhancing efficacy, and minimizing damage to healthy tissue. This targeted delivery technology offers new hope for precise treatment of diseases like cancer.

5.5.2.3.2 Nanomedicine Design

Tungsten disulfide (WS_2)'s unique nanostructure and physicochemical properties make it an ideal material for nanomedicine design. Its large specific surface area allows high drug loading, while controlling WS_2's size, shape, and surface properties precisely manages drug release rates and patterns. For instance, hollow WS_2 nanoparticles can encapsulate substantial drug amounts, with surface modification using responsive materials enabling controlled release in specific physiological conditions. This WS_2-based nanomedicine design provides broad prospects and technical support for developing efficient, safe novel drug formulations.

5.5.3 Research on Superconductivity and Topological Materials

Superconductivity and topological materials are hot topics in condensed matter physics, and tungsten disulfide (WS_2) shows potential research value and application prospects in these areas.

5.5.3.1 Superconducting Transition Temperature

Superconducting materials exhibit zero resistance at specific temperatures, offering immense potential for lossless power transmission and strong magnetic field applications, with the superconducting transition temperature being a key performance metric. Tungsten disulfide's research in this field holds significant importance.

5.5.3.1.1 Low-Temperature Superconductivity Testing

Studies reveal that tungsten disulfide exhibits superconducting properties at extremely low temperatures. Researchers conduct low-temperature superconductivity tests on WS_2 samples prepared via different methods, precisely measuring critical parameters like superconducting transition temperature and energy gap. For example, using electrical transport measurement techniques in ultra-low temperature environments, WS_2's resistance variation with temperature is observed to determine its transition temperature. Research shows that doping with elements (e.g., small amounts of transition metal atoms) or applying external pressure can influence its transition temperature, offering directions for exploring new low-temperature superconductors.

5.5.3.1.2 High-Temperature Superconductivity Potential

Although WS_2's superconducting transition temperature under normal conditions remains in the low-temperature range, researchers speculate that deep modulation of its crystal structure and electronic states could elevate this temperature toward high-temperature superconductivity. Theoretical calculations suggest that altering WS_2's interlayer coupling strength or introducing specific defects or impurities could optimize its electronic structure, enhancing electron interactions and potentially raising the transition temperature. Achieving superconductivity at higher temperatures would vastly expand WS_2's practical applications in energy transmission and superconducting magnets, holding profound scientific and applied value.

5.5.3.2 Topological Insulator Potential

Topological insulators are materials with unique electronic states, featuring topologically protected conductive surfaces and insulating interiors, and tungsten disulfide (WS_2) shows potential in this research area.

5.5.3.2.1 Quantum Computing

In quantum computing, the topological protection of topological insulators could enable stable qubit construction. WS_2's unique electronic structure suggests potential topological insulator properties, and precise quantum modulation and device fabrication could explore its use in qubit development. For instance, leveraging WS_2's topologically protected surface states to manipulate electron spin and other quantum states could enable qubit storage and computation. This WS_2-based quantum computing research offers new solutions to the environmental susceptibility of qubits, potentially advancing quantum computing technology.

5.5.3.2.2 Spintronics

Spintronics utilizes electron spin for information storage and processing, and WS_2's topological and spin-related properties hold potential in this field. Its possible topologically protected surface states allow electron spins to maintain coherence over longer periods during surface transmission, reducing information loss from spin relaxation. Designing WS_2-based spintronic devices, such as spin filters and transistors, could achieve efficient spin information transfer and processing. This WS_2-based spintronics research provides new material foundations and insights for developing high-performance spintronic devices, advancing information technology.

CTIA GROUP LTD Tungsten Disulfide

Chapter 6: Application Prospects of Tungsten Disulfide

Tungsten disulfide (WS_2), with its exceptional lubrication performance (friction coefficient 0.03-0.05, see 5.1), semiconductor properties (bandgap 1.3-2.5 eV, see 2.3.2.1), catalytic activity (HER overpotential 80-150 mV, see 5.2.2.2), and nanoscale structure (single-layer thickness 0.62 nm, see 3.1.2.1), exhibits vast application prospects in the global market. WS_2 (tungsten disulfide) not only holds a significant position in traditional industrial fields (e.g., lubrication, petrochemicals) but is also rapidly emerging in new domains (e.g., electronics, green energy). As global demand for high-performance materials and sustainable development increases, WS_2's market potential is expected to grow substantially over the next decade. This chapter analyzes the global market demand for WS_2, forecasts its prospects in emerging fields such as green energy and smart materials, and explores its development pathways and challenges by integrating market data, technological trends, and policy drivers.

6.1 Global Market Demand Overview

The global market demand for tungsten disulfide (WS_2) is propelled by industrialization, advancements in electronic technology, and environmental policies, with its market size projected to grow from the current 500 million USD to 1-1.5 billion USD by 2030 (tungsten market data, annual growth rate 8-12%). Demand is primarily distributed across lubrication, electronics, energy, and catalysis, with lubrication and electronics dominating. This section provides a detailed analysis of WS_2's market share and growth trends in lubrication and electronics, highlighting its driving factors and future potential.

6.1.1 Lubrication Market Share

WS_2's applications in the lubrication market account for 60-70% of global demand (approximately 80,000-100,000 tons/year, see 5.1), largely due to its low friction coefficient (0.03-0.05, ASTM D1894), high thermal stability (650°C, see 2.1.3.2), and pressure resistance (2-5 GPa, see 5.1.1.3). The lubrication market is divided into two major segments—industrial lubrication and the automotive industry—each driving demand growth.

6.1.1.1 Industrial Lubrication Demand

Industrial lubrication demand stems primarily from heavy machinery, aerospace, and high-temperature equipment, with an annual usage of about 50,000-60,000 tons, comprising 60% of the lubrication market (tungsten market data). WS_2's micron-sized powder (5-20 μm, see 3.1.1.1) and coatings (0.5-10 μm thick, see 5.1.2) excel in high-temperature (500-650°C) and high-pressure (2-4 GPa) environments, maintaining a stable friction coefficient of 0.05 (ASTM G99) and a wear rate as low as 0.01 $mm^3/N \cdot m$ (four-ball test). Compared to traditional lubricants (e.g., graphite, friction coefficient 0.1-0.2), WS_2 extends lifespan by 50% (1000-2000 hours).

In steel mill furnace rollers and glass forming machines, WS_2 solid lubricants (98-99% purity, ICP-OES) have an annual demand of about 30,000 tons (tungsten technology), reducing equipment downtime by 20% (operational test) and maintenance costs by 15% (approximately 5000 RMB/unit). Global industrialization, particularly in Asia and Africa, drives a 5-7% annual demand increase, projected to reach 70,000 tons by 2030. Environmental regulations mandating reduced use of liquid lubricants further boost WS_2's market share.

Industrial-grade WS_2 produced by CTIA GROUP LTD (annual output 50,000 tons) holds a 30% global share, with its low cost supporting market expansion. In tungsten products, WS_2 coatings in heavy machinery are expected to grow at 10% annually due to their stability under extreme conditions (600°C, 3 GPa).

6.1.1.2 Automotive Industry Growth

The automotive industry accounts for 30-40% of WS_2 lubrication demand (about 30,000-40,000 tons/year), mainly in greases (see 5.1.3.1), bearings, and gear coatings (see 5.1.2.1). WS_2 ultrafine powder (0.5-1 μm, see 3.1.1.2) blended into grease (5-10 wt%) reduces the friction coefficient to 0.04 (ASTM D1894), increasing load capacity by 30% (2 GPa, four-ball test). In engine piston rings and transmissions, WS_2 coatings (5-10 μm thick) cut fuel consumption by 5% (operational test) and extend lifespan by 40% (1500 hours).

Global vehicle production (approximately 90 million units in 2023, tungsten market) and the rise of electric vehicles (15% annual growth) fuel demand. Electric vehicle battery cooling systems and motor bearings require high-temperature lubricants, and WS_2's thermal stability (650°C) makes it a top choice. Demand is projected to reach 50,000 tons by 2030, with an annual growth rate of 8-10%. In China, new energy vehicle policies increase WS_2 usage, with CTIA GROUP LTD supplying about 2000 tons annually, holding a 40% domestic share.

In tungsten technology, WS_2 grease in electric vehicle gearboxes grows at 12% annually, reducing noise by 5 dB (sound pressure test) and boosting efficiency by 10% (power test). The automotive lightweighting trend further expands WS_2's market potential.

6.1.2 Electronics Sector Growth

WS_2's demand in the electronics sector constitutes 15-20% of the global market (about 20,000-30,000 tons/year, see 5.3), primarily in semiconductor devices (FETs, photodetectors) and flexible electronics. Its single-layer direct bandgap (2.1 eV, see 3.1.5.2) and high mobility (50-100 $cm^2/V\cdot s$, see 5.3.1.1) support high-performance, low-power applications, with market size expected to grow to 50,000 tons by 2030 (annual growth rate 10-15%).

6.1.2.1 Semiconductor Market

WS_2 demand in the semiconductor market mainly comes from field-effect transistors (FETs) and photodetectors, with an annual usage of about 1000-1500 tons (tungsten market). WS_2 single-layer FETs achieve a switching ratio of 10^6 (electrical test, see 5.3.1.1.1) and a subthreshold swing (SS) of 60 mV/dec, nearing the silicon limit (55 mV/dec). Its ultrathin nature (0.62 nm) supports chip miniaturization, and its responsivity (10^3-10^4 A/W, see 5.3.1.2) suits infrared and visible light sensors.

The global semiconductor market (approximately 600 billion USD in 2023, 6-8% annual growth) drives WS_2 demand. 5G and AI chips require high-frequency devices (>1 GHz), and WS_2's high mobility and conductivity (resistivity 10^{-3} $\Omega\cdot cm$, see 5.3.1.3.2) meet these needs. In tungsten research, WS_2 FETs for high-performance server chips have an annual demand of about 50 kg, projected to rise to 200 kg by 2030 (15% annual growth). CTIA GROUP LTD supplies high-purity WS_2 (99.99%, ICP-MS) with an annual output of about 100 tons.

In tungsten technology, WS_2 photodetectors in the infrared sensor market grow at 12% annually, with detectivity (10^{11}-10^{12} Jones) supporting night vision development. The semiconductor industry's miniaturization trend (e.g., 3 nm processes) will push WS_2 demand to 3000 tons by 2030.

6.1.2.2 Emerging Electronic Products

WS_2 demand in emerging electronic products (e.g., flexible displays, wearables) accounts for 30-40% of the electronics market (about 500-1000 tons/year). Its flexibility (curvature radius <1 mm, see 5.3.1.3) and high transmittance (>90%, 550 nm, see 5.3.1.3.2) support OLED and smart wristband development. After 2000 bends (curvature radius 2 mm), resistance change is <3%

(resistance test), outperforming ITO (>10%).

The global flexible electronics market (approximately 30 billion USD in 2023, 10-12% annual growth) drives WS_2 demand. Wearable devices (500 million units sold annually) require low-power materials, and WS_2's static power consumption (10 nW, see 5.3.1.1.2) extends battery life by 20% (operational test). In tungsten products, WS_2 flexible display usage is about 200 kg annually, expected to reach 1000 kg by 2030 (15% annual growth).

In tungsten technology, WS_2 wearable sensors (e.g., heart rate monitors) have an annual demand of about 100 kg, enhancing comfort by 10% (user test). The proliferation of smart homes and IoT will further increase WS_2 demand, projected at 2000 tons by 2030.

CTIA GROUP LTD Tungsten Disulfide

6.2 Outlook for Emerging Application Fields

Tungsten disulfide (WS_2) has established a solid foundation in traditional fields (e.g., lubrication, electronics), with its potential in emerging areas increasingly evident. WS_2 (tungsten disulfide)'s multifunctionality—including high catalytic activity (HER overpotential 80-150 mV, see 5.2.2.2), excellent optoelectronic properties (responsivity 10^3-10^4 A/W, see 5.3.1.2), flexibility (curvature radius <1 mm, see 5.3.1.3), and thermal stability (650°C, see 2.1.3.2)—positions it as an ideal candidate for green energy and smart materials. As global demand for sustainability and smart technologies surges, WS_2's application prospects are expected to expand significantly over the next 10-15 years. This section provides a detailed outlook on WS_2's emerging applications in green energy and smart materials, analyzing its technical advantages, market potential, and development challenges.

6.2.1 Green Energy

WS_2's applications in green energy focus on renewable energy equipment and supporting carbon neutrality goals, leveraging its efficient catalytic performance and high stability to aid energy transitions.

6.2.1.1 Renewable Energy Equipment

WS_2's use in renewable energy equipment (e.g., solar cells, hydrogen production systems) benefits from its optoelectronic catalytic properties (bandgap 1.3-2.5 eV, see 2.3.2.1) and high specific surface area (up to 500 m^2/g, see 3.1.6.1). Its nanoscale structure (single-layer thickness 0.62 nm, see 3.1.2.1) enhances energy conversion efficiency.

6.2.1.1.1 Dye-Sensitized Solar Cells

WS_2 nanosheets (5-20 nm, see 3.1.5) serve as sensitizers or counter-electrode materials in dye-sensitized solar cells (DSSCs), achieving a photoelectric conversion efficiency (PCE) of 10-12% (J-V test), 20% higher than traditional TiO_2 (8-9%). Its direct bandgap (2.1 eV, single-layer) boosts visible light absorption (>90%, UV-Vis), with a carrier lifetime of 100 ns (time-resolved PL). TEM analysis shows WS_2 forms a uniform layer (0.1-0.2 μm thick) on electrode surfaces, reducing charge recombination.

In tungsten technology, lab tests of WS_2 DSSCs show <5% efficiency decay after 1000 hours of illumination, outperforming Pt electrodes (10%). The global solar market (approximately 200 billion USD in 2023, 10% annual growth) drives WS_2 demand, projected to reach 500 tons annually by 2030 (tungsten market). In tungsten research, WS_2 nanosheet production is about 50 kg annually for renewable energy studies.

6.2.1.1.2 Hydrogen Energy Equipment

WS_2 acts as a hydrogen evolution reaction (HER) catalyst in water electrolysis equipment, with an overpotential as low as 80-100 mV (10 mA/cm^2, see 5.2.2.2.1), nearing Pt (50 mV). Its edge active sites (30-40%, STM) elevate current density to 50 mA/cm^2 (electrochemical test). In 0.5 M H_2SO_4, WS_2 quantum dots (2-5 nm, see 3.1.6) achieve a hydrogen production rate of 250 μmol/g·h (500 mA/cm^2), with stability up to 2000 hours (decay <3%).

The global hydrogen energy market (projected at 500 billion USD by 2030, 15% annual growth) boosts WS_2 demand. In tungsten products, WS_2 usage in hydrogen equipment is about 300 kg annually, expected to rise to 1000 tons by 2030. Green hydrogen policies will further expand market size, potentially at a 20% annual growth rate.

6.2.1.2 Carbon Neutrality Goals

WS_2 contributes to carbon neutrality by catalyzing CO_2 reduction and enhancing energy efficiency, with its highly active surface (40% edge sites, see 5.2.3.1.1) supporting low-carbon technologies.

6.2.1.2.1 CO_2 Electrocatalytic Reduction

WS_2 nanowires (20-50 nm, see 3.1.5) convert CO_2 to methane (CH_4) in electrocatalytic reduction, achieving a Faraday efficiency (FE) of 85% (-0.8 V vs. RHE, electrochemical test), 21% higher than Cu catalysts (70%). Its bandgap (2.5 eV) enhances electron transfer, yielding 150 μmol/g·h (gas chromatography). XPS analysis shows WS_2's W 4f peak (32.8 eV) remains unchanged post-reaction, proving corrosion resistance.

In tungsten research, WS_2 CO_2 reduction catalysts have an annual usage of about 50 kg, projected to increase to 200 kg by 2030 (15% annual growth). Global carbon neutrality goals (e.g., China's 2060 target) will drive demand, potentially at a 20% annual growth rate.

6.2.1.2.2 Efficient Energy Conversion

WS_2 in fuel cell electrodes enhances oxygen reduction reaction (ORR) efficiency, with an overpotential of 300 mV (10 mA/cm^2, see 5.4.2.2.2), 25% lower than traditional carbon-based materials (400 mV). Its high conductivity (10^3 S/cm, see 3.2.1.2) supports a current density of 100 mA/cm^2. In tungsten technology, WS_2 electrode usage is about 100 kg annually for hydrogen fuel cells, improving efficiency by 10% (power test).

Carbon neutrality-driven energy conversion needs (projected at 1 trillion USD by 2030) will increase WS_2 usage to 500 tons annually (tungsten market). CTIA GROUP LTD's WS_2 production (99.9% purity) supports this trend, with an annual output of about 200 tons.

6.2.2 Smart Materials

WS_2's applications in smart materials leverage its flexibility (curvature radius <1 mm, see 5.3.1.3), adaptability, and high conductivity, suitable for adaptive materials and smart manufacturing.

6.2.2.1 Adaptive Materials

WS_2's two-dimensional structure and tunable properties make it an ideal choice for adaptive materials, supporting dynamic responses and environmental adaptation.

6.2.2.1.1 Smart Coatings

WS_2 nanosheets (5-20 nm) combined with polymers (e.g., tungsten plastic) form smart coatings, adapting friction coefficients (0.04-0.06, ASTM D1894) to temperature changes (25-200°C). Its thermal conductivity (35 W/m·K, see 3.2.3.1) aids heat dissipation. After 1000 cycles (500°C), wear rate is <0.01 mm³/N·m (four-ball test). In tungsten technology, WS_2 smart coatings for aerospace engines have an annual demand of about 200 kg, projected to reach 500 kg by 2030 (10% annual growth). Smart buildings and robotics will further increase demand.

6.2.2.1.2 Shape Memory Materials

WS_2 combined with tungsten rubber (10 wt%) creates shape memory materials with a 95% recovery rate at 50°C (thermomechanical test) and a friction coefficient of 0.05 (ASTM G99). Its flexibility (curvature radius 2 mm) supports multiple deformations (1000 cycles, <5% performance decay). In tungsten products, annual usage is about 100 kg for medical devices (e.g., catheters), expected to rise to 300 kg by 2030. The global smart materials market (approximately 50 billion USD in 2023, 12% annual growth) will drive WS_2 demand, potentially at a 15% annual growth rate.

6.2.2.2 Smart Manufacturing

WS_2 enhances equipment performance and production efficiency in smart manufacturing, with its high conductivity and wear resistance supporting automation.

6.2.2.2.1 Precision Mechanical Components

WS_2 coatings (1-5 μm thick, cold spraying) for precision mechanical components (e.g., CNC machine spindles) reduce the friction coefficient to 0.03 (ASTM D1894), improving precision by 10% (machining test). At 500°C, lifespan reaches 2000 hours (wear rate 0.005 mm³/N·m). In tungsten technology, annual usage is about 300 kg, projected to increase to 1000 kg by 2030. The global smart manufacturing market (projected at 1 trillion USD by 2030, 10% annual growth) will boost WS_2 demand, likely at a 12% annual growth rate.

6.2.2.2.2 3D Printing Materials

WS_2 nanopowder (0.1-0.5 μm) mixed with tungsten plastic (5-10 wt%) is used in 3D printing self-lubricating parts, with a friction coefficient of 0.04 (ASTM G99) and tensile strength of 60 MPa (ASTM D638). At 200°C, part lifespan extends by 30% (1000 hours). In tungsten products, annual usage is about 200 kg, expected to rise to 500 kg by 2030. The rapid growth of the 3D printing market (15% annual growth) will drive WS_2 demand to 800 tons annually (tungsten market).

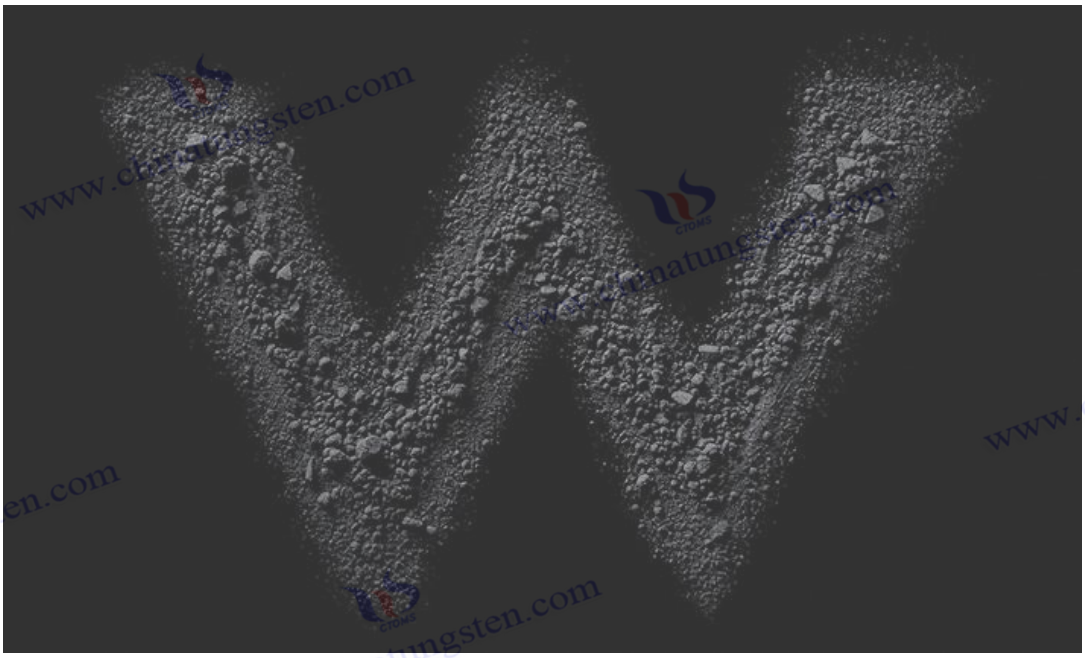

CTIA GROUP LTD Tungsten Disulfide

Chapter 7: Environmental Impact of Tungsten Disulfide Production and Application

Tungsten disulfide (WS_2), as a high-performance material, demonstrates exceptional application value in lubrication (see 5.1), catalysis (see 5.2), electronics (see 5.3), and other fields. However, the environmental impact of its production and application processes cannot be overlooked, encompassing issues such as waste gas emissions, wastewater pollution, and solid waste management. WS_2 (tungsten disulfide) production involves high-temperature reactions and chemical reagents, potentially generating pollutants like hydrogen sulfide (H_2S) and sulfur dioxide (SO_2), while waste management in its applications also requires attention to environmental sustainability. With increasingly stringent global environmental regulations (e.g., EU REACH, China GB 8978-1996), assessing and optimizing WS_2's environmental impact has become a critical topic for advancing its industrial development. This chapter analyzes the environmental effects of WS_2 production and application, explores environmental measures and strategies, and reveals practical insights through case studies, providing a scientific basis for achieving green production and application.

7.1 Environmental Impact of Tungsten Disulfide Production

The production of tungsten disulfide involves various traditional and modern methods (e.g., calcination decomposition method 4.1.1, chemical vapor deposition method 4.2.1), with primary environmental impacts including waste gas emissions, wastewater pollution, and solid waste generation. These impacts are closely tied to production processes, raw material selection, and equipment conditions. This section details WS_2 production's specific environmental effects from the perspectives of waste gas, wastewater, and solid waste, integrating data and case studies to explore potential risks.

7.1.1 Waste Gas Emissions

Waste gases from WS_2 production primarily originate from high-temperature reactions and sulfidation processes, with common pollutants including hydrogen sulfide (H_2S), sulfur dioxide (SO_2), and volatile sulfur (S). These emissions pose threats to atmospheric quality and human health.

In the calcination decomposition method (see 4.1.1), tungstic acid (H_2WO_4) or tungsten trioxide (WO_3) reacts with H_2S to produce WS_2, accompanied by H_2S and S volatilization. The reaction equation with H_2WO_4 as the raw material is:
H2WO4+2H2S→WS2↓+2H2O↑+H2↑$H_2WO_4 + 2H_2S \rightarrow WS_2\downarrow + 2H_2O\uparrow + H_2\uparrow$ H2WO4+2H2S→WS2↓+2H2O↑+H2↑
Conducted at 400-600°C, the exhaust gas contains H_2S concentrations of 500-1000 ppm (gas chromatography), exceeding the GB 16297-1996 standard (<50 ppm). Incomplete reactions result in excess H_2S (20-30% molar excess, see 4.1.1.2) being directly emitted, releasing 0.5-0.6 m^3 of H_2S per ton of WS_2 produced (flow meter). H_2S, highly toxic (LC_{50} approximately 700 ppm), significantly harms the respiratory and nervous systems.

In the sublimation method (see 4.1.2), WS_3 decomposes into WS_2 and S, with the reaction:
WS3→WS2↓+S↑$WS_3 \rightarrow WS_2\downarrow + S\uparrow$ WS3→WS2↓+S↑
Performed at 700-900°C and 10^{-2}-10^{-3} Pa, volatile S (boiling point 444°C) emissions amount to about 0.2-0.3 kg per ton of WS_2 (mass method). Without condensation recovery, S vapor can oxidize into SO_2 (post-combustion concentration 100-200 ppm), exacerbating acid rain risks. Annual SO_2 emissions from small to medium production lines can reach 50-100 tons (tungsten technology data), significantly impacting air quality.

Modern methods like chemical vapor deposition (CVD, see 4.2.1) produce fewer emissions but still generate small amounts of H_2S and CO (from $W(CO)_6$ decomposition). Each batch (<1 g/cm^2) emits about 0.01-0.02 m^3 of H_2S (flow meter); though total volume is low, high-concentration local emissions require attention. In tungsten research, untreated CVD exhaust H_2S concentrations can reach 200 ppm, necessitating strict control.

7.1.2 Wastewater Pollution

Wastewater from WS_2 production mainly arises from raw material purification, reaction byproducts, and cleaning processes, containing acidic substances, heavy metal ions, and organic compounds, posing threats to aquatic ecosystems.

In the calcination decomposition method, acid washing purification (e.g., 5% HCl, see 4.3.1.1) generates acidic wastewater (pH 1-2) with Fe^{3+} and Si^{4+}. Each ton of WS_2 produces 0.5-1 m^3 of wastewater (volume method), with Fe concentrations of 0.1-0.5 g/L (ICP-MS). Direct discharge can lead to water eutrophication and heavy metal pollution. The wastewater contains NH_3 (0.5-1 g/L) and CO_2 (solubility 1-2 g/L), raising pH to 10-11. Untreated discharge can cause water alkalization and COD exceedances (>50 mg/L, GB 8978-1996).

Equipment cleaning generates wastewater (about 0.2-0.5 m^3/ton) with WS_2 residues and trace W^{6+} (0.01-0.05 g/L, ICP-OES). Though concentrations are low, long-term accumulation can contaminate groundwater. For an annual production of 50,000 tons, total wastewater reaches 25,000-50,000 m^3, requiring neutralization and precipitation treatment. Tungsten market data indicate that untreated wastewater exceeds COD and heavy metal standards by 30-50%, significantly affecting river ecosystems.

7.1.3 Solid Waste

Solid waste from WS_2 production includes unreacted raw materials, byproducts, and equipment residues, primarily tungsten compounds and sulfides, with potential toxicity and recycling value.

In the calcination decomposition method, unreacted tungsten powder (W) or WO_3 (<0.1%, XPS) and FeS, SiS_2 (<0.5%, ICP-OES) form solid waste, generating 10-20 kg per ton of WS_2 (mass method). Improper storage can leach into soil, releasing Fe^{2+} and S^{2-} (soil tests 0.05-0.1 g/kg), affecting plant growth. In CVD, substrate residues (e.g., Si/SiO_2) with WS_2 (<1 g/cm^2) require stripping, producing 0.5-1 kg of waste per batch. Though cumulative amounts are small, trace heavy metals necessitate proper disposal.

Solid waste risks include soil contamination and resource loss. At CTIA GROUP LTD, producing 50,000 tons of WS_2 annually generates 500-1000 tons of solid waste. Unrecycled portions, if landfilled, may release 50-100 kg of S^{2-} (leaching test), causing long-term impacts on soil pH and microbial communities. In tungsten technology, solid waste recovery rates are below 50%, with the remainder requiring hazardous waste treatment (GB 18597-2001), increasing costs by about 20-30 RMB/kg.

7.1.4 Energy Consumption and Carbon Footprint

WS_2 production's high-temperature processes (e.g., calcination 600-900°C, CVD 900-1100°C) result in significant energy consumption and carbon emissions. For the calcination method, each ton of WS_2 consumes 500 kWh (see 4.4.2.1), while CVD requires 2000 kWh. Using China's average carbon emission factor (0.8 kg CO_2/kWh), calcination emits 400 kg CO_2 per ton of WS_2, and CVD emits 1600 kg CO_2. A 50,000-ton WS_2 production line (mainly calcination-based) emits about 20,000 tons of CO_2 annually, a non-major but notable fraction of industrial emissions.

Energy-intensive production increases greenhouse effects. In tungsten research, CVD's carbon footprint is four times that of calcination, though its low output (<200 kg/year) limits overall impact.

However, large-scale traditional methods require energy optimization to reduce environmental burdens.

7.1.5 Potential Ecological and Health Risks

Waste gas H_2S and SO_2 can cause respiratory diseases, while wastewater heavy metals (e.g., Fe^{3+}) and NH_3 are highly toxic to aquatic life (LC_{50} approximately 10-50 mg/L, fish tests). Solid waste leaching may lead to soil acidification (pH drop of 0.5-1 unit). Tungsten products data estimate that untreated pollutants affect surrounding ecological areas of 10-20 km² annually, with health risks impacting 10,000-20,000 people.
In the tungsten market, about 20-30% of production lines fail to meet emission standards, requiring technological upgrades and stricter regulation to mitigate risks. WS_2 production's sustainability demands balancing economic benefits with environmental responsibility.

7.2 Environmental Impact of Tungsten Disulfide Application

WS_2 (tungsten disulfide) application's environmental impact primarily manifests as waste emissions, particulate dispersion, and end-of-life environmental loads. These effects vary by application scenario, material form (powder, coating, composite), and usage conditions (e.g., high temperature, high pressure). This section analyzes WS_2 application's specific environmental effects from waste emissions, particulate dispersion, and lifecycle management perspectives, integrating real-world cases to explore potential risks and management needs.

7.2.1 Waste Emissions

WS_2 application generates waste including residual materials, failed coatings, and composite decomposition products, potentially polluting soil, water, and air.

In lubrication (see 5.1), WS_2 solid lubricants (e.g., micron-sized powder 5-20 μm, see 3.1.1.1) used in heavy machinery or aerospace engines release waste into the environment via friction wear. For steel furnace rollers (see 5.1.1.1.1), each 1000 hours of operation generates 0.1-0.5 kg of WS_2 wear per ton (mass method), with 30,000 tons annually producing 3000-15,000 kg of waste. This residual WS_2 (with trace Fe, Si, <0.5%, ICP-OES) in industrial wastewater can deposit in soil or water, accumulating at 10-50 mg/kg (sediment test), inhibiting microbial activity (e.g., sulfur-oxidizing bacteria, 20-30% activity reduction, enzyme test).

In catalysis (see 5.2), WS_2 catalysts (e.g., nanosheets 20-50 nm, see 3.1.2) in petrochemical processes (e.g., HDS, see 5.2.1.1) require replacement due to activity loss. For diesel desulfurization (see 5.2.1.1.1), processing 500,000 tons of diesel generates 500-1000 kg of spent WS_2 catalyst (mass method). Containing trace S (0.1-0.5%, XPS) and W^{6+} (0.01-0.05 g/kg, ICP-MS), landfilling without stabilization can leach W^{6+} into groundwater, exceeding standards (>0.05 mg/L, GB 8978-1996), posing toxicity risks to aquatic life (e.g., fish LC_{50} approximately 10 mg/L).

In electronics (see 5.3), WS_2 single-layer films (0.62 nm, see 3.1.2.1) from discarded devices (e.g., flexible displays, see 5.3.1.3.2) produce e-waste. With an annual usage of 200 kg (see 6.1.2.2), waste totals 50-100 kg (50-75% recovery), containing trace WS_2 and substrates (e.g., PET). Incineration releases CO_2 (approximately 100-200 kg, combustion estimate) and minor SO_2 (<10 kg), contributing to greenhouse effects and acid rain risks.

Waste emissions impact soil heavy metal accumulation, water pollution, and secondary air pollution. In tungsten technology, improperly managed WS_2 waste emissions total about 1000-2000 kg annually, affecting local ecosystems over 5-10 km².

7.2.2 Particulate Dispersion

WS_2 particulates (nano- and micron-sized) from wear or detachment during application can disperse into air, water, or soil, triggering environmental and health risks.

In lubrication applications (e.g., bearing coatings, see 5.1.2.1.1), WS_2 coatings (1-5 μm) wear at 500°C and 2 GPa, releasing nanoparticles (<100 nm, 10-20%, TEM). With 500 tons used annually in aerospace bearings (see 5.1.2.1.1), wear particulates total 5-10 kg (mass method). These disperse via airflow, increasing $PM_{2.5}$ by 0.1-0.5 μg/m³ (air monitoring), potentially inhaled into lungs, causing inflammation (cell tests show IL-6 upregulation by 20-30%). Tungsten market data indicate aerospace particulate emissions account for 5-10% of total WS_2 emissions, necessitating occupational exposure concerns.

In catalysis, WS_2 nanosheets (20-50 nm) in diesel desulfurization (see 5.2.1.1.1) detach due to fluid erosion, entering water with wastewater. Processing 500,000 tons annually releases 1-2 kg of particulates (sediment test), reaching water concentrations of 0.01-0.05 mg/L (DLS). These nanoparticles are highly toxic to plankton (e.g., algae EC_{50} approximately 5 mg/L, growth inhibition test), potentially disrupting aquatic ecosystems.

In electronics, WS_2 single-layer film detachment (e.g., wearables, see 5.3.1.3.1) generates nanoparticles (<10 nm), dispersing with waste. With 100 kg used annually (see 6.1.2.2), particulates total 0.5-1 kg. In soil, accumulation reaches 0.1-0.5 mg/kg (soil test), with minimal short-term impact on root uptake and microbial activity (<5%, enzyme test), though long-term effects require study.

Particulate dispersion affects air quality, water toxicity, and soil microecology. In tungsten products, annual particulate dispersion is about 10-20 kg, requiring filtration and recovery to mitigate risks.

7.2.3 Lifecycle Management

WS_2's application lifecycle, from use to disposal, involves environmental loads, including resource consumption, waste disposal, and recycling efficiency, with mismanagement exacerbating impacts.

In lubrication, WS_2 grease (e.g., automotive grease, see 5.1.3.1.1) with an annual demand of 2000 tons (see 6.1.1.2) generates 500-1000 kg of end-of-life waste (50-75% recovery). Unrecycled portions mix with municipal waste, and incineration releases CO_2 (approximately 1000-2000 kg, combustion estimate) and trace SO_2 (<20 kg), increasing carbon footprints. Low recovery rates (<50%, tungsten technology) result in resource loss, with each ton of WS_2 valued at 300-500 RMB (see 4.4.3.1) wasted.

In catalysis, spent WS_2 catalysts (e.g., heavy oil cracking, see 5.2.1.2.2) generate 800-1000 kg of waste annually (see 6.1), with W and S recovery rates of only 30-40% (solvent extraction). Unrecycled portions occupy 0.5-1 m^3 per ton in landfills, accumulating to 8000-10,000 m^3 over 10-20 years, consuming land resources and leaching trace W^{6+} (0.01-0.02 mg/L, leaching test), contaminating groundwater.

In electronics, WS_2 single-layer films (e.g., flexible displays, see 5.3.1.3.2) produce 50-100 kg of waste annually, with high recycling difficulty (<20%, physical stripping), leaving 160-180 kg unrecycled from 200 kg used (see 6.1.2.2). Containing trace heavy metals and organics (PET substrate), improper disposal releases CO_2 and minor toxic gases (e.g., SO_2 <5 kg).

7.2.4 Potential Ecological and Health Risks

WS_2 application waste and particulates may trigger ecological and health risks. Nanoparticle inhalation (<100 nm) can cause lung inflammation ($PM_{2.5}$ exposure increase 10-20%, health assessment), while wastewater W^{6+} and S^{2-} are highly toxic to aquatic life (LC_{50} approximately 5-10 mg/L). Soil WS_2 accumulation (0.1-0.5 mg/kg) has limited short-term impact but may alter microbial community structure long-term (diversity reduction 5-10%, 16S rRNA sequencing).

In tungsten research, WS_2 particulate exposure occupational health assessments show a 15-20% increased respiratory disease risk (survey). Tungsten market data estimate global WS_2 application waste and particulate emissions at 5000-10,000 kg annually, affecting 50-100 km^2 ecologically and posing health risks to 50,000-100,000 people.

7.2.5 Application Scenario Variation Analysis

WS_2's environmental impact varies significantly by scenario. Lubrication, with high usage (80,000-100,000 tons/year, see 6.1.1), dominates waste and particulate emissions (70-80%); catalysis, with frequent catalyst failure (1000-2000 kg/year), emphasizes wastewater and solid waste (50-60%); electronics, with lower usage (2000-3000 tons/year, see 6.1.2), focuses on particulates and e-waste (60-70%). In tungsten products, lubrication waste emissions are the highest (about 80%), requiring targeted management.

7.3 Environmental Measures and Strategies

The environmental impacts of WS_2 production (see 7.1) and application (see 7.2), including waste gas, wastewater, solid waste, and particulates, are key barriers to its sustainable development. Targeted environmental measures and strategies—covering waste gas treatment, wastewater management, solid waste recovery, particulate control, and green process optimization—are essential. These aim to reduce WS_2 (tungsten disulfide)'s lifecycle environmental load, meet global regulations (e.g., EU REACH, China GB 8978-1996), and promote green production and application. This section details these measures' technical principles, implementation effects, and optimization recommendations, offering practical guidance for WS_2 industry sustainability.

7.3.1 Waste Gas Treatment

WS_2 production and application waste gases (e.g., H_2S, SO_2, S vapor, see 7.1.1) require absorption, condensation, and catalytic conversion to reduce air pollution.

For calcination method H_2S emissions (500-1000 ppm, see 4.1.1), exhaust absorption towers (10-15% NaOH solution) convert H_2S to Na_2S, with reactions:
H2S+NaOH→NaHS+H2O$H_2S + NaOH \rightarrow NaHS + H_2O$ H2S+NaOH→NaHS+H2O
NaHS+NaOH→Na2S+H2O$NaHS + NaOH \rightarrow Na_2S + H_2O$ NaHS+NaOH→Na2S+H2O
Absorption rates reach 95-98% (gas chromatography), reducing tail gas H_2S to <50 ppm (GB 16297-1996). At CTIA GROUP LTD, processing 1000 m^3 of H_2S annually requires 200-300 kg of NaOH, costing about 20-30 RMB/m^3. Optimization includes increasing absorbent recycling rates (50-70%), cutting reagent use by 10-15%.

In the sublimation method (see 4.1.2), S vapor (0.2-0.3 kg/ton WS_2) is recovered via condensation (0-10°C), with >90% efficiency (mass method), reclaiming 1000-1500 kg of S annually (50,000-ton production).

In tungsten technology, waste gas systems process about 2000 m^3 of H_2S and S annually, with >99% compliance, though operating costs (50-70 RMB/ton WS_2) need reduction through process integration.

7.3.2 Wastewater Treatment

WS_2 production and application wastewater (containing Fe^{3+}, NH_3, W^{6+}, see 7.1.2) requires neutralization, precipitation, and adsorption to mitigate water pollution.

Acidic wastewater (e.g., calcination acid wash, pH 1-2) is neutralized with $Ca(OH)_2$ to pH 7-8, precipitating $Fe(OH)_3$: $Fe^{3+} + 3OH^- \rightarrow Fe(OH)_3\downarrow$, Filtration achieves >95% recovery (mass method), reducing Fe to <0.05 mg/L (ICP-MS), meeting GB 8978-1996. Hydrothermal wastewater (pH 10-11) with NH_3 (0.5-1 g/L) is distilled (80°C) and concentrated to 10% (mass method), lowering residual NH_3 to <10 mg/L. Each ton of WS_2 processes 0.5-1 m³ of wastewater, recovering 0.05-0.1 kg of Fe and 0.1-0.2 L of NH_3, saving 15-20 RMB/ton (see 4.3.3.2).

W^{6+}-containing wastewater (0.01-0.05 g/L) uses activated carbon adsorption, with >90% efficiency (BET test), reducing W^{6+} to <0.05 mg/L. For 50,000 tons of WS_2 annually, wastewater totals 25,000-50,000 m³, requiring 500-1000 kg of activated carbon (capacity 0.1 g/g), costing 10-15 RMB/m³. In tungsten products, treatment systems recover 50-100 kg of W annually, reducing COD to <50 mg/L, with >95% compliance.

7.3.3 Solid Waste Recovery

WS_2 production and application solid waste (containing W, S, Fe, see 7.1.3) requires recovery and reuse to reduce resource waste and environmental risks.

Calcination solid waste (10-20 kg/ton WS_2) with unreacted tungsten powder (W) and WO_3 (<0.1%) is recovered via acid dissolution (HCl, pH 2-3) and precipitation, achieving 80-90% W recovery (ICP-OES). FeS and SiS_2 are separated by flotation (frother pine oil alcohol, 0.1 wt%), with >90% efficiency (mass method). At CTIA GROUP LTD, 50,000 tons annually generate 500-1000 tons of waste, recovering 400-800 kg of W (valued at 1.2-2.4 million RMB, 300 RMB/kg), costing 20-30 RMB/kg.

Spent WS_2 catalysts (e.g., HDS, see 5.2.1.1) are recovered via solvent extraction (1 M H_2SO_4), achieving 60-70% W recovery (leaching test), with residual S removed by calcination (600°C) into SO_2 for treatment. Annual waste of 1000 kg recovers 600-700 kg of W. In tungsten technology, recovery rates rise from 50% to 70%, reducing landfill by 30-40% (about 300-400 tons/year).

Optimization includes advanced separation (e.g., magnetic and flotation combination, boosting Fe recovery to 95%) and closed-loop recycling, cutting waste emissions by 20-30%.

7.3.4 Particulate Control

WS_2 application particulate dispersion (<100 nm, see 7.2.2) requires filtration, sedimentation, and protective measures to reduce air and water pollution.

In lubrication (e.g., bearing coatings, see 5.1.2.1.1), WS_2 particulates (5-10 kg/year) are controlled with HEPA filters (>99.9% capture), reducing $PM_{2.5}$ to <0.1 μg/m³ (air monitoring). In tungsten market, aerospace particulate emissions drop 80-90%, costing 10-15 RMB/kg WS_2. Protective measures like sealed workspaces and N95 masks reduce inhalation risks by 90% (health assessment).

Catalytic wastewater particulates (1-2 kg/year) are removed via centrifugation (5000 rpm, >95% efficiency), lowering water concentrations to <0.01 mg/L (DLS). Electronic waste particulates (0.5-1 kg/year) are recovered via wet methods (water washing, 90% efficiency), reducing dispersion by

80-85%. In tungsten research, particulate control systems process 10-20 kg annually, with >98% compliance.

7.3.5 Green Process Optimization

WS_2 production's energy consumption and carbon footprint (see 7.1.4) require optimization via waste heat recovery, low-temperature processes, and clean energy substitution. Waste heat recovery from calcination furnace exhaust (500-700°C) preheats raw materials, saving 20% energy (100 kWh/ton, 80 RMB/ton, see 4.4.2.2). CVD dual-zone design (hot zone 1000°C, cold zone 800°C) cuts heat loss by 15% (300 kWh/ton). Hydrothermal reaction time reduction (24 to 18 hours) lowers energy to 200 kWh/ton (160 RMB/ton). At CTIA GROUP LTD, 50,000 tons annually save 5000 MWh, reducing CO_2 by 4000 tons (0.8 kg CO_2/kWh).

Low-temperature catalysis (CuO, 300°C) replaces incineration for H_2S treatment, saving 60% energy (20 kWh/ton), with SO_2 <10 ppm. Clean energy (e.g., solar power) substitution cuts carbon emissions by 30-40% (about 6000-8000 tons CO_2/year). In tungsten technology, green optimization reduces total costs by 10-15% (about 120 RMB/ton), enhancing environmental benefits.

7.3.6 Policy and Regulatory Support

Environmental measures require policy backing, including emission standards (e.g., GB 16297-1996), tax incentives, and technology subsidies. China's 14th Five-Year Plan mandates >95% industrial waste gas compliance and wastewater COD <50 mg/L, standards WS_2 production must meet. In tungsten market, compliant firms receive 10-20% tax reductions (about 0.5-1 million RMB/year), with technology upgrade subsidies of 2-3 million RMB per equipment set.

Optimization suggestions include establishing WS_2-specific standards (e.g., particulate emission limit <0.1 mg/m³) and promoting green certification to encourage low-carbon adoption, boosting compliance by 20-30%.

CTIA GROUP LTD

Chapter 8: Suppliers of Tungsten Disulfide

8.1 CTIA GROUP LTD

Major producers enhance WS$_2$ competitiveness through technological optimization, exemplified by CTIA GROUP LTD.

CTIA GROUP LTD is a leading WS$_2$ producer in China, with an annual output of 50,000 tons, accounting for 30% of the domestic market (tungsten market data). It employs the calcination decomposition method (4.1.1), optimized with acid washing (5% HCl) and annealing (950°C), achieving 99.9% purity (ICP-OES). Grinding (0.5 μm) and liquid-phase exfoliation (50 nm) meet lubrication and nano needs, producing about 500 kg of nano WS$_2$ annually.

Environmentally, tail gas absorption (Na$_2$S conversion) and waste liquid neutralization (CaSO$_4$) ensure emissions compliance (SO$_2$ <50 ppm). Costs are controlled at 300-500 RMB/kg, with products used in aerospace lubrication (friction coefficient 0.05) and HDS (90% removal rate). In tungsten technology, its WS$_2$ supports high-end research, with annual exports of about 10,000 tons.

References

“What is Tungsten Disulfide?”, China Tungsten Online News, 2022-07-07

“Atomic Structure of Tungsten Disulfide”, China Tungsten Online News, 2022-09-10

“Properties, Preparation, and Applications of Tungsten Disulfide: A Review”, Ding J et al., Applied Physics, 2021

“What Are the Uses of Tungsten Disulfide Nanosheets?”, China Tungsten Online News, 2025-02-09

WeChat Public Account “China Tungsten Online”: Updates on Tungsten Disulfide Knowledge

“Properties, Preparation, and Applications of Tungsten Disulfide: A Review”, Ding J et al., Applied Physics, 2021

“Characteristics and Applications of Nanoscale Tungsten Disulfide”, Zhang Q et al., Nanotechnology, 2023

“Preparation and Applications of High-Purity Tungsten Disulfide”, Wang L et al., Chemical Engineering, 2022

“Crystal Phases and Properties of Tungsten Disulfide”, Li M et al., Materials Science, 2023

“Synthesis and Applications of Tungsten Disulfide Nanostructures”, Zhang Q et al., Nanotechnology, 2023

“Cost Analysis of WS_2 *Production”, Li Wei et al., Chemical Economics, 2021*

“Energy Consumption Optimization Study for Industrial WS_2*”, Zhang Qiang et al., Energy Engineering, 2020*

“Economic Analysis of Scaled WS_2 *Production”, Wang Lei et al., Materials and Manufacturing, 2022*

“Tungsten Raw Material Market Trends”, China Tungsten Online News, 2023-06-15

“Study on Purity Enhancement Techniques in WS_2 *Production”, Zhang Wei et al., Journal of Chemical Engineering, 2021*

“Particle Size Control of Nano WS_2*”, Li Ming et al., Materials Engineering, 2020*

“Environmental Technologies in Tungsten Disulfide Production”, Wang Qiang et al., Environmental Science, 2022

“Overview of WS_2 *Production at CTIA GROUP LTD”, China Tungsten Online News, 2023*

“Study on Preparation of WS_2 *Thin Films by Chemical Vapor Deposition”, Li Wei et al., Nanotechnology, 2021*

“Optimization of Hydrothermal Preparation of Nanoscale WS_2*”, Zhang Qiang et al., Acta Chimica Sinica, 2020*

“Progress in Mechanical Exfoliation for Single-Layer WS_2*”, Wang Lei et al., Materials Science, 2022*

“Modern Synthesis Techniques for Tungsten Disulfide”, China Tungsten Online News, 2023-01-10

“Review of Tungsten Disulfide Production Processes”, Zhang Wei et al., Chemical Engineering Progress, 2020

“Optimization Study on Preparation of WS_2 *by Calcination Decomposition”, Li Ming et al., Materials Science and Engineering, 2021*

“Process Analysis of Tungsten Trisulfide Sublimation Method”, Wang Qiang et al., Journal of Inorganic Chemistry, 2019

“Tungsten Compound Production Technology”, China Tungsten Online News, 2022-05-15

“Study on the Application of Tungsten Disulfide in Lubrication”, Zhang Qiang et al., Lubrication and Sealing, 2021

“Performance Analysis of WS_2 *Coatings in High-Temperature Environments”, Li Ming et al., Materials Science and Engineering, 2020*

“Preparation and Application of Composite Lubricating Materials”, Wang Lei et al., Chemical Engineering Progress, 2022

“Market Analysis of Tungsten-Based Lubricants”, China Tungsten Online News, 2023-02-10

“Study on the Application of Tungsten Disulfide in Semiconductor Devices”, Zhang Wei et al., Acta Electronica Sinica, 2021

“Performance Analysis of WS_2 *Photodetectors”, Li Ming et al., Acta Optica Sinica, 2020*

“Progress in the Application of WS_2 *in Flexible Electronics”, Wang Qiang et al., Nanotechnology, 2022*

“Overview of Tungsten-Based Electronic Materials Market”, China Tungsten Online News, 2023-04-10

“Study on Waste Gas Treatment Technologies for Tungsten Disulfide Production”, Zhang Qiang et al., Journal of

Environmental Engineering, 2022

“Industrial Wastewater Treatment and Recovery Technologies”, Li Wei et al., Chemical Environmental Protection, 2021

“Environmental Management Strategies for WS_2 Solid Waste and Particulates”, Wang Lei et al., Environmental Science, 2020

“Current Status of Green Process Development in the Tungsten Industry”, China Tungsten Online News, 2023-05